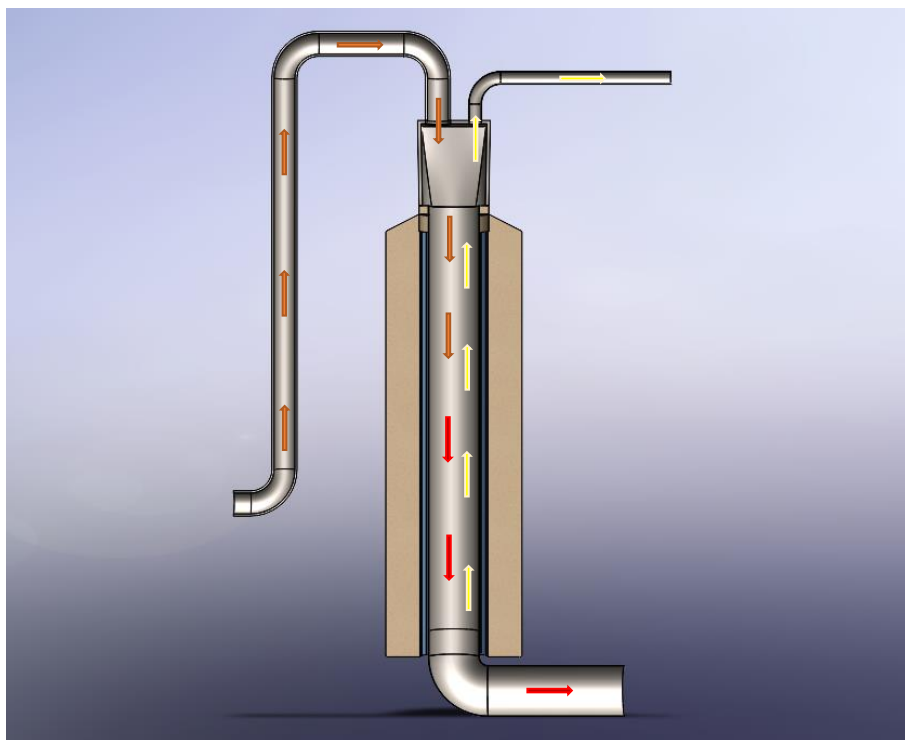# University of South-Eastern Norway

FMH606 Master's Thesis 2021

Energy and Environmental Technology

Calcination in an electrically heated drop tube calciner

Martin Hagenlund Usterud

Faculty of Technology, Natural sciences and Maritime Sciences

Campus Porsgrunn

University of South-Eastern Norway

Course: FMH606 Master's Thesis, 2021

Title: Calcination in an electrically heated drop tube calciner

Number of pages: 148

Keywords: Drop tube calciner, Electricity, Cement production, Decarbonization, Terminal settling velocity, Particle residence time, Heat transfer, Python 3.8 simulation, Cost estimation.

Student:	Martin Hagenlund Usterud
Supervisor:	Lars-André Tokheim
Co-supervisor	Ron M. Jacob
External partner:	Norcem AS Brevik w/Christoffer Moen

Summary:

About 70 % of the CO_2 emissions are generated through calcination (decarbonization) in a modern cement kiln system. The $CaCO_3$ in the limestone is the primary source of CO_2, and the rest comes from fuel combustion. Electrification of the calciner, i.e., replacing fuel combustion with electrically generated heat, will eliminate the fuel combustion exhaust gases. The calciner exit gas will then be pure CO_2 and removes the need for a separate CO_2 capture plant. For this reason, an electrically heated drop tube reactor was designed, and the applicability and cost estimation of the reactor and adjacent units were estimated.

Three system designs were evaluated: 1) counter-current flow of gas and particles, not considering cluster formations, 2) counter-current flow of gas and particles, applying clustering effect, 3) co-current flow of gas and particles.

Python 3.8 was used for modeling and simulation of the three designs. A modified shrinking core model, equilibrium pressure, and the partial pressure of CO_2 were used to determine the kinetics of calcination of calcium carbonate. Diameter of tubes, height, and the number of tubes necessary to process the meal were simulated, varying the key parameters: 1) velocity of CO_2 gas, 2) operating temperature.

Mass and energy balances were implemented to determine the net energy transfer required to preheat and calcine the raw meal. A feed rate of 207 t/h raw meal requires an energy supply of about 108 MW. Supertahl modules from Kanthal® APM are chosen as a viable option for heat transfer.

Design (2) and (3) were both found to be feasible. To achieve 94% calcination, a diameter of 5.3 meters, height of 23.2 meters, and four processing tubes result in an optimum solution for the counter-current design. To achieve the same degree of calcination with the co-current design, a diameter of 3.52 meters, height of 20.2 meters, and eight processing tubes are necessary.

The new system can be implemented into an existing cement clinker process by minimal alterations to the existing system. A de-dusting cyclone, two heat exchangers, and a fan are required. An elevator to transport the raw meal may be implemented if the reactor tubes are long.

Cost estimations show that the CAPEX for the counter-current design becomes about 104 MNOK and for the co-current design 105 MNOK. Cost of electricity is the major contributor to costs, and the OPEX was calculated to 224.54 MNOK/year.

The cost per captured unit (ton) CO_2 for both designs was estimated to be about 522 NOK/t_{CO2}.

Preface

This master's thesis titled "Calcination in an electrically heated drop tube calciner" was done at the University of South-Eastern Norway, Porsgrunn. It was written for partial fulfillment of a Master of Science degree in Energy and Environmental Technology.

The front-page picture is a concept sketch of the drop tube calciner, modelled in Solidworks.

This master thesis is a part of an ongoing research project that USN is a part of, ELSE. It has been an exciting and valuable experience for me to be involved in this project and work with Prof. Lars André Tokheim under close supervision.

I want to express my sincere gratitude to Prof. Lars André Tokheim for his support, interest, and valuable knowledge throughout this project. I would also like to express my gratitude to co-supervisor Ron M. Jacob for his suggestions and support. This thesis would not be possible without the external partner, so I would like to extend my thanks to Christoffer Moen and Norcem Brevik.

Porsgrunn, May 2021

Martin Hagenlund Usterud

Contents

Nomenclature

Symbol	Description	Unit
A_{cross}	Cross-sectional area	m^2
$A_{heat,section}$	Heat transfer area, general	m^2
$A_{heat,ph}$	Heat transfer area, preheating section	m^2
$A_{heat,cal}$	Heat transfer area, calcination section	m^2
$A_{surface}$	Surface area	m^2
$A_{footprint}$	Footprint of installation	m^2
$A_{maintenance}$	Space consideration maintenance	m^2
A_{HX}	Heat transfer area, heat exchanger	m^2
$A_{p,proj}$	The projected area of particle	m^2
Ar	Archimedes number	$-$
A	Frequency factor	$mol/m^2 s k Pa$
C_A	Cost of past unit	$
C_B	Cost of the present unit	$
C_D	Drag coefficient	$-$
C_p	Specific heat capacity	$J/kg\ K$
$C_{p,phm}$	Specific heat capacity preheated meal	$J/kg\ K$
$C_{p,phm,900°C}$	Specific heat capacity meal at 900°C	$J/kg\ K$
$C_{p,CO2,cal}$	Specific heat capacity of CO_2 produced by calcination	$J/kg\ K$
$C_{p,CO2,HX}$	Specific heat capacity CO_2 in a heat exchanger	$J/kg\ K$

$C_{p,air,HX}$	Specific heat capacity air in a heat exchanger	$J/kg\ K$
C_{tube}	Cost of tube	$
C_{mat}	Cost of material	$
C_{2021}	Cost in the year 2021	$
C_{2002}	Cost in the year 2002	$
$C_{2021,euro}$	Cost in 2021 euro	$euro$
$C_{2021,\$}$	Cost in 2021 dollar	$
C_{el}	Cost of electricity	NOK
$C_{el,NOK/kWh}$	Cost of electricity per kilo Watt-hour	NOK/kWh
$CAPEX_{CO2,captured}$	Capital expenditures per captured unit of CO_2	NOK/t_{CO2}
$OPEX_{CO2,captured}$	Operational expenditures per captured unit CO_2	NOK/t_{CO2}
$C_{total,CO2,captured}$	Cost of total CO_2 captured	NOK
$C_{90\%,10t/h}$	Cost of the tube, 90% calcination degree processing 10t/h	NOK
$C_{90\%,21,10t/h}$	Cost of 21 tubes, 90% calcination degree, 10t/h	NOK
$C_{fan,CS,2021,41m^3}$	Cost of fan in carbon steel in 2021 with capacity 41m3	NOK
$C_{HX,Inconel,2021,279m^3}$	Cost of heat exchanger in Inconel for 2021 and 279 m2	NOK
$C_{HX,2}$	Cost of two heat exchanger units	NOK
C_{In718}	Cost of Inconel 718 alloy	

$C_{cyc,ss316,2021,144.5m^3/s}$	Cost of cyclone in 2021 in stainless steel, capacity 144.5 m3/s	NOK
D_p	Particle diameter	m
D	Diameter	m
D_o	Outer wall diameter	m
D_i	Inner wall diameter	m
D_e	Diameter of exit gas, cyclone	m
E	Activation energy	kJ/mol
$E_{phm,in}$	The energy of preheated meal entering DTR	MW
E_{gen}	Generated energy	MW
$E_{meal,900°C}$	The energy of meal at 900°C	MW
$E_{gen,ph}$	Generated energy preheating section	MW
$E_{el,ph}$	Energy supply to preheating section	MW
$E_{el,supply,ph}$	Energy supply to preheating section including the efficiency of electricity to heat	MW
$E_{gen,cal}$	Generated energy calcination section	MW
$E_{out,cal}$	Energy out of the DTR	MW
$E_{el,cal}$	Energy supply to calcination section	MW
$E_{el,supply,cal}$	Energy supply calcination section including the efficiency of electricity to heat	MW
E_{cal}	The energy of calcination reaction	MW

$E_{other,cal}$	The energy of other meal-related reactions	MW
$E_{CO2,cal}$	The energy of produced CO_2	MW
EAC	Equivalent annual cost	$MNOK/y$
EAC_{CAPEX}	The equivalent annual cost of capital expenditures	$MNOK/y$
EAC_{OPEX}	The equivalent annual cost of operation expenditures	$MNOK/y$
$F_{dead,load}$	Normal force by the weight of the structure	N
F_{wind}	Wind force	N
F_G	Gravitational force	N
F_b	Buoyant Force	N
F_f	Frictional force	N
F_N	Future value	NOK
H	Inlet height cyclone	m
H_{cal}	Enthalpy calcination reaction	MJ/kg_{CO2}
$H_{other,cal}$	Enthalpy other meal-related reaction	MJ/kg_{CO2}
I_c	Electrical current	A
I	Second-order moment of inertia	m^4
K_D	Calcination rate	$mol/m^2 s\ atm$
K	Cyclone constant	$-$
L_c	Length of the cone, cyclone	m
L_b	Length of the body, cyclone	m
M	Molar mass of a substance	g/mol

M_{CaCO3}	Molar mass of calcium carbonate	g/mol
M_{CaO}	Molar mass of calcium oxide	g/mol
M_{CO2}	Molar mass of CO_2	g/mol
M_{air}	Molar mass of air	g/mol
M_b	Bending moment	$N\,m$
N	Rotations	$-$
N_{tubes}	Number of tubes	$-$
$N_{elements}$	Number of elements	$-$
N_u	Nusselt number	$-$
NPV	Net present value	NOK
NPV_{CAPEX}	Net present value of capital expenditures	NOK
NPV_{OPEX}	Net present value of operational expenditures	NOK
$NPV_{C,el}$	Net present value of electricity cost	NOK
N_i	Interest periods	$-$
PV	Present value	NOK
P	Pressure	bar
Pr	Prandtl number	$-$
P^*	Equilibrium pressure	bar
P_{CO2}	The partial pressure of CO_2	bar
Q	Duty	MW
$Q_{section}$	Sensible heat for a specific section	MW
Q_{ph}	Sensible heat preheating section	MW
Q_{cal}	Sensible heat calcination section	MW

$Q_{w,HX}$	Waste heat from the heat exchanger	MW
$Q_{refractory}$	Waste heat through refractory of DTR	MW
Re	Reynolds number	$-$
R	Universal gas constant	$m^3 Pa/K\ mol$
R_e	Electrical resistance	ohm
T	Temperature	K
T_{phm}	Temperature of preheated meal	K
$T_{m,phm}$	Median preheated meal temperature	K
T_{ref}	Reference temperature	K
T_{cal}	Calcination temperature	K
T_{wall}	Operating temperature of DTR	K
$T_{CO2,cooled}$	Temperature of cooled CO_2	K
$T_{air,exc}$	Excess cooling air temperature, heat exchanger	K
$T_{air,exc,hot}$	Excess hot air temperature, heat exchanger	K
T_s	Surface temperature	K
T_m	Mean fluid temperature	K
T_{part}	Surface particle temperature	K
$T_{h,in}$	Hot temperature inlet, heat exchanger	K
$T_{h,out}$	Hot stream effluent temperature, heat exchanger	K
$T_{c,in}$	Cold temperature inlet, heat exchanger	K
$T_{c,out}$	Cold temperature effluent, heat exchanger	K

T_{in}	Inlet temperature, fan	K
T_∞	Ambient temperature	K
$T_{outside}$	Temperature outside surface of refractory, DTR	K
U	Overall heat transfer coefficient	$W/m^2\,K$
$\dot{V}$	Volumetric flow rate	m^3/s
$\dot{V}_{CO2}$	Volumetric flow rate of CO_2	m^3/s
$\dot{V}_{fluid}$	Volumetric flow rate of fluid	m^3/s
V	Volume	m^3
V_c	Volume particle core	m^3
W	Inlet width, cyclone	m
W_{el}	Power, fan	MW
X	Calcination conversion factor	$-$

a_f	Annuity factor	$-$
d_{50}	Cut size diameter, cyclone	m
d_p	Diameter particle	m
d_o	Initial diameter core	m
e	Exponent cost estimation	$-$
f_{safety}	Safety factor	$-$
f_{tc}	Total installation cost factor	$-$
$f_{tc,cs}$	Total installation cost factor, carbon steel	$-$
$f_{eq,cs}$	Equipment cost factor, carbon steel	$-$
f_{mat}	Cost factor material	$-$

$f_{pi,cs}$	Piping cost factor, carbon steel	—
g	Gravitational acceleration	m/s^2
h_t	Height of tube	m
h	Convection heat transfer coefficient	$W/m^2\,K$
h_{out}	Convection heat transfer coefficient, ambient	$W/m^2\,K$
h_{rad}	Radiation heat transfer coefficient	$W/m^2\,K$
h_{ph}	Heat transfer coefficient, preheating section	$W/m^2\,K$
h_{cal}	Heat transfer coefficient, calcination section	$W/m^2\,K$
$h_{req,94\%}$	Height required for 94% calcination	m
$h_{req,90\%}$	Height required for 90% calcination	m
$h_{element}$	Height of heating element	m
i	Interest rate	—
k_r	Reaction rate constant	$m^{0.6}/s$
k	Conduction heat transfer coefficient	$W/m\,K$
m	Mass	kg
m_{part}	Mass of particle	kg
m_{gas}	Mass of gas	kg
$m_{hollow,cylinder}$	Mass of hollow cylinder	kg
$\dot{m}$	Mass flow rate	kg/s
$\dot{m}_{phm,in}$	Inlet mass flow rate of preheated meal	kg/s
$\dot{m}_{CO2,prod}$	Mass flow rate of produced CO_2	kg/s

$\dot{m}_{meal,cal}$	Mass flow rate of calcined meal	kg/s
$\dot{m}_{air,hot}$	Mass flow rate of hot air	kg/s
$\dot{m}_{CO2,prod,year}$	Produced CO_2 per year	kg/s
$m_{90\%,10t/h}$	Mass of tube when 90% calcination and 10t/h feed	kg
$\dot{n}$	Molar flow rate	mol/s
p_{out}	Pressure effluent of fan	bar
p_{in}	Pressure in front of the fan	bar
q''	Heat flux	W/m^2
q_{wind}	Even distributed wind force	N/m^2
q''_{conv}	Convection heat flux	W/m^2
q''_{rad}	Radiation heat flux	W/m^2
$q''_{section}$	Heat flux for a specific section, DTR	W/m^2
$q''_{wall,part,rad}$	Radiative heat flux from wall to particle	W/m^2
r_o	Radius of unreacted core	m
r_c	Radius of core	m
t	Wall thickness	m
t_{op}	Operating hours per year	h/y
t_{cal}	Calcination time	s
t_{res}	Particle residence time	s
u_m	Mean fluid velocity	m/s
u_i	Inlet velocity, cyclone	m/s
u_{CO2}	Velocity of CO_2 gas	m/s

v	Velocity	m/s
v_{air}	Velocity of air	m/s
v_{tp}	Terminal settling velocity, particle	m/s
$v_{t,turb}$	Turbulent settling velocity	m/s
$v_{t,lam}$	Laminar settling velocity	m/s
v_{mid}	Median settling velocity	m/s
$v_{uncalcinaed}$	Uncalcined settling velocity	m/s
$v_{94\%,cal}$	94% calcined settling velocity	m/s
$v_{t,counter}$	Terminal settling velocity, counter-current	m/s
$v_{t,co}$	Terminal settling velocity, co-current	m/s
$w_{CO2,phm}$	Weight fraction of CO_2 in raw meal	$-$
$w_{CaCO3,phm}$	Weight fraction of calcium carbonate in raw meal	$-$
α	Absorptivity	$-$
α_G	Absorptivity gas	$-$
α_{diff}	Thermal diffusivity	$-$
ΔT	Temperature difference	K
$\Delta T_{HX,min}$	Minimum temperature difference, heat exchanger	K
ΔT_{lm}	Logarithmic mean temperature	K
Δh	Height difference	m
ΔP_{DTR}	Pressure drop across DTR	bar
ΔP_{HX}	Pressure drop across the heat exchangers	bar

$\Delta P_{cyclone}$	Pressure drop across the cyclone	bar
ΔP_{tot}	Total pressure drop	bar
ε	Emissivity	$-$
ε_G	Emissivity gas	$-$
η	Efficiency	$-$
η_{fan}	Efficiency fan	$-$
$\eta_{el,heat}$	Efficiency electricity to heat conversion	$-$
μ	Dynamic viscosity	$Pa\ s$
μ_{gas}	Dynamic viscosity of a gas	$Pa\ s$
μ_s	Dynamic viscosity, specific	$Pa\ s$
ρ	Density	kg/m^3
ρ_{mat}	Density of a material	kg/m^3
ρ_{air}	Density of air	kg/m^3
ρ_{gas}	Density of a gas	kg/m^3
ρ_p	Density of particle	kg/m^3
ρ_{CO2}	Density of CO_2	kg/m^3
σ	Stefan-Boltzmann constant	$W/M^2\ K^4$
σ_b	Bending stress	MPa
σ_{max}	Maximum allowed stress	MPa
σ_e	Estimated stress	MPa
$\sigma_{dead,load}$	Stress by dead load	MPa
$\sigma_{tensile,max}$	Maximum allowed tensile stress	MPa
$\sigma_{yield,max}$	Maximum allowed shear stress	MPa

τ	Transmissivity	$-$
ν	Kinematic viscosity	m^2/s

List of abbreviations:

IEA	International Energy Agency
DTR	Drop Tube Reactor
FB	Fluidized bed
CAPEX	Capital Expenditures
OPEX	Operational Expenditures
PSD	Particle Size Distribution
LEILAC	Low Emissions Intensity Lime And Cement
SCM	Shrinking Core Model
XRF	X-Ray Fluorescence
HE	High efficiency
HX	Heat Exchanger
CS	Carbon Steel
SS	Stainless Steel
1-2 STHE	STHE with a shell and 2 passes

List of figures and tables

List of figures

List of tables

1 Introduction

This chapter includes the background, description, and objectives of the study. Chapter 1.4 describes the organization of the report.

1.1 Background

One of the most used construction materials in the world is concrete. The key additive in concrete is cement, and 4.1 billion tonnes of cement are produced globally every year. The production results in 5-8% of global anthropogenic CO_2 emission. [1, 2]

Producing cement clinkers has two major sources of CO_2 emission: 1) calcination, 2) fuel combustion. Equation (1.1) is the chemical reaction of the calcination process where limestone ($CaCO_3$) is decarbonized to lime (CaO) and carbon dioxide (CO_2). Calcination accounts for about 65% of the CO_2 emission, while fuel combustion accounts for about 35%. [3, 4]

$$CaCO_3(s) + heat \rightarrow CaO(s) + CO_2(g) \qquad (1.1)$$
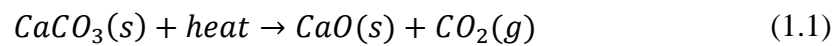
Cement production has remained relatively constant since 2014. However, as emerging countries and regions - especially Asia and Africa - are developing their infrastructure, cement demand is expected to increase. According to the International Energy Agency (IEA), the annual production of cement is expected to grow 0.5% annually from 2020 to 2030. [5]

Several key strategies to face this demand include: [3]

- Improving the energy efficiency of existing cement plants.
- Usage of lower carbon fuels and green electricity.
- Reduce clinker-to-cement ratio and total demand.
- Advancing process and carbon capture technology.

The task background, description and a flow diagram is presented in Appendix A. Included in Appendix A is a flow diagram of a cement kiln process. Appendix B presents the project's work breakdown structure, and the project schedule is in Appendix C.

1.2 Problem description

Expecting a green future, the cement clinker process will be powered by renewable energy sources, such as green electricity. Implementing green electricity to power the calciner instead of fossil fuels can prove an efficient way to reduce CO_2 emissions. The CO_2 produced from standard fuel combustion is eliminated, and the CO_2 produced from the calcination process is pure, which implies that a more simple method of capturing the CO_2 can be applied.

"Combined calcination and CO_2 capture in cement clinker production by use of CO_2-neutral electrical energy" is an ongoing research project that USN is a part of. The acronym ELSE is short for the project name. The goal is to replace carbon-containing fuels with electricity to decarbonate the raw meal in the cement kiln process and capture the CO_2 from the decarbonization of the calcium carbonate.

In the ELSE project, different reactors are investigated and evaluated to decarbonize the raw meal. In this master thesis, an electrically heated drop tube reactor (DTR) is developed. The meal is fed at the top of the tube and will drop down as it is heated and calcined by electrically

heated tube walls. By replacing the traditional calciner with an electrically heated DTR, post-combustion CO_2 capture facilities might be neglected, resulting in a less expensive operation.

Previously in 2020, a master's thesis on "Calcination in an electrically heated bubbling fluidized bed (FB) applied in calcium looping" was conducted by Nastaran Ahmadpour Samani. The FB reactor is quite different from the DTR. However, some of the knowledge and findings from Samani's thesis can be adapted to this study. Energy requirements, cost estimations, CO_2 emissions, and recycling are topics included in Samani's thesis of interest. According to Samani, one of the challenges is the fine particle size distribution of limestone particles and how to handle cohesive Geldart C particles – one proposal was to introduce coarser Geldart B particles. A similar problem might be present in the current thesis. [6]

1.3 Objectives

The main objective of this study is to investigate how the calciner in a cement kiln process can be designed as an electrically heated drop tube reactor (DTR) and evaluate the applicability and cost of this concept.

Several sub-objectives needs to be completed to meet the requirements of the main goal:

1. Evaluating the DTR reactor and investigate its ability to calcine the raw meal using resistance heating.
2. Suggesting a design for the DTR and create a flow diagram of a design reference case.
3. Investigating the need for gas recycling.
4. Identification and quantification of waste heat streams for the new system design.
5. Making mass and energy balances and calculate flow rates, temperatures, and duties.
6. Simulating the DTR calciner varying key parameters.
7. Creating flow diagrams of the selected cases.
8. Describing the impacts to the original kiln system by implementing the new calciner.
9. Evaluate the required size of the DTR calciner and other relevant equipment units.
10. Estimating the investment cost (CAPEX) and operational cost (OPEX) of the suggested process per avoided CO_2 unit ($€/t_{co2}$)

Each introduction of the following main chapters has a list of questions that should be answered to meet the above-listed sub-goals.

1.4 Outline of the thesis

This thesis consists of eight chapters. Chapter 1 describes the background and objective of the study. Chapter 2 emphasizes the theory associated with the DTR concept. Fluidization, kinetic modeling, heating concepts, and the modern cement kiln system are topics being described. The design of the system, mass and energy balances, pressure drop, specific heat capacities, and heat transfer are discussed in Chapter 3. Three design cases: 1) counter-current flow of gas and particles with single-particle theory, 2) counter-current flow of gas and particles applying clustering effect, 3) co-current flow of gas and particles, and several calculation examples regarding the design are discussed in Chapter 4. Chapter 5 includes the simulation setup. Python 3.8 is used for the simulation where key parameters are varied. The cost estimation theory is included in Chapter 6. Simulation results, results of cost estimation, and a discussion regarding the three design cases are included in Chapter 7. Chapter 8 concludes the thesis.

2 Theory

This chapter includes the general theory on fluidization, particle settling velocity, kinetics, heat transfer, and theory necessary to understand the DTR concept. The following questions should be answered within Chapter 2:

- What concepts are the DTR based upon?
- How are the particles influenced fluid mechanically and thermally at the top of the drop tube?
- What conditions are influencing the particles settling?
- During the calcination process, what happens to the gas, and does the gas influence the limestone particles?
- What are the advantages/disadvantages of a DTR compared to existing calcination reactors?
- Which units in the existing system should be replaced or modified?

2.1 Electrically heated drop tube reactor concept

Figure 2.1 illustrates the concept of calcination by use of an electrically heated DTR. The tube walls are heated in sections by electricity. At the top of the DTR, the raw meal, $CaCO_3$, is supplied. The tube walls heat the $CaCO_3$ particles due to radiation heat transfer from the tube walls, conduction heat transfer from particle collisions, and convection between the fluid and the particles. As the particles are heated to the required calcination temperature (about 900 °C), the CO_2 is extracted from the $CaCO_3$, and the product particles are CaO. Since the tube is heated by electricity, the only gas existing is CO_2 from the calcination process. Thus, the need for advanced carbon capture facilities is eliminated. CaO particles can further be transformed into cement clinkers by sintering in a kiln at a temperature of 1400 °C. [7, 8]
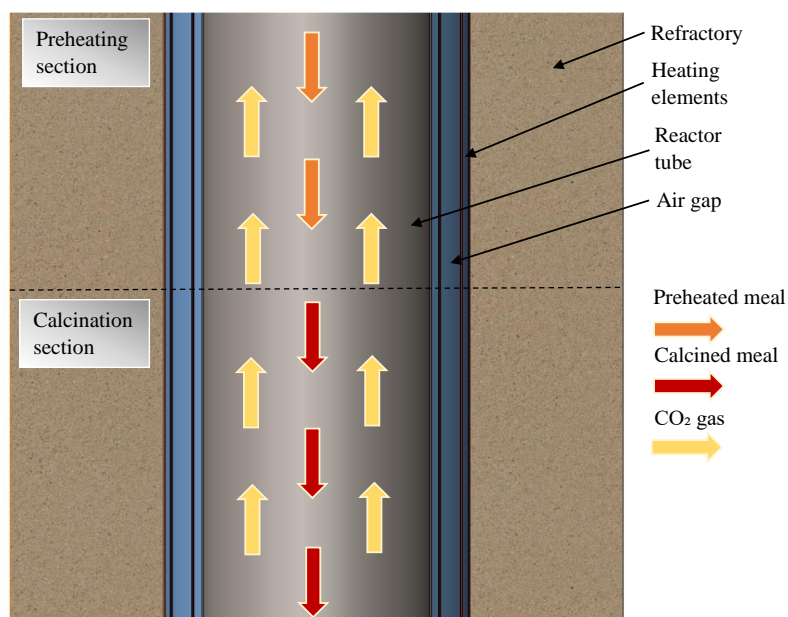
Figure 2.1: Sketch of reactor concept with the arrangement: refractory material, heating elements on the edge of the refractory, air gap, tube. Inside the tube is the preheated meal indicated with orange arrows, calcined meal red arrows, and CO_2 gas are yellow arrows.

A similar project, LEILAC (Low Emissions Intensity Lime And Cement), has been carried out with support from the European Union. In the LEILAC project, the calcination of $CACO_3$ was performed in a steel reactor. The method of direct separation as done in the LEILAC project indicates a potential of 60% reduction in CO_2 emissions. If fossil fuels are replaced with green electricity, such as with the electrically heated DTR, the reduction in CO_2 emissions can be as high as 85%. [8]

2.2 Geldart's classification

Geldart presented a classification system of powders/particles in 1973. The classification system is widely accepted and accounts for the two most important particle properties, particle density and size. The system is derived from experiments of fluidization in ambient air. According to the classification, particles can be divided into four categories, A, B, C, and D, illustrated in Figure 2.2 [9]. Geldart classification is often used for fluidized bed reactors. However, using this classification system, the flow in the system can be determined to be dilute or dense. Most likely, the system operates in an area between dense and dilute. [10]
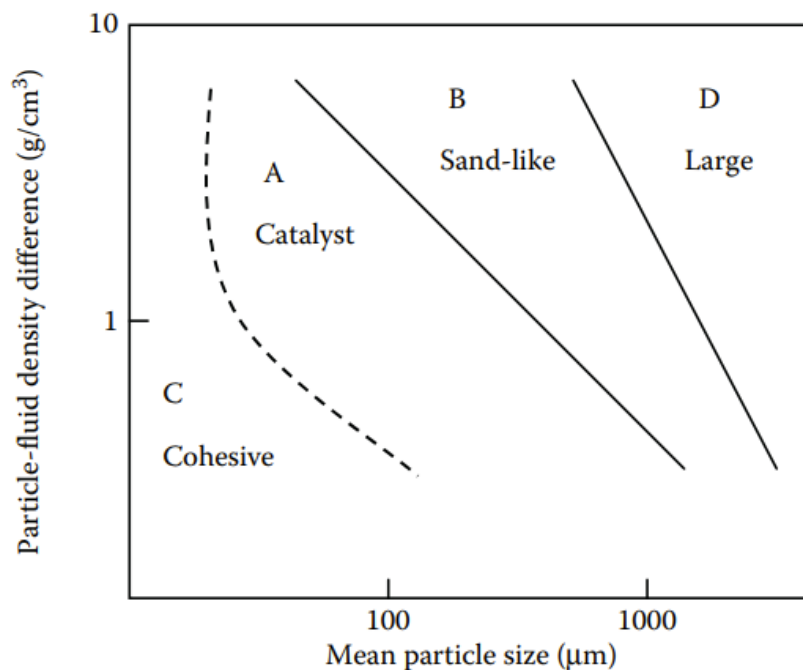
Figure 2.2: Geldart's classification of powders/particles [9]

According to Gas Fluidization Technology, reviewed by Geldart, the groups are divided by particle size [10]:

- Group C: cohesive powders are in this category. This type of powders is complicated to fluidize due to interparticle forces greater than those which the fluid can exert on the particle. The size of these particles is very small ($d_p < 20$ μm). [10]
- Group A: aeratable powders, which fluidize well. The size of these particles is small (20 μm $< d_p < 100$ μm), and the density is relatively low (< 1400 kg/m^3). Interparticle forces are present for these particles. [10]
- Group B: sand-type powders. The size ranges of these particles depend on their density. Interparticle forces are negligible for these particles. [10]
  - 60 μm $< d_p < 500$ μm when $\rho_p = 4000$ kg/m^3
  - 250 μm $< d_p < 1000$ μm when $\rho_p = 1000$ kg/m^3

- Group D: Large or dense particles or a combination of both. Fluidization of these particles can occur. The particles may have high momentum, and the particle interaction is low. [10]

2.3 Terminal settling velocity

When moving in a quiescent fluid, the maximum velocity a particle can obtain is called the terminal settling velocity. The terminal settling velocity depends on the particle characteristics, flow conditions, and fluid characteristics. [11]

A single particle settling in a fluid is affected by three forces, gravitational, friction, and buoyancy. The gravitational force pulls the particle in the settling direction while the friction and buoyancy forces work in the opposite direction, illustrated in Figure 2.3. [12]
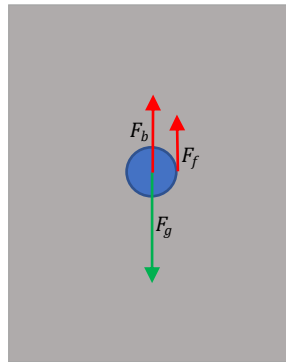
Figure 2.3: Illustration of gravitational, friction, and buoyancy forces acting on a spherical particle in quiescent fluid.

Equations (2.1 – 2.3) are describing the forces:

$$F_g = m_p \cdot g \tag{2.1}$$

$$F_b = m_{gas} \cdot g \tag{2.2}$$

$$F_f = C_D \cdot \frac{1}{2} \cdot \rho_{gas} \cdot v^2 \cdot A_{p,proj} \tag{2.3}$$

Where F_g, F_b, F_f, $[N]$ are the gravitational, buoyancy, and frictional forces, respectively. m_p, $m_{gas}[kg]$ are the masses of the particle and gas, respectively. $C_D[-]$ is the drag coefficient, ρ_{gas} $\left[\frac{kg}{m^3}\right]$ is the density of the gas, v $\left[\frac{m}{s}\right]$ is the velocity and $A_{p,proj}$ $[m^2]$ is the projected area.

Equation (2.4) is describing the force balance:

$$F_g = F_b + F_f \tag{2.4}$$

The terminal settling velocity is highly dependent on the flow regime and particle size. It is expected that the settling velocity is lower with turbulent conditions than laminar due to the random motion caused by eddies. The laminar settling velocity can be calculated using Equation (2.5), assuming relatively small spherical particles in the Stokes regime (Re <<1). [12]

$$v_t = \frac{g \cdot D_p^2 \cdot (\rho_p - \rho_{gas})}{18 \cdot \mu} \tag{2.5}$$

Where $D_p \ [m]$ is the particle diameter, $\rho_p \ \left[\frac{kg}{m^3}\right]$ is the density of the particle, and $\mu \ [Pa \ s]$ is the dynamic viscosity.

For bigger particles, where the Reynolds number is greater than 1, the settling is turbulent. The terminal settling velocity is dependent on two dimensionless numbers, the Archimedes number and the Reynolds number, described by Equations (2.6) and (2.7), respectively. [12]

$$Ar = \frac{\rho_{gas} \cdot (\rho_p - \rho_{gas}) \cdot g \cdot D_p^3}{\mu^2} \tag{2.6}$$

$$Re = 0.1334 \cdot Ar^{0.7016} \tag{2.7}$$

The terminal settling velocity in the turbulent flow regime can be calculated using Equation (2.8).

$$v_{t,turb} = \frac{Re \cdot \mu}{\rho_{gas} \cdot D_p} \tag{2.8}$$

During the calcination process, the particle's mass reduces due to conversion from $CaCO_3$ to CaO. Thus, the terminal settling velocity is reduced. Therefore, the velocity is determined as the median value of an uncalcined particle and a 94% converted particle (Equation (2.9)).

$$v_{mid} = \frac{v_{uncalcined} + v_{94\%,calcined}}{2} \tag{2.9}$$

2.4 Kinetic models for the reaction of solids

Several models have been developed to predict the kinetics of solids. According to Levenspiel, [13] the most appropriate model can be selected by investigating the reaction chemistry and physical property of the particle in the reaction:

- Is the particle porous?
- Does the porosity change during the reaction?
- Does a shell of the product surround the reactant core?
- Does the product appear flaky?
- Is the reaction a thermal decomposition?
- Is the reaction a straight chemical action between constituents of the solid?
- Is the reaction between two solids?
- Is it a reaction between two solids and a gas?

The goal of using such a kinetic model is to describe reacting particles' behavior, using simple mathematics adequately. [13]

2.4.1 Shrinking core model

The shrinking core model (SCM) describes the changes in solid particles during a chemical reaction. Gas-solid heterogeneous reactions often consist of gaseous species in both reactants

and products. However, in the calcination reaction, the only gaseous specie is in the reaction product, namely CO_2. [14, 15]

Thermal decomposition is a chemical reaction where a substance is decomposed caused by heat. For most cases, the reaction is endothermic as the reaction requires heat to break the molecular bonds in the substance that is decomposed. As mentioned above, the decomposition of calcium carbonate produces a gaseous product of CO_2, and this gas may negatively impact the reaction. Therefore, having a model such as the shrinking core model to understand the kinetics can help define the necessary parameters and design of the DTR, such as residence time, required heat, and the energy required. [15, 16]

According to Levenspiel [13], the controlling mechanisms of the reaction in a SCM are either ash diffusion control or reaction control. The control mechanisms are dependent on particle size, and large particles are controlled by ash diffusion. The limestone particles of interest in this study are relatively small, thus, reaction control. As the reaction occurs, the solid reactant ($CaCO_3$) depletes, and a more porous solid product (CaO) layer is formed. The CO_2 diffuses through the porous product until the conversion is complete, indicated by Figure 2.4.
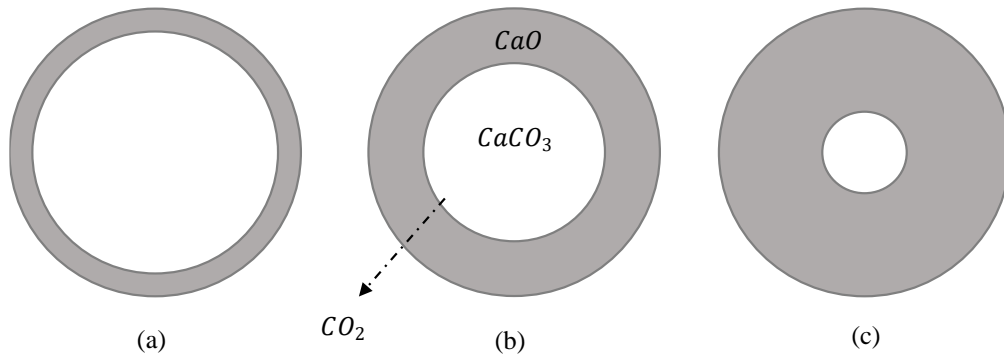
Figure 2.4: Shrinking core of a single particle. (a) Illustrates a large core with a thin layer of product. (b) illustrates the diffusion of CO_2 through the porous layer of CaO. (c) Illustrates an almost fully calcined particle.

The classic SCM of decomposition is derived assuming the rate of change of volume of the particle's unreacted core is proportional to the surface area of the unreacted spherical particle (Equation (2.10)). [17]

$$\frac{dV_c}{dt} = -k_r \cdot 4 \cdot \pi \cdot r_c^3 \tag{2.10}$$

Equation (2.11) is the formula for the volume of unreacted core V_c.

$$V_c = (1 - X)\frac{4}{3} \cdot \pi \cdot r_0^3 \tag{2.11}$$

Where:

$$1 - X = \left(\frac{r_c}{r_0}\right)^3 \tag{2.12}$$

By combining equations (2.11 and 2.12) with Equation (2.10) and integrating Equation (2.10), the ratio between reaction rate and the initial radius can be found, assuming that the calcination occurs at equal rates (Equation (2.13)). [17]

$$\frac{k_r}{r_0} = \frac{1 - (1 - X)^{\frac{1}{3}}}{t_{cal}}$$

(2.13)

The above equations describe a simplified model of the reaction kinetics of limestone. The classic SCM for calculating the conversion factor is given by Equation (2.14), substituting the radius with the diameter.

$$X = 1 - \left(1 - \frac{k_r}{d_0} \cdot t_{cal}\right)^3$$

(2.14)

Equation (2.14) does not fit the reaction time expected when calcining $CaCO_3$ as the reaction is more complex. However, a modified SCM is proposed by Milne et al. [17], where d_0 has a slope of -0.6 should fit the reaction more correctly. Substituting the radius with the diameter and implementing the slope to Equation (2.13) and solving for conversion factor X, the conversion factor can be described with Equation (2.15). [17]

$$X = 1 - \left(1 - \frac{k_r}{d_0^{0.6}} \cdot t_{cal}\right)^3$$

(2.15)

Where $k_r \left[\frac{m^{0.6}}{s}\right]$ is the reaction rate coefficient, $d_0^{0.6}$ [m] is the modified diameter and t [s] is time. The reaction rate coefficient can be calculated using Equation (2.16).

$$k_r = K_D \cdot (P^* - P_{CO2}) = [A \cdot \exp\left(\frac{-E}{R \cdot T}\right) \cdot (P^* - P_{CO2})$$

(2.16)

Where $A = 0.012 \frac{mol}{m^2 s\, kPa}$ is a frequency factor, $E = 33.47 \frac{kJ}{mol}$ is the activation energy and T [K] is the calcination temperature [18]. The reaction rate coefficient is dependent on the equilibrium pressure, P^* [atm] described by Equation (2.17), and partial pressure of CO_2, P_{CO2} [atm].

$$P^* = 4.192 \cdot 10^9 \cdot \exp\left(\frac{-20474}{T}\right)$$

(2.17)

Rearranging Equation (2.15), the reaction time of the calcination can be calculated (Equation 2.18):

$$t_{cal} = \frac{(1 - (1 - X)^3 d_o^{0.6})}{k_r}$$

(2.18)

2.5 Residence time

The residence time for a particle can be defined as the time that a specific particle resides in a vessel or stage during a continuous process. [19]

Several factors need to be considered to determine the residence time necessary for the particles. During the calcination of $CaCO_3$, CO_2 gas is released into the reactor tube (described in chapter 2.4). Due to the density of the CO_2 gas under atmospheric pressure at high temperature, the gas will rise, and impact the smaller particles, since the buoyancy and

frictional forces acting on the particles are more significant than the gravitational force. Particle interactions such as collisions, cluster formation, frictional forces, and electrostatic forces need to be considered. The particle size distribution naturally occurring when producing cement from $CaCO_3$ is wide. Due to the forces and flow regime described in chapter 2.3, the residence time is different for each particle size.

Equation (2.19) can be applied to calculate the residence time, where the height of the reactor is divided by the terminal settling velocity.

$$t_{res} = \frac{h_t}{v_t} \tag{2.19}$$

2.5.1 Sections of the DTR

The height of the DTR can be divided into a preheating section and a calcination section. The preheating section of the DTR raises the temperature of the particles to the calcination temperature. Thus, the height of the tube must be determined from the residence time of the particles. The same approach can be applied to the calcination part, where enough heat must supply the particles to reach the desired calcination degree. When dividing the reactor into these two sections, some assumptions are made:

- The partial pressure of the produced CO_2 is 1 atm.
- The calcination reaction appears only at the calcination temperature (900 °C), i.e., the calcination section.

2.5.2 CO₂ atmosphere

The atmosphere inside the reactor consists of pure CO_2, which leads to more simple post-processing of the gas. However, some challenges become apparent.

The gaseous CO_2 that forms during the calcination reaction has a low density due to the high temperature. The gas will rise due to buoyancy and create a counter-current flow with the particles. However, fine particles in the particle size distribution described later in Chapter 3.1, some of the particles rise and exit with the gas at the top of the reactor. The dusty gas requires de-dusting before the gas can be processed and stored. One additional benefit from the buoyant CO_2 gas is enhanced convection heat transfer between the fluid and particles due to the high-temperature gas.

Carbonation is the chemical reaction where CaO entraps CO_2 and produces $CaCO_3$ (Equation (2.20)). [20]

$$CaO_{(s)} + CO_{2(g)} \rightarrow CaCO_{3(s)} \tag{2.20}$$
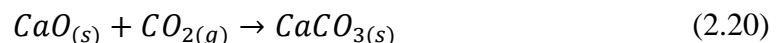
The $CaCO_3$ forms at a temperature of about 650 °C, thus, below a modern calcination reactor's operational temperature (900 °C). i.e., calcination and carbonation reactions occur at the same time within the reactor. The carbonation may inhibit the calcination of limestone. However, it is expected that the operational conditions are favored calcination. [20]

2.6 The modern cement kiln system

Figure 2.5 is a schematic of the kiln 6 system at Norcem AS Brevik [21]. The units of interest regarding this master thesis are the cyclone towers, the pre-calcination unit, the rotary kiln, and the clinker cooler.
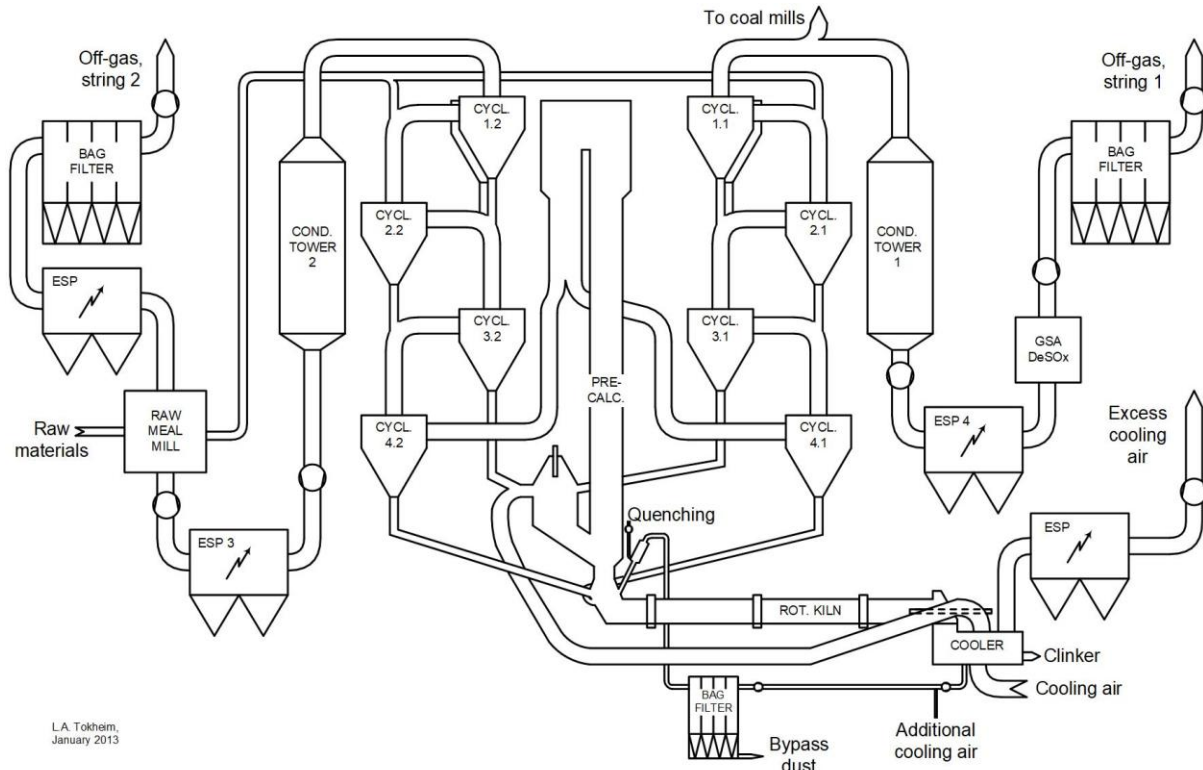
Figure 2.5: Sketch of kiln 6 system including bypass and GSA [21]

The system has two sets of 4-stage cyclone preheaters, which heats the raw meal to about 650 °C before the meal enters the pre-calcination reactor from cyclone tower (3.1) and (3.2). In the pre-calcination reactor, the meal is heated to about 900 °C, of which the calcination of the meal occurs. Pre-calcination is a process where the raw meal is thermally decomposed from limestone to lime and CO_2 gas, and the degree of calcination is 94%. The pre-calcined meal is then fed to the rotary kiln where the meal is calcined 100%, and the clinker is produced. The operating temperature is usually 1400 °C. Thus, a cooler is used to obtain the desired temperature of the clinker. [22]

Figure 2.5 is the basis for the process flow diagram discussed in Chapter 3.2, where the units of interest are illustrated.

2.7 The electrically modified cement kiln system

The DTR is to be implemented in an existing cement kiln system, with as few changes as possible, to reduce the impact of the system and the cost. However, some changes are required. Figure 2.5 is the basis of the evaluation: 1) The DTR is replacing the pre-calciner, 2) de-dusting cyclone(s) to clean the exiting gas, 3) Heat exchanger to cool down the CO_2 before it is stored, 4) a fan, to overcome the pressure losses of the DTR, cyclone and heat exchangers, 5) electrical power supply to heat and calcine the raw meal.

Some units in addition to the existing pre-calciner may also be excluded, such as a cyclone. The quencher, bag filter, and additional recycle lines can also be expected to be excluded. A process flow diagram shows the intended system with the units of interest in Figure 3.3.

2.8   Resistance heating and heat transfer

Conversion from electrical to thermal energy can be done through resistance heating. The rate of the generated energy can be described by Equation (2.21), where the current, $I\ [A]$, is passing through a medium with a resistance (electrical), $R_e\ [\Omega]$. [23]

$$\dot{E}_{gen} = I^2 R_e \tag{2.21}$$

Resistance heating ensures high electricity to heat conversion efficiency (typically 95-99%). Losses related to the conversion to thermal energy may be due to the resistive material glowing. A minor part of the electric energy is converted to light which may not contribute to the heat transfer.

The heated medium, such as a metal vessel, can transfer the heat to another medium through conduction, convection, and radiation. In this study, the reactor tube walls are heated by resistance heating, and the heat transfer mechanisms are calcining the meal differently [4]:

- Conduction: If the limestone particles are directly in contact with the reactor wall.
- Convection: The reactor wall transferring the heat to the CO_2 gas generated from the calcination.
- Radiation: From the reactor wall through the gas medium and directly affect the limestone particles.

The limestone particles are moving continuously throughout the reactor. Thus, the contribution of conduction heat transfer might be negligible. The contribution depends on the particles' behavior inside the reactor - how the particles are fed into the reactor, the flow regime inside the reactor, particle interaction, etc.

Small particles might be carried in the opposite direction of the falling particles due to the buoyancy of CO_2 gas. By assuming these particles are calcined, the temperature of the particles is about 900 °C. Thus, these hot particles transfer heat to the colder particles, which have a lower temperature range of 650-900 °C (preheating section).

2.8.1   Convection heat transfer

Newton's law of cooling is used to describe thermal convection, and this law states that the cooling rate of a body is proportional to the difference between the body (surface) and the fluid temperatures. Equation (2.22) expresses the convective heat flux, $q''_{conv}\ \left[\frac{W}{m^2}\right]$, as the product of the convective heat transfer coefficient, $h\ \left[\frac{W}{m^2 K}\right]$, and the temperature difference between the surface, $T_s\ [K]$, and the mean fluid temperature, $T_m\ [K]$: [23]

$$q''_{conv} = h \cdot (T_s - T_m) \tag{2.22}$$

The convective heat transfer coefficient is dependent on the surface geometry, the fluid motion, and several fluid thermodynamic and transport properties. Equation (2.23) can be applied to

calculate the coefficient. Where, $k \left[\frac{W}{m\,K}\right]$, is the thermal conductivity, $Nu\,[-]$, is the Nusselt number, and $D\,[m]$, is the diameter of the tube.[23]

$$h = \frac{k \cdot Nu}{D} \qquad (2.23)$$

2.8.2 Radiation heat transfer

Heat in the form of radiation is transmitted from an object with a nonzero temperature. Equation (2.24) is the Stefan-Boltzmann law, which describes the radiation heat flux, $q''_{rad}\left[\frac{W}{m^2}\right]$. In Equation (2.24), the emissivity, $\varepsilon\,[-]$, has a value in the range ($0 \leq \varepsilon \leq 1$), the Stefan-Boltzmann constant, $\sigma = 5.67 \cdot 10^{-8}\left[\frac{W}{m^2\,K^4}\right]$, and $T_{part}\,[K]$, is the surface temperature of the particles and, $T_{sur}\,[K]$ is the temperature of the surroundings. [23]

$$q''_{rad} = \varepsilon \cdot \sigma \cdot \left(T^4_{part} - T^4_{sur}\right) \qquad (2.24)$$

For convenience, Equation (2.24) can be rewritten and expressed in the same form as Equation (2.22). Equation (2.25) is the radiation heat transfer expressed with the radiation heat transfer coefficient, $h_{rad}\left[\frac{W}{m^2\,K}\right]$. [23]

$$q''_{rad} = h_{rad} \cdot (T_{part} - T_{sur}) \qquad (2.25)$$

Where the radiation heat transfer coefficient is described with Equation (2.26):

$$h_{rad} \equiv \varepsilon \cdot \sigma \cdot \left(T_{part} + T_{sur}\right) \cdot \left(T^2_{part} + T^2_{sur}\right) \qquad (2.26)$$

2.8.3 Combined heat transfer

In this thesis, the heat is transferred to the meal by convection and radiation. The radiation heat transfer coefficient depends heavily on temperature, whereas the convection heat transfer coefficient has a relatively weak temperature dependence.

By combining the heat transfer additions from both convection and radiation, the total heat flux is given by Equation (2.27): [23]

$$q''_{tot} = q''_{conv} + q''_{rad} = h \cdot (T_s - T_m) + h_{rad} \cdot \left(T_{part} - T_{sur}\right) \qquad (2.27)$$

3 Design

This section describes the necessary equations and theory in order to design the DTR and adjacent units. The following questions should be answered:

- What is the typical particle size distribution (PSD) of the raw meal?
- What countermeasures can be implemented to process the particles influenced by the buoyancy of the gas from calcination?
- What are the requirements to modify/replace the units?
- What sizes need to be specified to evaluate the design?
- What should the design values be?
- What is the total energy demand of the pre-heating and calcination process?
- How long should the reactor be? What is the minimum required height?
- Which factors affect the size of the reactor?
- What equipment units should be included in the process flow diagram?
- What reference case should be accounted for in the process flow diagram?
- What reference case/design values are the mass and energy balances dependent on?
- What are the resulting calculated values?
- What conditions specified from sub-objective one are dictating the need for gas recycling?
- What is the required need for recycling?
- What are the sources of heat loss?
- Are the heat losses an addition to existing losses?
- At what temperatures are losses happening?

To connect all considerations of designing a DTR, an overview of the report is shown in Figure 3.1. The procedure is based on the upcoming chapters and includes dimensioning, energy balances and heat transfer, strength analysis, tube arrangement, pressure drop, simulations, and cost estimation.

Total procedure

1. The PSD and cumulative frequency of particles are investigated to get an overview of fluidization properties.

2. A process flow diagram is created to get an overview of the DTR system with adjacent units.

3. Based on the process flow diagram, mass and energy balances are created. The specific heat capacities are calculated.

4. Equations to determine the dimensions of the DTR are listed.

5. The possibility of buckling, impact of wind force, and the outside surface temperature are used to evaluate reactor wall thickness.

6. Dimensioning theory of cyclones, HX's, and the required power of the fan to compensate for the pressure drop.equations are listed.

7. Heat transfer correlations by convection and gas absorption radiation are described.

8. Calculation example design 1: Counter-current flow of gas and particles – single particle theory.

9. Calculation example design 2: Counter-current flow of gas and particles – applying clustering effect.

10. Calculation example design 3: Co-current flow of gas and particles.

11. Pressure drop calculation across the units within the system, and efficiency of de-dusting cyclone.

12. Reactor wall thickness calculations.

13. Simulations: Python script for evaluating the diameter, length and number of reactor tubes are included in Appendix K and L.

14. Cost estimation theory.

15. Cost estimation theory, material selection, heating element selection and adjacent units are described.

16. Implementing the cost estimation theory, and estimating the total cost (CAPEX, OPEX), including the cost per captured CO_2 unit.

17. Results, discussion, conclusion

Figure 3.1: Overview of the following chapters

3.1 Particle size distribution

Information regarding the particle size distribution (Appendix D) of the raw meal is collected from Norcem Brevik in 1996. There have not been any significant changes to the meal since 1996, and the data is regarded as valid. The size of the particles ranges from 0.2 µm to 180 µm, and the majority are small ($d_p < 30$ µm). From Appendix D the median of the PSD is 21.25 µm.

Figure 3.2 is the cumulative frequency of particles according to Appendix D. The figure indicates that Geldart C particles are represented by approximately 48%, which are of particular interest due to the challenging fluidization of the particles. The classification criterion is described in detail in Chapter 2.2.
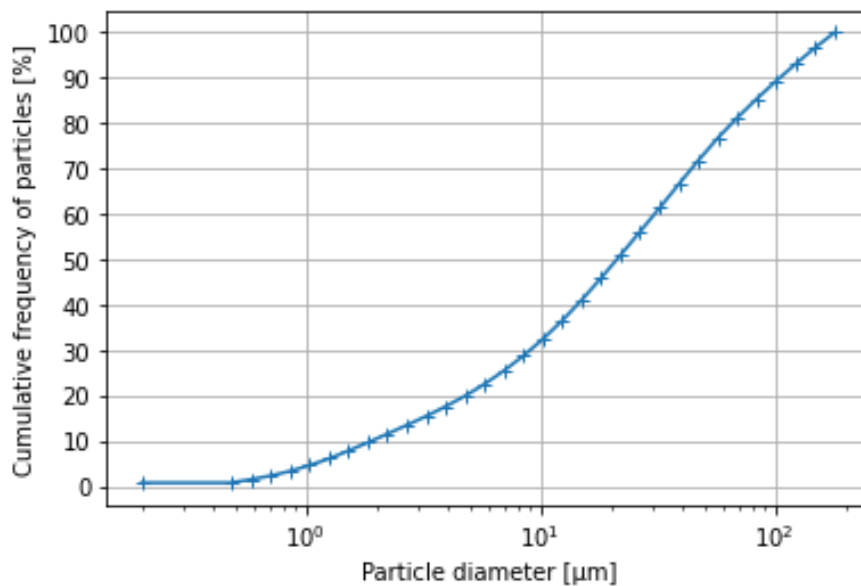
Figure 3.2: Cumulative frequency of particles based on Appendix D. Large fraction of the particles shows to be included as Geldart C particles, approximately 48%.

3.1.1 Chemical composition of raw meal

The chemical composition of limestone particles can be determined by X-ray fluorescence analysis (XRF). The analysis is conducted on the limestone particles by making a melt where the particles are fully calcined. The melt mass is reduced as it is produced; this is mainly due to off-driven CO_2. This reduction in mass is referred to as loss on ignition (LoI). Thus, the composition of the particle-melt presented in Table 3.1 is on loss on ignition-free basis. The chemical composition of the PSD presented in Table 3.1 is not the same as presented in Chapter 3.1. However, the difference in chemical composition is assumed to be negligible.

Table 3.1: Chemical composition (data provided by Norcem AS Brevik)

Grain size [µm]	> 200	200-125	125-90	90-63	63-32	< 32	Total
Portion [wgt%]	1.65	3.50	4.30	9.11	25.45	53.45	97.46
SiO_2	48.24	44.75	36.61	26.51	18.98	17.01	20.80
Al_2O_3	12.57	8.72	6.85	5.18	3.97	4.21	4.66
Fe_2O_3	4.32	3.75	3.24	3.62	4.07	3.37	3.60
CaO	37.19	42.15	51.77	61.19	67.78	69.55	65.99
MgO	1.41	1.66	2.21	2.55	3.01	3.22	2.97
SO_3	0.91	0.91	0.91	0.91	0.91	0.91	0.91
K_2O	2.66	2.21	1.72	1.31	1.01	1.00	1.13
Na_2O	0.61	0.52	0.46	0.42	0.41	0.42	0.43
Sum	107.91	104.64	107.77	101.69	100.14	99.69	100.49

Table 3.1 shows that the particle's chemical composition is very dependent on the particle size.

The larger particles ($d_p > 125$ µm) have a high content of quartz (SiO_2) compared to the smaller particles ($d_p < 32$ µm). Opposite, the CaO content in the smaller particles is nearly twice the amount of the larger particles. The high amount of SiO_2 in the large particles –a hard mineral – indicates why these particles are not ground to such small size as the particles containing less quartz and more calcite (CaO).

Assuming 100% conversion of $CaCO_3$ to CaO and all other oxides being weighted as the XRF analysis determined in Table 3.1, the initial composition of the raw meal before calcination can be determined. The chemical composition can be used to determine the particles' reactivity by the individual particles' size and their chemical composition. The smaller particles, given the high amount of $CaCO_3$, are expected to thermally decompose more quickly – not only by the small size – but also by the composition.

Table 3.2 represents the chemical composition of the raw meal. The content of $CaCO_3$ is based on the CaO content in Table 3.1, and the weight of other oxides is kept constant. Thus, it is assumed that none of these oxides undergo a reaction. All components of the compound have been normalized. An Excel spreadsheet of the calculation is attached to Appendix E.

Table 3.2: Calculated chemical composition of raw meal based on table provided by Norcem AS Brevik

Grain size [µm]	> 200	200-125	125-90	90-63	63-32	< 32	Total
Portion [wgt%]	1.65	3.50	4.30	9.11	25.45	53.45	97.46
SiO_2	33.16	29.64	23.39	17.88	14.34	13.43	15.28
Al_2O_3	8.64	7.72	6.09	4.66	3.74	3.50	3.98
Fe_2O_3	2.97	2.65	2.09	1.60	1.28	1.20	1.37
$CaCO_3$	51.39	56.54	65.72	73.79	78.98	80.31	77.60
MgO	0.97	0.87	0.68	0.52	0.42	0.39	0.45
SO_3	0.63	0.56	0.44	0.34	0.27	0.25	0.29
K_2O	1.83	1.63	1.29	0.99	0.79	0.74	0.84
Na_2O	0.42	0.37	0.30	0.23	0.18	0.17	0.19
Sum	100.00	100.00	100.00	100.00	100.00	100.00	100.00

3.2 Cluster formation

Cluster formation of the particles is expected to occur. Based on Chapter 2.2, the Geldart C particles tend to agglomerate. The particles can form relatively large clusters due to intermolecular forces, particles melting on the reactor walls' surface, and sintering (the latter two due to high temperature). This phenomenon is essential to address for industrial applications, as the sintering can cause fluidization difficulties. [24]

Another phenomenon is the effect of mass load. Several models have been developed to address this phenomenon in cyclones. If the ratio of mass load to gas load is high, the mass tends to overload the cyclone and increases the cyclone's efficiency. The same phenomenon may occur in the DTR, where the raw meal forms clusters and the effective particle size happens to be much larger than the initial PSD suggest.

3.3 Process flow diagram

Figure 3.3 is an illustration of the DTR with nearby units of interest. The raw meal is preheated in the cyclone between lines (1) and (2), which corresponds to cyclone three in the modern cement plant at Norcem AS Brevik (presented in Chapter 2.6). The height difference between cyclone three (2) and the expected height of the inlet of the DTR (3) requires an elevator (or another conveying unit) to transport the preheated raw meal. During the transport, there are heat losses. However, the losses are regarded as negligible for the setup of the process flow diagram. Thus, the preheated raw meal is fed into the DTR at a temperature of 658 °C (3). The feed rate is based on a capacity of 4968 t/d, resulting in 207 t/h [22, 25]. With the buoyancy of CO_2 gas, small particles may be dragged with the gas upwards in the DTR. Thus, a cyclone unit to de-dust the gas is installed between lines (6) and (7). The calcined dust is separated from the gas in the de-dusting cyclone.

Further, the dust follows line (10), connecting to the main-line (5). Pure CO_2 (7) exits the cyclone, but due to the high temperature of 900 °C, a heat exchanger is installed, which utilizes the air from the clinker cooler (11) to cool down the CO_2 gas (7). The hot air (12) produced at the heat exchanger is recycled back to the preheating cyclones. A fan is used to effectively suck the cooled CO_2 gas (8) from the heat exchanger, and further, the gas is sent to storage (9).

The DTR utilizes electrical energy to preheat the raw meal to 900 °C in the first section of the DTR (preheat zone), then, at 900 °C, the electrical energy is used for calcination ($CaCO_3 \rightarrow CO_2 + CaO$) of the raw meal (reaction zone). The supply of electrical energy is different for the preheat zone and the reaction zone. Thus, in Figure 3.3, this is indicated using two coils. The calcined meal exits the DTR at a temperature of approximately 900 °C (4), where the meal line (4) is connected to the dust line (10) and is further sent to the rotary kiln for clinker production (5).
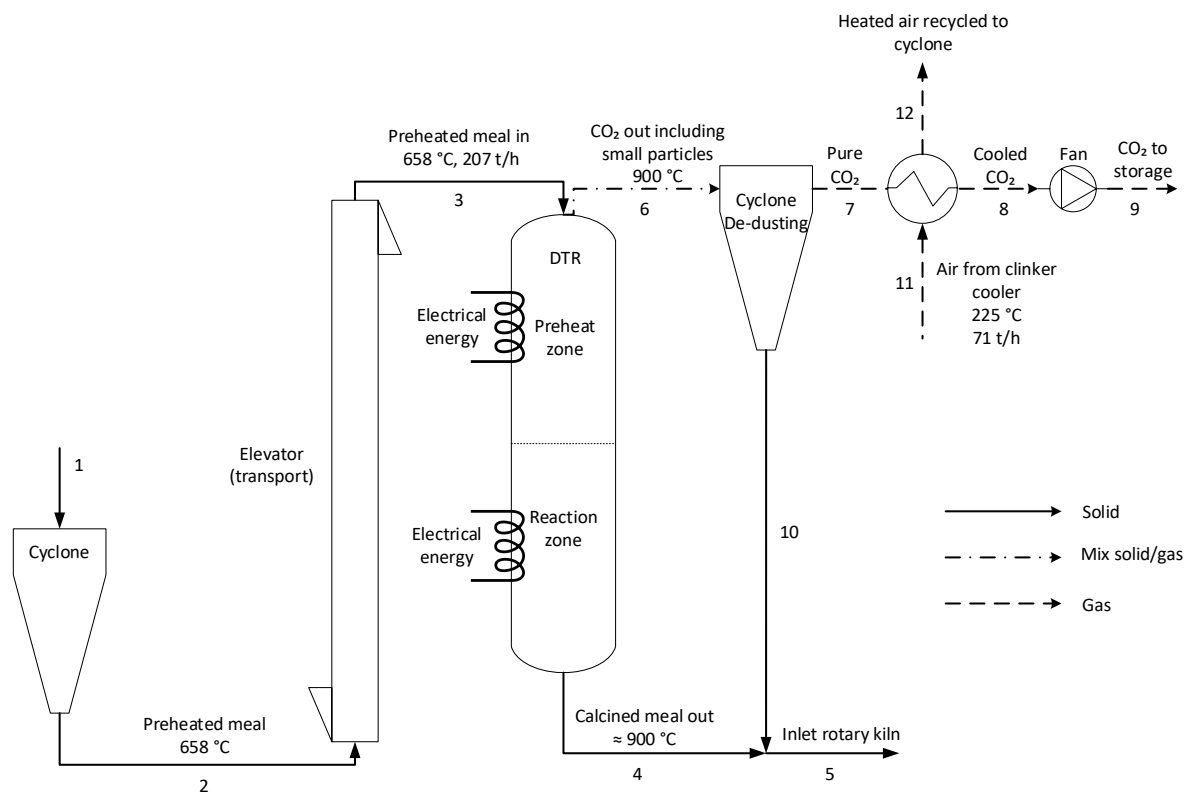
Figure 3.3: Process flow diagram of the DTR and units of interest.

3.3.1 Mass balance

Based upon Figure 3.3, a mass balance for the DTR can be derived. The system is evaluated assuming steady-state conditions. Design basis values of the weighted calcium carbonate content in the raw meal is calculated from the chemical composition discussed in Table 3.1. The calcination degree is based on the typical value effectively used in modern cement clinker production [25].

Table 3.3: Design basis values - mass balance

Parameter	Unit	Design basis value
$\dot{m}_{phm,in}$	$\dfrac{t}{h}$	207
$w_{CaCO3,phm}$	$\dfrac{kg}{kg}$	0.77
X	–	94%

By assuming steady state, Equation (3.1) describes the mass balance:

$$\dot{m}_{phm,in} = \dot{m}_{CO2,prod} + \dot{m}_{meal,cal} \tag{3.1}$$

Where $\dot{m}_{phm,in} \left[\frac{t}{h}\right]$ is the mass feed rate of the preheated raw meal into the DTR, $\dot{m}_{CO2,prod} \left[\frac{t}{h}\right]$ is the mass of the CO_2 gas produced during calcination and $\dot{m}_{meal,cal} \left[\frac{t}{h}\right]$ is the mass of the calcined meal.

The weight fraction of CO_2 produced in the calciner can be determined by the $CaCO_3$ content in the raw meal (Equation (3.2)):

$$w_{CO2,phm} = w_{CaCO3,phm} \frac{M_{CO2}}{M_{CaCO3}} \tag{3.2}$$

The weight fraction of the $CaCO_3$ ($w_{CaCO3,phm}$) in the raw meal is listed in Table 3.3, $M_{CO2} \left[\frac{g}{mol}\right]$ and $M_{CaCO3} \left[\frac{g}{mol}\right]$ are the molecular mass of CO_2 and $CaCO_3$, respectively.

The mass of the CO_2 generated during calcination assuming 100% conversion can be found by Equation (3.3):

$$\dot{m}_{CO2,phm,100\%} = w_{CO2,phm} \dot{m}_{phm,in} \tag{3.3}$$

Equation (3.3) does not account for the calcination degree X. Thus, this correction is included in Equation (3.4):

$$\dot{m}_{CO2,prod} = \dot{m}_{CO2,phm,100\%} X \tag{3.4}$$

The calcined meal flow rate ($\dot{m}_{meal,cal}$) out of the DTR can be calculated by Equation (3.5):

$$\dot{m}_{meal,cal} = \dot{m}_{phm,in} - \dot{m}_{CO2,prod} \tag{3.5}$$

3.3.2 Energy balances

Based on Figure 3.3, three energy balances can be made to describe the DTR and the nearby units of interest: 1) Calciner, 2) Heat exchanger.

Design basis values for the energy balances are collected partly from Samani's master thesis and a report from phase 1 of the ELSE project. The parameters are listed in Table 3.4 [6, 26]. R. Jacob's master thesis, "Gas-to-gas heat exchanger for heat utilization in hot CO_2 from an

electrically heated calcination process," is used to define the design basis values for the heat exchanger energy balance [26].

Table 3.4: Design basis values - energy balances

Parameter	Unit	Design basis values
T_{ref}	°C	25 $(p_{ref} = 1\ atm)$
T_{phm}	°C	658
T_{cal}	°C	900
$T_{air,exc}$	°C	225
$T_{CO2,cal}$	°C	900
$\Delta T_{HX,min}$	K	100
H_{cal}	$\frac{MJ}{kg_{CO2}}$	−3.6
$H_{other,cal}$	$\frac{MJ}{kg_{CO2}}$	0.3
$\eta_{el,heat}$	−	98%
$\dot{m}_{air}$	$\frac{t}{h}$	71

3.3.2.1 Energy balance DTR

The DTR can be viewed as a two-part system composed of two sections, where the top section is reserved for preheating of the raw meal, and the bottom section is where the calcination reaction occurs; thus, two energy balances can be derived. The heat loss from the DTR to the surroundings is neglected.

Preheat zone:

Assuming steady-state, the energy balance of the DTR's preheat zone can be described by Equation (3.7), where the sum of the inlet energy, $E_{phm,in}$ $[MW]$, and the generated energy, $E_{gen,ph}$ $[MW]$, equals the energy of the heated meal before calcination occurs, $E_{meal,900°C}$ $[MW]$:

$$E_{phm,in} + E_{gen,ph} = E_{meal,900°C} \tag{3.7}$$

The energy provided into the system is calculated using Equation (3.8) and consists only of the raw meal's energy.

$$E_{phm,in} = \dot{m}_{phm,in} C_{p,phm}(T_{phm} - T_{ref}) \tag{3.8}$$

The mass flow rate, $\dot{m}_{phm,in}$ $\left[\frac{kg}{s}\right]$ is given in Table 3.3, $C_{p,phm}$ $\left[\frac{J}{kg\ K}\right]$ is the specific heat of the preheated meal at constant pressure evaluated at the inlet temperature of the meal (T_{phm} $[K]$) and T_{ref} $[K]$ is the reference temperature listed in Table 3.4.

Energy generated in the preheat zone, $E_{gen,ph}$ [MW] only consist of one element, the electric energy for preheating the meal, $E_{el,ph}$ [MW], (Equation (3.9)).

$$E_{gen,ph} = E_{el,ph} \qquad (3.9)$$

The electrical energy used in the preheat zone is calculated using Equation (3.10), which is the energy the meal obtain just before calcination occurs minus the inlet energy:

$$E_{el,ph} = E_{meal,900°C} - E_{phm,in} \qquad (3.10)$$

Further, $E_{meal,900°C}$ [MW] is the energy used to heat the meal to calcination temperature from the reference temperature, T_{ref} [K], described by Equation (3.11):

$$E_{meal,900°C} = \dot{m}_{phm,in} C_{p,phm,900°C} (T_{cal} - T_{ref}) \qquad (3.11)$$

The energy supplied required to heat the meal to desired calcination temperature, $E_{el,supply,ph}$ [MW], can be determined by Equation (3.12):

$$E_{el,supply,ph} = \frac{E_{el,ph}}{\eta_{el,heat}} \qquad (3.12)$$

The efficiency of transforming the electricity to heat is a design basis value (Table 3.1).

Reaction zone:

The governing energy balance of the reaction zone is expressed by Equation (3.13), where the energy into the reaction zone is the outlet of the preheat zone, $E_{meal,900°C}$ [MW] (described by Equation (3.11)), plus the energy generated by the calcination, $E_{gen,cal}$ [MW], minus the energy out the DTR, E_{out} [MW]:

$$E_{meal,900°C} + E_{gen,cal} - E_{out,cal} = 0 \qquad (3.13)$$

The energy out is the sum of the energy in the CO_2 gas, $E_{CO2,cal}$ [MW], and in the calcined meal, $E_{meal,cal}$ [MW] (Equation 3.14):

$$E_{out,cal} = E_{CO2,cal} + E_{meal,900°C} \qquad (3.14)$$

The generated energy in the reaction zone consists of three terms, energy due to electrical heating, $E_{el,cal}$ [MW], calcination, E_{cal} [MW], and other meal-related reactions, $E_{other,cal}$ [MW] (Equation (3.15)):

$$E_{gen,cal} = E_{el,cal} + E_{cal} + E_{other,cal} \qquad (3.15)$$

The energy provided by the CO_2 gas from the calcined meal is expressed by Equation (3.16):

$$E_{CO2,cal} = \dot{m}_{CO2,cal} C_{p,CO2,cal} (T_{cal} - T_{ref}) \qquad (3.16)$$

$C_{p,CO2,cal}$ $\left[\frac{J}{kg\,K}\right]$ and $C_{p,meal,cal}$ $\left[\frac{J}{kg\,K}\right]$ are the specific heat of the CO_2 and meal at constant pressure evaluated at T_{cal} [K], respectively.

The generation terms for the calcination and other meal-related reaction are expressed by Equation (3.17) and (3.18), respectively:

$$E_{cal} = \dot{m}_{CO2,cal} H_{cal} \tag{3.17}$$

$$E_{other} = \dot{m}_{CO2,cal} H_{other} \tag{3.18}$$

The enthalpy of calcination H_{cal} $\left[\frac{MJ}{kg_{CO2}}\right]$ and other meal-related reactions $H_{other,cal}$ $\left[\frac{MJ}{kg_{CO2}}\right]$ are listed as basis design values in Table 3.4.

Electrical energy for the calcination can be expressed with Equation (3.19):

$$E_{el,cal} = E_{out,cal} - E_{meal,900°C} - E_{cal} - E_{other} \tag{3.19}$$

Thus, the supply of electrical energy required for calcination is obtained with Equation (3.20):

$$E_{el,supply,cal} = \frac{E_{el,cal}}{\eta_{el,heat}} \tag{3.20}$$

The same conversion efficiency, $\eta_{el,heat}$ $[-]$, is valid for both the preheat zone and calcination zone. The design basis value for the efficiency is listed in Table 3.4.

3.3.2.2   Energy balance heat exchanger

The exiting CO_2 gas from the calciner carries a significant amount of sensible heat. To utilize this heat, the heat should be transferred to another medium, such as air. Figure 3.3 includes a heat exchanger that aims to cool down the CO_2 gas exiting the DTR and heat air used for preheating purposes in the cyclone towers.

Two alternatives based on the heat capacity rate definition ($C \stackrel{\text{def}}{=} \dot{m}_{gas} C_{p,gas}$) can be applied to calculate either the temperature of the exiting CO_2 gas, $T_{CO2,cooled}$ $[K]$, or the air exit temperature, $T_{air,exc,hot}$ $[K]$. If the heat capacity rate is higher for the air than the CO_2 stream, then Equation (3.21) can be applied. If the heat capacity rate is lower for the air stream than for the CO_2 stream, Equation (3.22) can be applied.

The temperature of the cooled CO_2 gas is given as the sum of excess cooling air temperature $T_{air,exc}$ $[K]$ and a minimum temperature difference in the heat exchanger, $\Delta T_{HX,min}$ $[K]$ (Equation (3.21)):

$$T_{CO2,cooled} = T_{air,exc} + \Delta T_{HX,min} \tag{3.21}$$

The excess hot air temperature can be calculated by subtracting the minimum temperature difference in the heat exchanger $\Delta T_{HX,min}$ $[K]$ from the hot CO_2 temperature, T_{cal} $[K]$ (Equation (3.22)):

$$T_{air,exc,hot} = T_{cal} - \Delta T_{HX,min} \tag{3.22}$$

By applying a heat balance for the heat exchanger, the temperature of the excess cooling air can then be given as in Equation (3.23):

$$T_{air,exc,hot} = T_{air,exc} + \frac{\dot{m}_{CO2,cal} \cdot C_{p,CO2,HX} \cdot (T_{cal} - T_{CO2,cooled})}{\dot{m}_{air,hot} \cdot C_{p,air,HX}} \tag{3.23}$$

Where $C_{p,CO2,HX}$ $\left[\frac{J}{kg\,K}\right]$ is the specific heat at a constant pressure of CO_2 at the average temperature of the hot side of the heat exchanger, $C_{p,air,HX}$ $\left[\frac{J}{kg\,K}\right]$ is the specific heat at a constant pressure of the air at the average temperature of the cold side of the heat exchanger, and $\dot{m}_{air,hot}$ $\left[\frac{t}{h}\right]$ is the mass flow rate of air from the clinker cooler.

3.3.3 Specific heat capacity

The specific heat capacities $\left[\frac{kJ}{mol\,K}\right]$ for CO_2 and air under constant pressure are found using Equation (3.24), while the specific heat capacity of $CaCO_3$ is found using Equation (3.25). [26]

$$C_p = a + bT + cT^2 + dT^2 \tag{3.24}$$

$$C_p = a + bT + cT^{-2} \tag{3.25}$$

The parameters a, b, c, and d are listed in Table 3.5. [26]

Table 3.5: Parameters for calculating the specific heat capacities.

Compound	Temp. unit	a 10^3	b 10^5	c 10^8	d 10^{12}	Validity [Temp. unit]
Calcium carbonate	[K]	82.34	4.975	$-12.87 \cdot 10^{10}$	-	273-1033
Carbon dioxide	[°C]	36.11	4.233	-2.887	7.464	0-1500
Air	[°C]	28.94	0.4147	0.3191	-1.965	0-1500

Specific heat capacity is a temperature-dependent parameter, and the validity for the adjustable parameters (a, b, c, d) are given in Table 3.5. The C_p value calculated using this information is assumed to be valid for $CaCO_3$, though the temperature might be below the validity limit.

3.4 Design of DTR and adjacent units

The following subchapters describe equations and theories on designing the DTR and the adjacent units of the DTR.

3.4.1 DTR

To effectively process the raw meal to desired calcination degree, the design of the DTR is important. Essential design factors include:

- The volumetric flow rate of raw meal
- The volumetric flow of produced gaseous CO_2
- Heat transfer rate
- Cross-sectional area
- Terminal settling velocity (particles)
- Velocity medium (fluid)

- Diameter
- Height
- Arrangement of tubes
- Simplicity regarding manufacturing
- Number of units (tubes)
- Footprint (area)
- Costs

The volumetric flow rate can be determined by Equation (3.26), and equal to the mass flow rate, $\dot{m}\left[\frac{kg}{s}\right]$, divided by the density, $\rho\left[\frac{kg}{m^3}\right]$.

$$\dot{V} = \frac{\dot{m}}{\rho} \tag{3.26}$$

Applying the ideal gas law, the density of a substance can estimated (Equation 3.27).

$$\rho = \frac{P \cdot M}{R \cdot T} \tag{3.27}$$

Where $P\ [Pa]$ is pressure, $M\left[\frac{kg}{mol}\right]$ is the molecular weight, $R\left[\frac{m^3 Pa}{K \cdot mol}\right]$ is the universal gas constant, and $T\ [K]$ is the temperature.

Based on the energy balances discussed in Chapter 3.3.2, the heat transfer rate can be calculated.

The cross-sectional area is determined by the volumetric flow rate divided by the fluid velocity, $u_m\left[\frac{m}{s}\right]$, given by Equation (3.28).

$$A_{cross} = \frac{\dot{V}}{u_m} \tag{3.28}$$

Further, by applying Equation (3.29), the diameter of a cylinder can be determined based on the cross-sectional area.

$$D = \sqrt{\frac{4 \cdot A_{cross}}{\pi}} \tag{3.29}$$

The heat transfer area is determined by the heat transfer rate and the heat flux. Thus, the heat transfer area for each section of the DTR is calculated with Equation (3.30).

$$A_{heat,section} = \frac{Q_{section}}{q''_{section}} \tag{3.30}$$

The height of each section of a cylinder can be equated by Equation (3.31) from the heat transfer area.

$$h_{t,section} = \frac{A_{heat,section}}{\pi \cdot D} \tag{3.31}$$

3.4.1.1   Pressure drop

The height lead to a pressure drop across the tube and can be calculated with Equation (3.32). [28]

$$\Delta P_{DTR} = \rho \cdot g \cdot \Delta h \tag{3.32}$$

Where $\rho \left[\frac{kg}{m^3}\right]$ is the fluid density, $g \left[\frac{m}{s^2}\right]$ is the gravitational acceleration and $\Delta h \, [m]$ is the height difference.

3.4.1.2   Strength analysis

To dimension the wall thickness of the reactor, some assumptions are made:

- The wind is the major external force acting on the DTR wall, which is the only contributor to shear stress.
- The weight "dead load" of the reactor is the primary source of internal forces acting on the DTR.

The impact of particle collisions on the inside wall and other minor contributors is assumed to be minimal and neglected in this study.

The thickness of the wall can be estimated by evaluating the size of the stresses acting on the DTR, with the allowable tensile and yield stresses for a specific material. To assess the impact of dead load on the DTR, Equation (3.33) can be applied. [29, 30]

$$\sigma_{dead,load} = \frac{F_{dead,load}}{A_{cross}} \tag{3.33}$$

Where $F_{dead,load} \, [N]$ is the force of the dead load, and $A_{cross} \, [m^2]$ is the cross-sectional area. The cross-sectional area is estimated using Equation (3.34) and the force by Equation (3.35).

$$A_{cross} = \frac{\pi}{4} \cdot (D_o^2 - D_i^2) \tag{3.34}$$

Where $D_o, D_i \, [m]$ is the outer and inner diameter, respectively.

$$F_{dead,load} = m \cdot g \tag{3.35}$$

Where $m \, [kg]$ is the mass of the cylinder, and $g \left[\frac{m}{s^2}\right]$ is the gravitational acceleration.

The mass can be calculated with Equation (3.36).

$$m = \rho_{mat} \cdot V \tag{3.36}$$

Where $\rho_{mat} \left[\frac{kg}{m^3}\right]$ is the density of a specific material, and $V \, [m^3]$ is the volume of the cylinder and calculated with Equation (3.37).

$$V = \frac{\pi}{4} \cdot (D_o^2 - D_i^2) \cdot h_t \tag{3.37}$$

Where $h_t \, [m]$ is the height of the cylinder tube.

The external wind force acting on the tube is by nature varying in intensity and strength. Thus, to dimension the wall thickness, a guide such as NORSOK N-003 can be applied. [31]

In this study, the wind is regarded as an evenly distributed force acting on the reactor wall. The reactor tube is fixed at the top and bottom to some sort of framework. Equation (3.38) is used to calculate the wind force. [32]

$$F_{wind} = \frac{C_D \cdot \rho_{air} \cdot A_{surface} \cdot v_{air}^2}{2} \tag{3.38}$$

Where C_D $[-]$ is the drag coefficient, ρ_{air} $\left[\frac{kg}{m^3}\right]$ is the density of air, $A_{surface}[m^2]$ is the surface area projected normal to the wind, and v_{air} $\left[\frac{m}{s}\right]$ is the wind velocity.

The drag coefficient is different for all geometries, and for a tall upright cylinder, 0.8 is the proposed value [32]. The projected area exposed to the wind can be regarded as half a cylinder, i.e., the wind is blowing from one side and is calculated using Equation (3.39).

$$A_{surface} = \pi \cdot \left(\frac{D}{2}\right) \cdot h_t \tag{3.39}$$

In compliance with NORSOK N-003, the wind velocity must be based on wind measurements over a period of time at the location of interest. Norsk Klimaservicesenter's database of wind measurements can be used (Figure 3.4). [33]
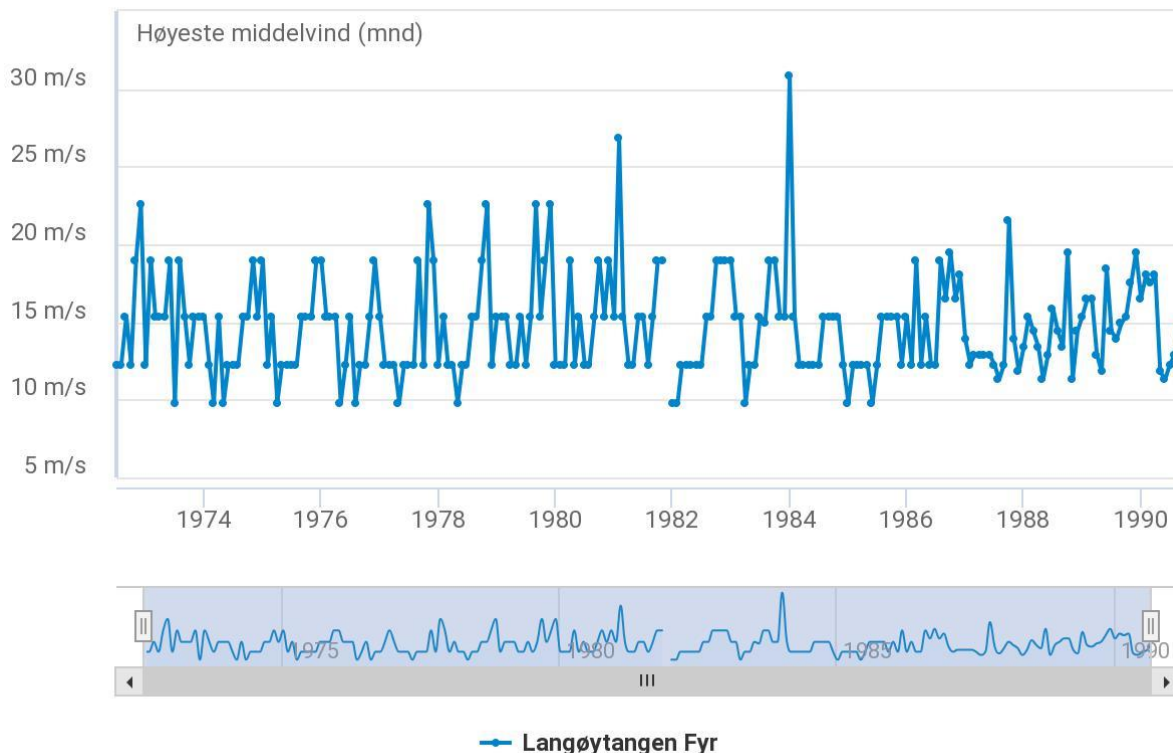
Figure 3.4: Wind measurements collected from Langøytangen Fyr. Measurement from 1974 to 1990. [33]

The impact of the wind force is regarded as an even distributed load. Since the cylinder is fixed at both ends, the maximum stresses are largest in the middle. Equation (3.40) equates the evenly distributed wind load:

$$q_{wind} = \frac{F_{wind}}{h_t} \tag{3.40}$$

The wind force applied to the reactor wall induces a bending moment on the cylinder, which can be equated applying Equation (3.41).

$$M_b = \frac{q_{wind} \cdot h_t^2}{8} \tag{3.41}$$

The stress due to bending can be calculated with Equation (3.42).

$$\sigma_b = \frac{M_b}{I} \tag{3.42}$$

Where $I\ [m^4]$ is the second-order moment of inertia.

As before mentioned, the maximum allowable stress, yield and tensile, must be evaluated for a specific material at specific operating conditions. An example of a maximum stress chart is shown in Figure 3.5. [34]
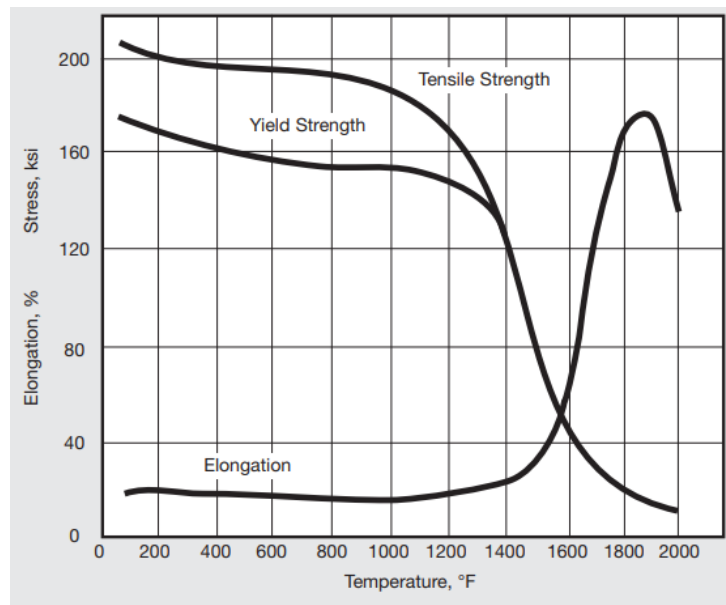
Figure 3.5: Maximum yield and tensile stresses, Inconel 718 [34]

With specified allowable stresses and estimated stresses, a trial-and-error analysis can determine the thickness of the reactor wall. The minimum thickness is found when the allowable stress multiplied with a safety factor, and the calculated stress is equal (Equation (3.43)).

$$\sigma_{max} = \sigma_e \cdot f_{safety} \tag{3.43}$$

The heating elements should transfer heat efficiently to the particles through the reactor wall. Thus, a thin wall is desired, which contradicts the requirement of the strength analysis. Equation (3.44) is used to calculate the necessary outside surface temperature $T_{outside}\ [K]$.

$$T_{outside} = T_{inside} + \frac{q''}{\left(\frac{k}{t}\right)} \tag{3.44}$$

Where $q'' \left[\frac{W}{m^2 K}\right]$ is the heat flux, $k \left[\frac{W}{mK}\right]$ is the thermal conductivity of the material, and $t\ [m]$ is the thickness of the wall. Further, the temperature on the outside must be evaluated against the properties of the material.

3.4.1.3 Tube arrangement

Several tubes may be necessary to process the raw meal effectively. All the factors mentioned earlier must be analyzed to find the optimized solution. The space available and the units footprint, and how to optimize the space available must be considered. Three arrangements are evaluated: 1) Single-tube, 2) several tubes with quadratic spacing, 3) several tubes in a circular spacing. Some arrangements are illustrated in Figure 3.6.
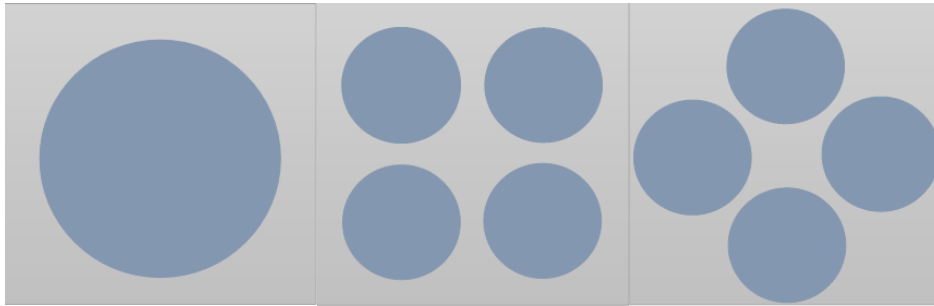
Figure 3.6: Arrangement tubes of a single tube, four tubes arranged quadratically, and four tubes in a circular arrangement.

The arrangement that impacts the total floor footprint can be evaluated by the cross-sectional area of the tube (for the circular arrangement), including spacing for maintenance and refractory, by Equation (3.45).

$$A_{footprint} = \left(\frac{\pi \cdot D^2}{4} + A_{maintanance} + A_{ref}\right) \cdot N_{tubes} \tag{3.45}$$

Where $A_{maintanance}\ [m^2]$ is an extension of the cross-sectional area (evaluated for the needed space for maintenance). $A_{ref}\ [m^2]$ is the required area of the refractory material.

3.4.2 Cyclone

In this thesis, there are two different uses of the cyclone: 1) co-current flow, where the calcined meal and gas is sent from the effluent tubes to a manifold, then further sent to a cyclone, 2) counter-current flow, where the gas exits at the top of the tubes are sent to a manifold, then a cyclone is implemented to separate fine particles from the gas.

Briefly explained in Chapter 3.3, the cyclone's purpose is to separate the dust particles from the gas. One cyclone may not be enough to process the total flow. Thus, several small cyclones may be implemented. In this thesis, only one cyclone is evaluated. Figure 3.7 shows an illustration of a Lapple cyclone with design lengths.
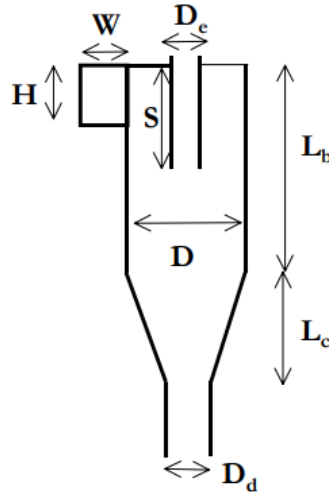
Figure 3.7: Lapple cyclone with design lengths [35]

Three cyclone design values depend on the application: 1) High efficiency, 2) Conventional, 3) High throughput. Design parameters for Lapple cyclones, with these three designs, are listed in Table 3.6. [35]

Table 3.6: Lapple cyclone design parameters [35]

	High Efficiency	Conventional	High throughput
Height of inlet: H/D	$0.5 - 0.44$	0.5	$0.75 - 0.8$
Width of inlet: W/D	$0.2 - 0.21$	0.25	$0.375 - 0.35$
Diameter of exit gas: D_e/D	$0.4 - 0.5$	0.5	0.75
Length of vortex finder: S/D	$1.5 - 1.4$	$2.0 - 1.75$	$1.5 - 1.7$
Length of body: L_b/D	$1.5 - 1.4$	$2.0 - 1.75$	$1.5 - 1.7$
Length of cone: L_c/D	2.5	2	$2.5 - 2$
Diameter of dust outlet: D_d/D	$0.375 - 0.4$	$0.25 - 0.4$	$0.375 - 0.4$

The cyclone must be able to separate fine particles from the gaseous flow, and the efficiency can be calculated with Equation (3.46). [35]

$$\eta(d_p) = \frac{1}{1 + \left(\frac{d_{50}}{d_p}\right)^2} \tag{3.46}$$

Where d_{50} is the cut size, i.e., particles with a diameter (d_p) larger than the cut size diameter has more than 50% removal efficiency. [35]

Equation (3.47) describes the cut size.

$$d_{50} = \sqrt{\frac{9 \cdot \mu_{gas} \cdot W}{2 \cdot \pi \cdot u_i \cdot N \cdot (\rho_p - \rho_{gas})}} \tag{3.47}$$

Where $\mu_{gas}\ [Pa\ s]$ is the dynamic viscosity of the gas, $u_i\ \left[\frac{m}{s}\right]$ is the inlet velocity of the gas, $\rho_{part}\ \left[\frac{kg}{m^3}\right]$ and $\rho_{gas}\ \left[\frac{kg}{m^3}\right]$ are the densities of particles and the gas, respectively. N is the number of rotations the gas flow makes before turning upwards, given by Equation (3.48) and defined by the length of the cyclone body, length of cone, and inlet height. [35]

$$N = \frac{L_b + \frac{1}{2} \cdot L_c}{H} \tag{3.48}$$

An essential characteristic of the cyclone is the pressure drop. The pressure drop is dependent on design dimensions ($H, W, and\ D_e$ Table 3.6), a constant K value in the range of 12-18 (16 recommended), the density of gas, and the inlet velocity. Equation (3.49) describes the pressure drop.[35]

$$\Delta P = \frac{1}{2} \frac{\rho_{gas} \cdot u_i^2 \cdot K \cdot H \cdot W}{D_e^2} \tag{3.49}$$

3.4.3 Heat exchanger

How to design a heat exchanger (HX) is not included in this thesis. However, to estimate the number of HX's needed to cool down the gaseous CO_2 to an appropriate storage temperature, the pressure drop across the HX's, and the cost, Jacob's thesis is used as inspiration. [26]

The area of the HX is calculated applying Equation (3.50).

$$A = \frac{Q}{U \Delta T_{lm}} \tag{3.50}$$

Where $Q\ [MW]$ is the duty, and $U\ \left[\frac{W}{m^2\ K}\right]$ is the overall heat transfer coefficient. The logarithmic mean temperature can be estimated by evaluating the hot and cold streams in and out of the heat exchanger (Equation (3.51)). [26]

$$\Delta T_{lm} = \frac{(T_{h,in} - T_{c,out}) - (T_{h,out} - T_{c,in})}{\ln\left(\frac{T_{h,in} - T_{c,out}}{T_{h,out} - T_{c,in}}\right)} \tag{3.51}$$

The pressure drop across the HX is dependent on several factors. However, according to Jacob, the pressure drop mainly increase due to an increase in fluid velocity and the number of tube passes. Figure 3.8 shows how the pressure drop along the tubes reduces with an increasing number of HX's in parallel. The same behavior is observed in the pressure drop along with the shell (Figure 3.9). [26]

Pressure drop along tube
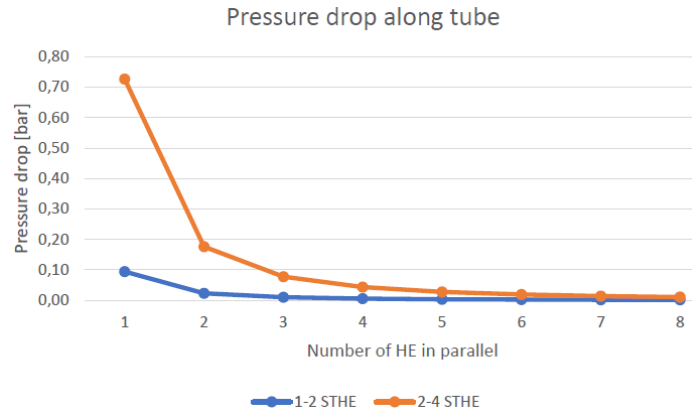
Figure 3.8: Pressure drop along tube with an increasing number of HX's, calculated by Jacob [26]

Pressure drop along shell
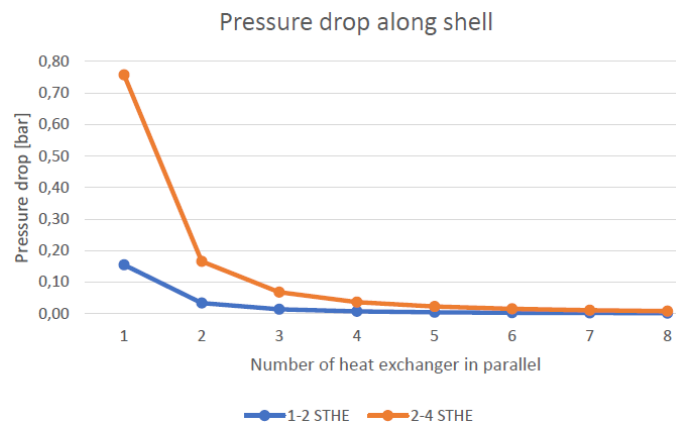
Figure 3.9: Pressure drop along shell with an increasing number of HX's, calculated by Jacob [26]

3.4.4 Fan

The implemented fan must compensate for the pressure drops across the DTR, cyclone, and HX(s). One of the design cases – the co-current flow of particles and gas – requires the fan to do additional work to counteract the natural buoyancy of the CO_2 gas.

The power required to compensate for the pressure drop can be obtained using Equation (3.52), assuming isothermal conditions for the fan. [36]

$$W_{el} = \frac{C_p \cdot T_{in} \cdot \dot{n}_{CO2}}{\eta_{fan}} \cdot \left(\left[\frac{p_{out}}{p_{in}} \right]^{\frac{R}{C_p}} - 1 \right) \tag{3.52}$$

Where $C_p \left[\frac{kJ}{mol\,K} \right]$ is the specific heat capacity of the fluid, $T_{in}\,[K]$ is the inlet temperature, $\dot{n}_{fluid} \left[\frac{mol}{s} \right]$ is the molar flow of the fluid, $\eta_{fan}\,[-]$ is the efficiency of the fan, $p_{out}\,[bar]$ and $p_{in}\,[bar]$ is the outlet and inlet pressures of the fan, respectively, and $R \left[\frac{m^3 Pa}{mol\,K} \right]$ is the universal gas constant.

3.5 Heat transfer in the DTR

As mentioned in Chapter 2.8, the heat transfer from the reactor walls to the raw meal is convection and radiation. How these heat transfer mechanisms affect the particles, the CO_2 gas, relevant parameters, and other factors are described in this chapter.

3.5.1 Nusselt number

The Nusselt number can be determined from an empirical correlation. According to Incropera et al., for a fully developed hydrodynamically and thermally turbulent flow in a smooth circular tube, the empirical correlation of the Nusselt number (Equation 3.53) is recommended. This correlation is based on the Reynolds number (flow regime), the Prandtl number (ratio of momentum and thermal diffusivity), and the dynamic viscosity. [37]

$$Nu_D = 0.027 \cdot Re_D^{\frac{4}{5}} \cdot Pr^{\frac{1}{3}} \cdot \left(\frac{\mu}{\mu_s}\right)^{0.14} \tag{3.53}$$

$$0.7 \leq Pr \leq 16700$$
$$Re_D \geq 10000$$
$$\frac{L}{D} \geq 10$$

All properties except μ_s should be evaluated at the mean temperature of the fluid $T_m\ [K]$. The mean temperature is calculated by determining the maximum temperature the CO_2 gas will be heated, by the contribution of radiative and convective heat transfer [37].

To use Equation (3.53), the Reynolds number must be above 10000, the Prandtl number must be larger or equal to 0.7 and less or equal than 16700, and the ratio of height to the diameter of the tube must be larger or equal to 10. [37]

The Reynolds number can be determined by Equation (3.54), where $\rho_g\ \left[\frac{kg}{m^3}\right]$ is the density of the gas, $u_m\ \left[\frac{m}{s}\right]$ is the mean velocity of the fluid, $D\ [m]$ is the characteristic length of the tube (diameter) and $\mu\ [Pa \cdot s]$ is the dynamic viscosity of the gas:

$$Re_D = \frac{\rho_g \cdot u_m \cdot D}{\mu} \tag{3.54}$$

The Prandtl number for the CO_2 gas is found by Equation (3.55), where $\nu\ \left[\frac{m^2}{s}\right]$ is the kinematic viscosity and $\alpha_{diff}\ \left[\frac{m^2}{s}\right]$ is the thermal diffusivity. [37]

$$Pr = \frac{\nu}{\alpha_{diff}} \tag{3.55}$$

3.5.2 Gas radiation absorption

Gases with a dipole moment and higher polyatomic gases can emit and absorb radiation (transmissivity $\tau < 1$, emissivity $\varepsilon > 0$, absorptivity $\alpha > 0$). Such gas is CO_2, which is the

only gaseous specie within the DTR. To determine the maximum temperature the CO_2 gas can be heated to, the impact of radiation heat on the gas must be determined. [37]

The heat flux between the CO_2 gas and the reactor walls is given by Equation (3.56), where ε_G is the emissivity of the gas, T_G is the temperature of the gas, and α_G is the gas absorptivity [38]:

$$q''_{CO2,rad} = \sigma(\varepsilon_G T_G^4 - \alpha_G T_{sur}^4) \tag{3.56}$$

Further, the characteristic mean beam length, which depends on the enclosure's geometry, needs to be determined. Table 3.7 is a table adapted from Geankoplis' "Transport processes and unit operations." [38]

Table 3.7: Mean beam length for gas radiation, adapted from [38]

Geometry of enclosure	Mean beam length, L
Sphere, diameter D	0.65D
Infinite cylinder, diameter D	0.95D
Cylinder, length = diameter D	0.60D

The total emissivity of CO_2 gas at a total pressure of 1 atm can be found using Figure 3.10. The emissivity is found by multiplying the partial pressure of CO_2 with the characteristic mean beam length $(P_G L)$ and read of the graph at temperature T_G. The absorptivity can be found in a similar matter. However, the temperature T_{sur} and the parameter $(P_G L \frac{T_{sur}}{T_G})$ is replacing $(P_G L)$. Finally, the value read of the y-axis is multiplied with $(\frac{T_G}{T_{sur}})$ to obtain the absorptivity (α_G). [38]
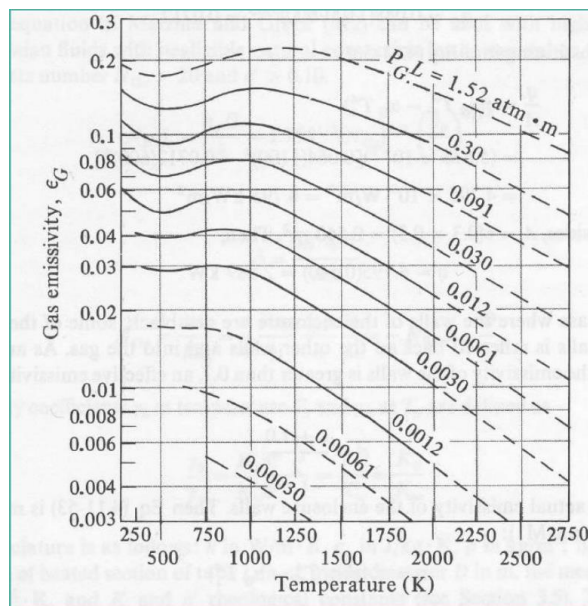
Figure 3.10: Emissivity diagram of CO_2 at a total pressure of 1 atm [38]

3.6 Gas recycling and waste streams

One of the main objectives of this thesis is to assess the need for gas recycling. The reactor does not require any recycling. However, investigating the surrounding system, heated air is sent to cyclone towers to preheat the raw meal, as explained in Chapter 3.3. Throughout the system of interest, there are sources of heat loss:

- Tall tubes may require the use of elevators to process the meal. Thus, heat loss due to transport is expected.
- The hot gas exiting the heat exchanger contains heat with no use, which is expected to be a significant loss.
- Heat losses from the surface of tubes.
- Heat loss through reactor refractory wall.

The waste heat from the HX can be estimated by Equation (3.57).

$$Q_{w,HX} = \dot{m} \cdot C_p \cdot \left(T_{CO2,cooled} - T_\infty\right) \tag{3.57}$$

Where $\dot{m} \left[\frac{kg}{s}\right]$ is the mass flow rate, $C_p \left[\frac{J}{kg\,K}\right]$ is the specific heat capacity of the mass, $T_{CO2,cooled} [K]$ is the outlet temperature of the HX, and $T_\infty [K]$ is the ambient temperature.

A composite calculation approach can be used to determine the heat loss through the refractory of the reactor. Equation (3.58) is the general formula for composite calculations.

$$q'' = U \cdot \Delta T \tag{3.58}$$

Where $U \left[\frac{W}{m^2\,K}\right]$ is the overall heat transfer coefficient calculated with Equation (3.59), and $\Delta T [K]$ is the temperature difference of the inside and outside.

$$U = \frac{1}{\frac{1}{h} + \frac{1}{k/t}} \tag{3.59}$$

The conduction and convective heat fluxes can be expressed with Equation (3.60) and (3.61), respectively.

$$q''_{cond} = \frac{k}{t} \cdot (T_{in} - T_{out}) \tag{3.60}$$

$$q''_{conv} = h \cdot (T_{out} - T_\infty) \tag{3.61}$$

Where $h \left[\frac{W}{m^2 K}\right]$ is the convective heat transfer coefficient, $k \left[\frac{W}{mK}\right]$ is the conductive heat transfer coefficient, and $t [m]$ is the thickness of the wall.

The heat loss can be calculated by Equation (3.62), where the flux is multiplied with the surface area.

$$Q_{refractory} = q'' \cdot A_{surface} \tag{3.62}$$

4 Design calculations

The following chapter determines the sizing of the system, both regarding dimensions and heat transfer. The following questions should be answered:

- How are the residence time and settling velocity influenced by the particle size? – Single particles and the entire PSD.
- What is the ideal heat transfer coefficient from the tube wall to the particle?
- How long do the particles need to be heated to inlet temperature, and how long does it take to heat the particle to the calcination temperature?
- How significant are the losses?
    a. If there are losses, can they be utilized to contribute to the system?
- What are the sizes, dimensions, numbers of equipment that are not already accounted for in sub-objective 2?
- How is the maintenance of equipment/system accounted for (area)?

4.1 Design 1: Counter-current flow of gas and particles – single particle theory

One of the main objects of this study is to determine the height of the DTR – most likely a big contributor to total cost – and ultimately the determinator if the concept is realizable or not. To do so, a calculation procedure (Figure 4.1) is developed. The procedure is based on the energy balances listed in 3.3.2, an overall heat transfer coefficient $U\left[\frac{W}{m^2 K}\right]$, and a design basis feed rate.

The raw meal consist of a wide range of particles diameters, all with different terminal settling velocity. Thus, the mean velocity of the gas should be optimized such that only the smallest particles are affected by the buoyancy of gaseous CO_2

1. Choose a design basis feedrate.

2. Calculate the amount of CO_2 gas produced during calcination. (94% calcination degree)

3. Calculate the heat transfer supplied both in the preheat zone and calcination zone. ($Q = Q_{ph} + Q_{cal}$)

4. Determine the heat transfer area. ($Q = UA\Delta T_{lm}$)

5. Calculate the volumetric flow rate of the CO_2 gas.

6. Choose a mean velocity of the gas based on the terminal settling velocity of the particles.

7. Calculate the cross sectional area required for the DTR based on the volumetric flow rate and the mean velocity.

8. Calculate the diameter of the DTR. ($D = sqrt(4A_{cross}/\pi)$)

9. Calculate the required length of the reactor. ($h_t = A_{heat,transfer}/D$)

10. Calculate the number of tubes necessary to process the meal of interest. ($n_{tubes} = h_t/h_{available}$)

Figure 4.1: Design calculation procedure, height DTR to evaluate the single particle theory of counter-current flow of gas and particles.

4.1.1 Calculation example assuming single particles (no clustering)

Following the steps suggested by the procedure (Figure 4.1), this example aims to determine the height of tubes necessary in the DTR unit to process a chosen feed rate of raw meal. The calculations are done on a mol-basis.

Table 4.1: Design basis values single particle theory procedure

Parameter	Unit	Design basis values
$\dot{m}_{phm,in}$	$\dfrac{t}{h}$	10
w_{CaCO3}	$-$	0.7760
T_{ref}	°C	25 $\left(p_{ref} = 1\,atm\right)$
T_{phm}	°C	658
T_{cal}	°C	900
T_{wall}	°C	1050
U	$\dfrac{W}{m^2\,K}$	250
u_m	$\dfrac{m}{s}$	0.2
H_{cal}	$\dfrac{MJ}{mol_{co2}}$	-0.1584
$H_{other,cal}$	$\dfrac{MJ}{mol_{co2}}$	0.0132
$\eta_{el,heat}$	$-$	98%

(1) The feed rate is given 10 [t/h]:

$$\dot{m}_{phm,in} = 10\,\frac{t}{h} = 2.78\,\frac{kg}{s}$$

$$\dot{n}_{phm,in} = \frac{\dot{m}_{phm,in}}{M_{w,CaCO_3}} = \frac{2.78}{100.0869 \cdot 10^{-3}} = 27.75\,\frac{mol}{s}$$

(2) Applying Equation (3.2) and (3.4) the amount of CO_2 produced from the calcination process can be determined:

$$w_{CO2,prod} = w_{CaCO3} \cdot \frac{M_{CO2}}{M_{CaCO3}} = 0.7760 \cdot \frac{44.01}{100.087} = 0.3412$$

$$\dot{m}_{CO2,phm,100\%} = w_{CO2,prod} \cdot \dot{m}_{phm,in} = 0.3412 \cdot 2.78 = 0.948\,\frac{kg}{s}$$

$$\dot{m}_{CO2,prod} = \dot{m}_{CO2,phm,100\%} \cdot X = 0.948 \cdot 0.94 = 0.891\,\frac{kg}{s}$$

$$\dot{n}_{CO2,prod} = \frac{0.891}{44.01 \cdot 10^{-3}} = 20.24 \, \frac{mol}{s}$$

(3) The heat transfer rate ($\dot{Q}$) from the reactor walls to the meal can be found as the sum of heat transferred in the preheat zone ($\dot{Q}_{ph}$) and the calcination zone ($\dot{Q}_{cal}$). The specific heat capacity of $CaCO_3$ is evaluated at an average temperature of $1052.15 \, K$, ($C_{p,phm} = 133.52 \, \frac{J}{mol \, K}$). The temperatures are given in Table 4.1. From the energy balance equations derived in Chapter 3.3.2, the sensible heat is calculated.

$$\dot{Q}_{ph} = E_{el,supply,ph} = \frac{E_{el,ph}}{\eta_{el,heat}}$$

$$E_{el,ph} = E_{meal,900°C} - E_{phm,in}$$

$$E_{phm,in} = \dot{n}_{phm,in} \cdot C_{p,phm} \cdot (T_{phm} - T_{ref})$$

$$= 27.75 \cdot 133.52 \cdot (931.15 - 298.15)$$

$$E_{phm,in} = 2.34 \, MW$$

$$E_{meal,900°C} = \dot{n}_{phm,in} \cdot C_{p,phm} \cdot (T_{cal} - T_{ref})$$

$$= 27.75 \cdot 133.52 \cdot (1173.15 - 298.15)$$

$$E_{meal,900°C} = 3.24 \, MW$$

$$E_{el,ph} = E_{meal,900°C} - E_{phm,in} = 3.24 - 2.34 = 0.9 \, MW$$

The effective heat transfer rate is calculated using the efficiency of electricity to heat conversion of 98%, listed in Table 4.1.

$$E_{el,supply,ph} = \frac{0.9}{0.98} MW = 0.92 \, MW = \dot{Q}_{ph}$$

The sensible heat for the calcination section ($\dot{Q}_{cal}$), is calculated with the specific heat capacity of the CO_2 gas is evaluated at the calcination temperature of $1173.15 \, K$, ($C_{p,CO2,cal} = 58.9 \, \frac{J}{mol \, K}$).

$$\dot{Q}_{cal} = E_{supply,cal} = \frac{E_{el,cal}}{\eta_{el,heat}}$$

$$E_{el,cal} = E_{out,cal} - E_{meal,900°C} - E_{cal} - E_{other,cal}$$

$$E_{CO2,cal} = \dot{n}_{CO2,prod} \cdot C_{p,CO2,cal} \cdot (T_{cal} - T_{ref})$$

$$= 20.24 \cdot 58.9 \cdot (1173.15 - 298.15)$$

$$E_{CO2,cal} = 1.04 \, MW$$

$$E_{out,cal} = E_{CO2,cal} + E_{meal,900°C} = 1.04 + 3.24 = 4.28 \, MW$$

The energies from the calcination and other meal reactions can be calculated as the product of the molar flow rate of CO_2 and the enthalpies of the calcination and other meal-related reactions, using Equation (3.17) and (3.18):

$H_{cal} = -0.1584 \frac{MJ}{mol_{CO2}}$ and $H_{other} = 0.0132 \frac{MJ}{mol_{CO2}}$.

$E_{cal} = \dot{n}_{CO2,prod} \cdot H_{cal} = 20.24 \cdot (-0,1584) = -3.21 \ MW$

$E_{other,cal} = \dot{n}_{CO2,prod} \cdot H_{other} = 20.24 \cdot 0.0132 = 0.27 \ MW$

The electrical energy in the calcination zone is then:

$E_{el,cal} = 4.28 - 3.24 - (-3.21) - 0.27 = 3.98 \ MW$

$\dot{Q}_{cal} = E_{supply,cal} = \frac{3.98}{0.98} = 4.06 \ MW$

The sensible heat contribution from both preheated and calcination zone is then:

$\dot{Q} = \dot{Q}_{ph} + \dot{Q}_{cal} = 0.92 + 4.06 = 4.98 \ MW$

(4) Calculating the heat transfer area can be done by applying Equation (3.50).

$$\dot{Q} = U \cdot A \cdot \Delta T_{lm} \rightarrow A_{heat} = \frac{\dot{Q}}{U \cdot \Delta T_{lm}}$$

$\Delta T_{lm} \ [K]$ is the logarithmic mean temperature and can be calculated for the preheated section using the operating temperature of the reactor ($T_{wall} = 1323.15 \ K$), the calcination temperature ($T_{cal} = 1173.15 \ K$) and the temperature of the preheated meal ($T_{phm} = 931.15 \ K$).

$$\Delta T_{lm} = \frac{(T_{wall} - T_{cal}) - (T_{wall} - T_{phm})}{\ln\left(\frac{T_{wall} - T_{cal}}{T_{wall} - T_{phm}}\right)}$$

$$\Delta T_{lm} = \frac{(1323.15 - 1173.15) - (1323.15 - 931.15)}{\ln\left(\frac{1323.15 - 1173.15}{1323.15 - 931.15}\right)} = 251.9 \ K$$

$$A_{heat,ph} = \frac{0.92 \cdot 10^6}{250 \cdot 251.9} = 14.6 \ m^2$$

The mean temperature in the calcination section ($T_{m,cal}$) is the average of the operating temperature and the calcination temperature.

$$T_{m,cal} = \frac{T_{wall} + T_{cal}}{2} = 1248.15 \ K$$

By substituting T_{phm} with $T_{m,cal}$, the logarithmic mean temperature for the calcination section becomes:

$\Delta T_{lm,cal} = 108.2 \ K$

The heat transfer area required for calcination is then:

$$A_{heat,cal} = \frac{4.06 \cdot 10^6}{250 \cdot 108.2} = 150.1 \ m^2$$

The total heat transfer area becomes:

$A_{heat} = 14.6 + 150.1 = 164.7 \ [m^2]$

(5) By Equation (3.26) the volumetric flow rate of CO_2 gas can be found by dividing the mass flow rate of CO_2 previously calculated in step (2) by the density of CO_2, which is given by the ideal gas law (Equation (3.27)) evaluated at the calcination temperature.

$$\dot{V}_{CO2} = \frac{\dot{m}_{CO2,prod}}{\rho_{CO2}}$$

The partial pressure of CO_2 (P_{CO2}) is approximately equal to 1 atm. $R = 8.314 \frac{m^3 Pa}{mol\,K}$ is the universal gas constant.

$$\rho_{CO2} = \frac{P_{CO2}M_{w,CO2}}{RT_{cal}}$$

$$\rho_{CO2} = \frac{101325 \cdot 44.01 \cdot 10^{-3}}{8.314 \cdot 1173.15} = 0.457 \frac{kg}{m^3}$$

$$\dot{V}_{CO2} = \frac{0.891}{0.457} = 1.95 \frac{m^3}{s}$$

(6) The chosen mean velocity ($u_m \left[\frac{m}{s}\right]$) of the fluid is based on the terminal settling velocity presented in Chapter 2.3. The higher the velocity, the more particles would be influenced by the buoyancy of gas. However, too low velocity requires a larger cross-sectional area, which ultimately leads to a large diameter of the DTR. In this example $u_m = 0.2 \frac{m}{s}$ is chosen, but this might not be optimal.

(7) The cross-sectional area is found by Equation (3.28) by dividing the volumetric flow rate by the mean velocity of the fluid.

$$A_{cross} = \frac{\dot{V}_{CO2}}{u_m} = \frac{1.95}{0.2} = 9.75\ m^2$$

(8) The diameter of the DTR (cylinder) is then (Equation 3.29)):

$$D = \sqrt{\frac{4 \cdot A_{cross}}{\pi}} = \sqrt{\frac{4 \cdot 9.75}{\pi}} = 3.52\ m$$

(9) If the chosen amount of raw meal were to be processed and calcined in one tube, the total height would then according to Equation (3.31) be:

$$h_t = \frac{A_{heat}}{D\pi} = \frac{146.7}{3.52 \cdot \pi} = 13.26\ m$$

4.2 Design 2: Counter-current flow of gas and particles – applying clustering effect

The calculation procedure (Figure 4.3) assumes cluster formation. In practical systems, clustering is expected. Thus, the effective particle diameter is 500 µm. The terminal settling velocity of this particle size is greater at this effective particle size than the 180 µm particles. As a result, the fluid velocity can be higher, and the diameter of the tube becomes smaller. The layout of the process is shown in Figure 4.2.
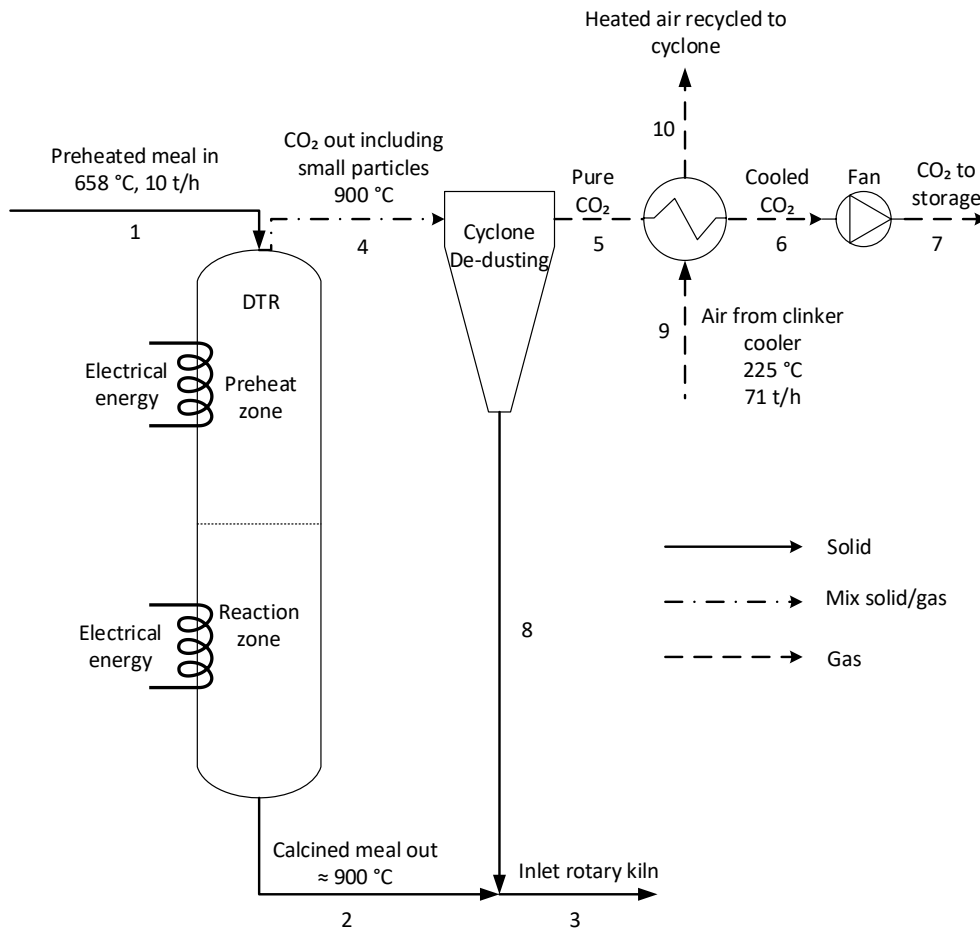
Figure 4.2: Process flow diagram - counter-current flow of gas and particles. The gas exits at the top of the DTR with some fine particles carried by the gas.

1. Choose a design basis feedrate.

2. Calculate the amount of CO_2 gas produced during calcination. (94% calcination degree)

To optimize the system, the fluid velocity can be altered. The chosen fluid velocity will impact the sizing, which ultimately could lead to big differences in cost.

3. Choose a mean velocity based on the settling velocity of the effective particle cluster formation size.

4. Calculate the volumetric flow rate of the CO_2 gas.

5. Calculate the cross-sectional area and tube diameter.

6. Calculate the convective and radiative heat flux to the meal. (Both from reactor walls and gas)

7. Calculate the heat rate which is required to preheat and calcine the meal. (Q_{ph} and Q_{cal})

8. Calculate the heat transfer areas for both sections based on the heat fluxes and heat rates.

9. Calculate the required height of the sections based on the heat transfer area and diameter.

10. Calculate the total height of the reactor.

Figure 4.3: Calculation procedure with an effective particle size of 500 µm to determine the necessary height of one tube.

4.2.1 Calculation example with an effective cluster formation size of 500 µm

Applying the calculation procedure (Figure 4.3), the height of the DTR is calculated. The feed rate of raw meal is $10\frac{t}{h}$. It can be expected that the heat transfer contribution from radiation is much greater than the contribution from convection. Thus, the calculation is based on radiation only. Radiation gas absorption discussed in Chapter 3.5.2 is neglected as the fluid is regarded as non-absorbing for the following example. Appendix F consists of convection contribution and how the absorbing CO_2 gas affects the heat transfer.

Table 4.2: Design basis values cluster formation

Parameter	Unit	Design basis values
$\dot{m}_{phm,in}$	$\dfrac{t}{h}$	10
w_{CaCO3}	–	0.7760
T_{ref}	°C	$25 \ (p_{ref} = 1 \ atm)$
T_{phm}	°C	658
T_{cal}	°C	900
T_{wall}	°C	1050
ε[1]	–	0.9
u_m	$\dfrac{m}{s}$	1.0
Q_{ph}	MW	0.9
Q_{cal}	MW	4.06

(1) Raw meal feed rate:

$$\dot{m}_{phm,in} = 10 \frac{t}{h} = 2.78 \ \frac{kg}{s}$$

$$\dot{n}_{phm,in} = \frac{\dot{m}_{phm,in}}{M_{w,CaCO3}} = \frac{2.78}{100.0869 \cdot 10^{-3}} = 27.75 \ \frac{mol}{s}$$

(2) CO_2 produced (Equation (3.2) and (3.4)):

$$w_{CO2,prod} = w_{CaCO3} \frac{M_{CO2}}{M_{CaCO3}} = 0.7760 \cdot \frac{44.01}{100.087} = 0.3412$$

$$\dot{m}_{CO2,phm,100\%} = w_{CO2,prod} \cdot \dot{m}_{phm,in} = 0.3412 \cdot 2.78 = 0.948 \ \frac{kg}{s}$$

$$\dot{m}_{CO2,prod} = \dot{m}_{CO2,phm,100\%} \cdot X = 0.948 \cdot 0.94 = 0.891 \ \frac{kg}{s}$$

$$\dot{n}_{CO2,prod} = \frac{0.891}{44.01 \cdot 10^{-3}} = 20.24 \ \frac{mol}{s}$$

(3) The mean fluid velocity is chosen based on the terminal settling velocity for an effective particle cluster size of 500 μm.

$$u_m = 1.0 \ \frac{m}{s}$$

---

[1] Emissivity of a grey body [39]

(4) The volumetric flow rate is calculated by Equation (2.6):

$$\dot{V}_{CO2} = \frac{\dot{m}_{CO2,prod}}{\rho_{CO2}} = \frac{0.891}{0.457} = 1.95 \ \frac{m^3}{s}$$

(5) The cross-sectional area and diameter are calculated by Equation (3.28) and (3.29):

$$A_{cross} = \frac{\dot{V}_{CO2}}{u_m} = \frac{1.95}{1.0} = 1.95 \ m^2$$

$$D = \sqrt{\frac{4 \cdot A_{cross}}{\pi}} = \sqrt{\frac{4 \cdot 1.95}{\pi}} = 1.57 \ m$$

(6) The radiative heat flux from the wall to the particles can be calculated using the theory listed in Chapter 2.8.2.

Preheat section:

The radiation heat flux from the reactor walls to the particles is dependent on two temperatures, the operating temperature T_{wall} $[K]$, and the mean temperature of the preheated meal $T_{m,phm}$ $[K]$.

The mean temperature of the raw meal is the sum of calcination temperature $T_{cal} = 1173.15 \ K$ and inlet temperature of the meal $T_{phm} = 931.15 \ K$ divided by two.

$$T_{m,phm} = \frac{T_{cal} + T_{phm}}{2} = 1052.15 \ [K]$$

Radiation heat flux (Equation (2.25)):

$$q''_{ph,wall,part,rad} = h_{rad} \cdot (T_{m,phm} - T_{wall})$$

Where radiation heat transfer coefficient is according to Equation (2.26):

$$h_{rad,ph} \equiv \varepsilon \cdot \sigma \cdot (T_{m,phm} + T_{wall}) \cdot (T^2_{m,phm} + T^2_{wall})$$

The emissivity $\varepsilon = 0.9$, $\sigma = 5.67 \cdot 10^{-8} \ \frac{W}{m^2 K^4}$, [39]

$$h_{rad,ph} = 0.9 \cdot 5.67 \cdot 10^{-5} \cdot (1052.15 + 1323.15) \cdot ((1052.15^2) + (1323.15^2))$$

$$h_{rad,ph} = 346.4 \ \frac{W}{m^2 K^4}$$

$$q''_{ph,wall,part,rad} = 346.4 \cdot (1052.15 - 1323.15) = -93874 \ \frac{W}{m^2}$$

Calcination section:

In this section of the DTR, the temperature of the raw meal is constant at calcination temperature T_{cal} $[K]$. Thus, the radiation heat flux is given:

$$q''_{cal,wall,part,rad} = h_{rad,cal} \cdot (T_{cal} - T_{wall})$$

$$h_{rad,cal} = 0.9 \cdot 5.67 \cdot 10^{-5} \cdot (1173.15 + 1323.15) \cdot ((1173.15)^2 + (1323.15)^2)$$

$$h_{rad,cal} = 398.3 \ \frac{W}{m^2 \ K}$$

$$q''_{cal,wall,part,rad} = 398.3 \cdot (1173.15 - 1323.15) = -59745 \, \frac{W}{m^2}$$

(7) The next step is to calculate the heat rate (Q_{ph} and Q_{cal}). Both calculated in Example 4.1.1 for the same feed rate of the raw meal (10 t/h):

$$Q_{ph} = 0.9 \, MW$$

$$Q_{cal} = 4.06 \, MW$$

(8) The heat transfer area is determined by dividing the heat flux by the respective heat rate for each section.

Preheating section:

Equation (3.30):

$$A_{heat,ph} = \frac{0.9 \cdot 10^6 \, W}{93874 \, \dfrac{W}{m^2}} = 9.59 \, m^2$$

Calcination section:

(Equation (3.30))

$$A_{heat,cal} = \frac{4.06 \cdot 10^6 \, W}{59745 \, \dfrac{W}{m^2}} = 67.96 \, m^2$$

(9) Each respective height of section is determined with Equation (3.31) by dividing the heat transfer area by the diameter and π.

$$h_{ph} = \frac{A_{heat,ph}}{\pi \cdot D} = \frac{9.59}{\pi \cdot 1.57} = 1.9 \, m$$

$$h_{cal} = \frac{A_{heat,cal}}{\pi \cdot D} = \frac{67.96}{\pi \cdot 1.57} = 13.8 \, m$$

The total required height to process the chosen feed rate:

$$h_t = 1.9 + 13.8 = 15.7 \, m$$

4.3 Design 3: Co-current flow of gas and particles

By forcing the fluid flow of CO_2 gas downwards by implementing a fan, as shown in Figure 4.4, the particles are not affected by the upwards motion of the gas. Thus, all particles will exit the DTR at the bottom exit. The systems arrangement makes it possible to calcine particles of fine size ($0.2 – 20 \, \mu m$), which reduces the sizing of the DTR, and ultimately the cost.
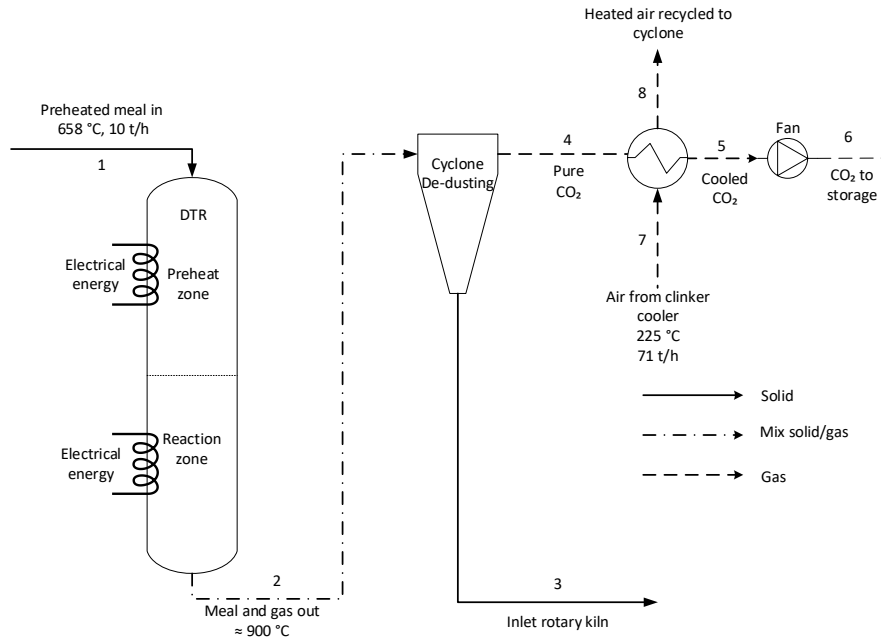
Figure 4.4: Process flow diagram: co-current flow of gas and particles. The gas exits with the calcined meal at the effluent of the reactor. The fluid is sent to a manifold before entering the cyclone (manifold is not included in process flow diagram)

4.3.1 Calculation example with Co-current flow of gas and particles

As stated in Chapter 4.2, the exact heat transfer mechanisms apply, radiation only, neglecting the heat transfer of convection. However, the exit processing of the particles and gas changes. The fluid flow and the particles are assumed to have equal velocity, which can be altered by the design of the fan. This design arrangement forces the gas downwards with the particles, and the troublesome buoyancy effect on the fine small particles is removed. Design values for further calculations in this subchapter are listed in Table 4.3.

Table 4.3: Design basis values - Co-current flow of gas and particles

Parameter	Unit	Design basis values
$\dot{m}_{phm,in}$	t/h	10
w_{CaCO3}	$-$	0.7760
T_{ref}	$°C$	$25\ (p_{ref} = 1\ atm)$
T_{phm}	$°C$	658
T_{cal}	$°C$	900
T_{wall}	$°C$	1050
ε	$-$	0.9
u_m	m/s	2.0
Q_{ph}	MW	0.9
Q_{cal}	MW	4.06

Applying the calculation procedure presented in Chapter 4.2, it is shown in Table 4.4 that the same heat transfer occurs. However, since there is more freedom to choose a fluid velocity, the dimensions of the reactor are different based on the selected fluid velocity.

Table 4.4: Calculated values co-current flow of gas and particles.

Calculated parameter	Unit	Value
$\dot{V}_{CO2}$	$\dfrac{m^3}{s}$	1.95
A_{cross}	m^2	0.97
D	m	1.11
$q''_{ph,wall,part,rad}$	$\dfrac{W}{m^2}$	93874
$q''_{cal,wall,part,rad}$	$\dfrac{W}{m^2}$	59745
$A_{heat,ph}$	m^2	9.59
$A_{heat,cal}$	m^2	67.96
L_{ph}	m	2.87
L_{cal}	m	20.00

4.4 Residence time and tube height

The residence time and the terminal settling velocity are used to determine the necessary tube height. Table 4.5 includes design basis values.

Table 4.5: Design basis values - tube height based on residence time

Parameter	Unit	Design basis values
u_m	$\dfrac{m}{s}$	0.5
v_{tp}	$\dfrac{m}{s}$	1.2
$t_{res,94}$	s	35
$t_{res,90}$	s	22

The terminal settling velocity is different from the counter-current and co-current design cases. The counter-current settling velocity becomes:

$$v_{t,counter} = v_{tp} - u_m$$

$$v_{t,counter} = 1.2 - 0.5 = 0.7\frac{m}{s}$$

While the co-current becomes:

$$v_{t,co} = v_{tp} + u_m$$

$$v_{t,co} = 1.2 + 0.5 = 1.7\frac{m}{s}$$

According to the required residence time of the particles, i.e., to achieve 94 % or 90 % calcination, the required height of the tubes for the co – and counter-current designs is calculated, rearranging Equation (2.19):

$$h_{req,co,94} = v_t \cdot t_{res,94} = 1.7 \cdot 35 = 59.5 \, m$$

$$h_{req,co,90} = v_t \cdot t_{res,90} = 1.7 \cdot 22 = 37.4 \, m$$

$$h_{req,counter,94} = v_t \cdot t_{res,94} = 0.7 \cdot 35 = 24.5 \, m$$

$$h_{req,counter,90} = v_t \cdot t_{res,90} = 0.7 \cdot 22 = 15.4 \, m$$

4.5 Pressure drop calculations

The pressure drop of the DTR and the adjacent units needs to be evaluated to calculate the required power of the fan. Pressure drop calculations across the cyclone are based on equations from Chapter 3.4.2, while the pressure drop for the HX is based on the results calculated by Jacob, discussed in Chapter 3.4.3 [26].

4.5.1 DTR

The large volume of the DTR and the low fluid velocity does not increase the unit's pressure drop. However, the elevation does, and the pressure drop can be calculated by applying Equation (3.32) in Chapter 3.4.1. The pressure drop is calculated using the design basis values listed in Table 4.6.

Table 4.6: Design basis values to calculate pressure drop, DTR.

Parameter	Unit	Design basis values
ρ_{CO2}	$\frac{kg}{m^3}$	0.457
g	$\frac{m}{s^2}$	9.807
Δh	m	20

$$\Delta P_{DTR} = \rho \cdot g \cdot \Delta h$$

$$\Delta P_{DTR} = 0.457 \cdot 9.807 \cdot 20 = 89.64 \, Pa$$

4.5.2 Cyclone

Based on the dimensions of the cyclone discussed in Chapter 3.4.2, the diameter can be determined by choosing a maximum allowed pressure drop. Table 4.7 consists of design basis values for the pressure calculation.

Table 4.7: Cyclone design values.

Parameter	Unit	Design basis values
ΔP	Pa	1000
K[2]	–	16
ρ_g	$\dfrac{kg}{m^3}$	0.457
$\dot{V}_{fluid}$	$\dfrac{m^3}{s}$	41
ρ_{part}	$\dfrac{kg}{m^3}$	2711
μ_{fluid}	$Pa \cdot s$	$4.65 \cdot 10^{-5}$
D_p	μm	30

By trial and error, the suggested diameter of the tube (from the manifold to cyclone) must be 1.76 meters in diameter to achieve the desired pressure drop. The following values have been calculated.

The inlet velocity:

$$u_i = \frac{\dot{V}_{fluid}}{\pi \cdot \left(\frac{D}{2}\right)^2} = \frac{41}{\pi \cdot \left(\frac{1.76}{2}\right)^2} = 16.85 \frac{m}{s}$$

The inlet height H $[m]$, width W $[m]$ And the diameter of the exit gas D_e $[m]$ is calculated using the following relations, tabulated in Table 3.6:

$$H = 0.47 \cdot D = 0.47 \cdot 1.76 = 0.83 \; m$$

$$W = 0.205 \cdot D = 0.205 \cdot 1.76 = 0.36 \; m$$

$$D_e = 0.45 \cdot D = 0.45 \cdot 1.76 = 0.79 \; m$$

The pressure drop across the cyclone becomes by Equation (3.49):

$$\Delta P = \frac{1}{2} \frac{\rho_{gas} \cdot u_i^2 \cdot K \cdot H \cdot W}{D_e^2} = \frac{1}{2} \frac{0.457 \cdot 16.85^2 \cdot 16 \cdot 0.83 \cdot 0.36}{0.79^2} = 988 \; Pa$$

4.5.2.1   Cyclone efficiency

The efficiency of the cyclone can be described as a function of particle size and calculated by Equation (3.46).

$$\eta(D_p) = \frac{1}{1 + \left(\frac{D_{50}}{D_p}\right)^2}$$

Where the cut size (D_{50} $[\mu m]$) is calculated using Equation (3.47).

---

[2] Suggested value of 16 [35]

$$D_{50} = \sqrt{\frac{9 \cdot \mu_{gas} \cdot W}{2 \cdot \pi \cdot u_i \cdot N \cdot (\rho_{part} - \rho_{gas})}}$$

Where N is the number of rotations the gas flow makes before returning upwards and found by Equation (3.48).

$$N = \frac{L_b + \frac{1}{2}L_c}{H}$$

Referring to Table 3.6, the dimensions L_b and L_c are:

$L_b = 1.45 \cdot D = 1.45 \cdot 1.76 = 2.56 \, m$

$L_c = 2.5 \cdot D = 2.5 \cdot 1.76 = 4.4 \, m$

Further:

$$N = \frac{2.56 + \frac{1}{2} \cdot 4.4}{0.83} = 5.75$$

And the cut size:

$$D_{50} = \sqrt{\frac{9 \cdot 4.65 \cdot 10^{-5} \cdot 0.36}{2 \cdot \pi \cdot 16.85 \cdot 5.75 \cdot (2711 - 0.457)}} = 9.55 \, \mu m$$

Efficiency for a particle size of 30µm:

$$\eta_{cyclone}(D_p = 30\mu m) = \frac{1}{1 + \left(\frac{9.55}{30}\right)^2} = 0.9079 = 90.79\%$$

4.5.3 Heat exchanger

The pressure drop across the shell side of the HX's is collected from the results of Jacob's master thesis, as discussed in Chapter 3.4.3. Jacobs' system basis is quite similar to the basis of the design in this thesis. Thus, the required work of the DTR is expected to be like Jacobs's results. [26]

Two 1-2 STHE are chosen, which gives a pressure drop of 0.18 bar over the shell. [26]

4.6 Reactor wall thickness

Based on Chapter 3.4.1.1, the thickness of the reactor wall can be estimated. In the following calculation example, an assumed material with good heat transfer and mechanical properties is chosen. To find the optimized thickness w.r.t. stresses, a trial-and-error approach is applied. The outer diameter is based on the results obtained from Chapter 4.3.1. Design basis values for the stress analysis are listed in Table 4.8.

Table 4.8: Design basis values - wall thickness.

Parameter	Unit	Design basis values
$\sigma_{tensile,max}$[3]	MPa	20
$\sigma_{yield,max}$	MPa	20
D_o	m	1.11
D_i	m	1.10
ρ_{mat}	$\dfrac{kg}{m^3}$	8193
g	$\dfrac{m}{s^2}$	9.807
h	m	30
f_{safety}	$-$	1.3
v_{air}[4]	$\dfrac{m}{s}$	40
C_d	$-$	0.8
T_{air}	$[K]$	293.15
P	Pa	101325
M_{air}	g/mol	28.97
R	$\dfrac{m^3 Pa}{K\ mol}$	8.314
I	m^4	0.00548
q''	$\dfrac{W}{m^2}$	93874
k	$\dfrac{W}{mK}$	30

4.6.1 Stress analysis

First, the axial stress by the weight of the cylinder is calculated by Equation (3.33).

$$\sigma_{dead,load} = \frac{F_{dead,load}}{A_{cross}}$$

---

[3] Inconel 718 is the inspiration of the maximum allowed tensile and yield stresses. The material described in this chapter is not Inconel 718. [34]

[4] The velocity of the wind is based on Figure 3.4.

The cross-sectional area of a hollow cylinder can be calculated by applying Equation (3.34) and the chosen inner and outer diameter listed in Table 4.8.

$$A_{cross} = \frac{\pi}{4} \cdot (D_o^2 - D_i^2)$$

$$A_{cross} = \frac{\pi}{4} \cdot (1.11^2 - 1.10^2) = 0.01736 \; m$$

The force of the dead load is the product of the mass multiplied by the gravitational acceleration (Equation (3.35)).

$$F_{dead,load} = m \cdot g$$

The mass of the cylinder is found with Equation (3.36) by the density of chosen material, multiplied by the volume of the shell.

$$m = \rho_{mat} \cdot V$$

Further, Equation (3.37) is used to calculate the volume.

$$V = A_{cross} \cdot h = \frac{\pi}{4} \cdot (D_o^2 - D_i^2) \cdot h$$

$$V = A_{cross} \cdot h = 0.01736 \cdot 30 = 0.521 \; m^3$$

The mass becomes:

$$m = 8193 \cdot 0.521 = 4266 \; kg$$

And the force of the dead load:

$$F_{dead,load} = 4266 \cdot 9.807 = 41839 \; N$$

The axial stress becomes:

$$\sigma_{dead,load} = \frac{F_{dead,load}}{A_{cross}} = \frac{41839}{0.01736} = 2410462 \; Pa = 2.41 \; MPa$$

The next step is to evaluate the bending of the cylinder due to wind force with Equation (3.38).

$$F_{wind} = \frac{C_D \cdot \rho_{air} \cdot A_{surface} \cdot v_{air}^2}{2}$$

The density of air is calculated using the ideal gas law (Equation (3.27)):

$$\rho_{air} = \frac{P \cdot M}{R \cdot T_{air}} = \frac{101325 \cdot 28.97 \cdot 10^{-3}}{8.314 \cdot 293.15} = 1.204 \, \frac{kg}{m^3}$$

It is assumed that the surface area affected by the wind is half the cylinder, thus Equation (3.39) can be utilized.

$$A_{surface} = \pi \cdot \left(\frac{D_o}{2}\right) \cdot h = \pi \cdot \left(\frac{1.11}{2}\right) \cdot 30 = 52.3 m^2$$

The wind force becomes:

$$F_{wind} = \frac{C_D \cdot \rho_{air} \cdot A_{surface} \cdot v_{air}^2}{2} = \frac{0.8 \cdot 1.204 \cdot 52.3 \cdot 40^2}{2} = 40319 \; N$$

The evenly distributed load is found with Equation (3.40), across the height of the cylinder:

$$q_{wind} = \frac{F_{wind}}{h} = \frac{40319}{30} = 1344 \frac{N}{m}$$

The bending moment can be calculated with Equation (3.41) by evaluating the height of the tube and the wind force acting on the surface.

$$M_b = \frac{q_{wind} \cdot h^2}{8} = \frac{1344 \cdot 30^2}{8} = 151196 \; Nm$$

Finally, the shear stress by the wind according to Equation (3.42) becomes:

$$\sigma_b = \frac{M_b}{I} = \frac{151196}{0.00548} = 27.58 \; MPa$$

The allowable stress is given by Equation (3.44).

$$\sigma_{b,max} = f_{safety} \cdot \sigma_{yield,max} = 1.3 \cdot 27.58 = 35.86 \; MPa$$

The impact of the wind is far greater than the dead load of the vessel. Thus, this force is evaluated when deciding on an appropriate thickness of the reactor wall. By trial-and-error, the minimum thickness is found and shown in Table 4.9. The calculation sheet is included in Appendix G.

Table 4.9: Thickness results.

Thickness	Shear stress	
10 mm	74.19 MPa	Failure
12 mm	61.20 MPa	Failure
25 mm	30.29 MPa	Below critical stress, not optimum
18 mm	41.67 MPa	Failure
20 mm	37.60 MPa	Failure
21 mm	35.86 MPa	Ok!

The calculated thickness can be used to determine the required outside temperature of the reactor with Equation (3.44). This temperature must be considered when deciding on material. The highest heat flux is apparent in the preheating section of the DTR. Thus, this is used in this calculation.

$$T_{outside} = T_{inside} + \frac{q''}{\left(\frac{k}{t}\right)} = 1323.15 + \frac{93874}{\left(\frac{30}{21 \cdot 10^{-3}}\right)} = 1389 \; [K]$$

4.7 Waste stream calculations

To calculate the heat losses of interest, the design basis values in Table 4.10 are used.

Table 4.10: Design basis values - heat loss.

Parameter	Unit	Design basis values
T_{wall}	K	1373.15
T_∞	K	293.15
$T_{CO2,cooled}$	K	616
k	$\dfrac{W}{m\,K}$	0.2
h_{out}	$\dfrac{W}{m^2\,K}$	5
t	m	0.2
$A_{surface}$	m^2	250
$\dot{m}_{CO2}$	$\dfrac{kg}{s}$	18.3
$C_{p,CO2}$	$\dfrac{kJ}{kg\,K}$	1.086

Heat loss through refractory:

The heat flux through the refractory to the ambient can be expressed by Equation (3.58):

$$q'' = U \cdot (T_{wall} - T_{out})$$

Conductive and convective heat fluxes given by Equation (3.59) and (3.60):

$$q''_{cond} = \frac{k}{t} \cdot (T_{wall} - T_{out})$$

$$q''_{conv} = h_{out} \cdot (T_{out} - T_\infty)$$

The heat fluxes must be equal.

$$q''_{cond} = q''_{conv} = q''$$

Thus:

$$\frac{q''}{\frac{k}{t}}(T_{wall} - T_{out}) = \frac{q''}{h_{out}}(T_{out} - T_\infty) \rightarrow \frac{q''}{\frac{k}{t}} + \frac{q''}{h} = T_{wall} - T_{out} + T_{out} - T_\infty$$

This leads to:

$$q'' = \frac{T_{wall} - T_\infty}{\frac{1}{k/t} + \frac{1}{h}} = \frac{1373.15 - 293.15}{\frac{1}{0.2/0.2} + \frac{1}{5}} = 895.83 \, \frac{W}{m^2}$$

The heat loss is found by Equation (3.62), multiplying the flux by the area of the cylinder (neglecting top and bottom).

$$Q = q'' \cdot A = 895.83 \cdot 250 = 223957.5 \, W = 0.224 \, MW$$

Heat loss from gas exiting HX:

The heat loss can be found by Equation (3.57):

$$Q_{HX} = \dot{m}_{CO2} \cdot C_{P,CO2} \cdot \left(T_{CO2,cooled} - T_\infty \right)$$

$$Q_{HX} = 18.3 \cdot 1.086 \cdot 10^3 \cdot (616 - 293.15) = 6416256 \, W = 6.42 \, MW$$

5 Simulations of DTR design

The cases described in Chapter 4 are implemented to Python 3.8 to be simulated. Two key parameters are expected to have the most significant impact on the DTR design: 1) Fluid velocity, 2) Operating temperature. The optimized diameter, height, and the number of tubes necessary to process the raw meal can be determined by changing these key parameters.

The following questions should be answered in this chapter:

- What are the interest for each case?
- What is the purpose of each case?
- Which key parameters are of interest to vary?
- What are the new resulting outputs?
- Which parameter influences the system most?

5.1 Simulation cases

To optimize the design of the DTR, several cases with varying key parameters are simulated in Python 3.8. The simulation programs are attached to Appendices J and K. All the simulated cases are based on the same design basis values, which are also included in Appendices J and K.

5.2 The effect of fluid velocity

The first parameter expected to have the most significant influence on the system is the fluid velocity. Included in Appendix K is the code used to simulate the effext of fluid velocity. The diameter is a function of fluid velocity, and by reducing/increasing this parameter, the diameter is expected to change accordingly. First, the cases are simulated by keeping the operating temperature constant.

Table 5.1 shows the key parameters of each simulation case.

Table 5.1: Simulation cases varying fluid velocity.

Case	Fluid velocity [m/s]	Operating temperature [K]	Available height [m]
Case **1**	0.5	1323.15	30
Case **2**	1.0	1323.15	30
Case **3**	2.0	1323.15	30

This simulation aims to determine the optimum height and number of tubes by varying only the fluid velocity. Further, in Chapter 7, the simulation results are discussed and evaluated against cost estimates to find the most viable designs.

5.3 The effect of temperature

To evaluate the effect of temperature, the fluid velocity is kept constant, while a set of selected temperatures and the effect of these temperatures are simulated (Appendix L). The cases are listed in Table 5.2.

Table 5.2: Simulation cases with varying temperature.

Case	Fluid velocity [m/s]	Operating temperature [K]	Available height [m]
Case 4	1.0	1500.00	30
Case 5	1.0	1400.00	30
Case 6	1.0	1323.15	30
Case 7	1.0	1200.00	30

The expected outcome of the temperature-based simulation is that the height is drastically reduced by implementing a higher temperature. Accordingly, the height is reduced by lowering the temperature. Thus, higher temperature increases the calcination rate of the particles, leading to a reduced requirement in size and number of heating tubes.

6 Cost estimation

One of the primary objectives of this thesis is to estimate the economic feasibility of the electrically heated DTR implemented in an existing cement plant. The cost estimation aims to establish an overview of the total cost and the uncertainties of the DTR project.

The following questions need to be answered:

- Which elements are contributing to CAPEX?
- Which elements are contributing to OPEX?
- How should the avoided CO_2 be calculated?
- Which estimation methods can be applied?
- What are the most important factors affecting the cost?

6.1 Theory

Several methods of estimating costs for the DTR can be implemented based on the information at hand. In this thesis, two factor methods are applied, the detailed factor estimation and the capacity factor method. Further, time adjustment, net present value, and cost per captured unit CO_2 are discussed.

6.1.1 Detailed factor estimation

This estimation method relies on a factor that accounts for the cost of equipment and the non-equipment items, such as piping, electrical power, etc. The detailed factor estimation considers direct cost, engineering cost, administrative cost, and cost of material types and different sizes. The method is used to estimate the total capital cost of any equipment unit in a plant, such as the DTR. [40]

N. H. Eldrup at USN Porsgrunn created a detailed factor table (Table 3.1) valid for 2020. The equipment cost is given in carbon steel. If a material other than carbon steel is used, the equipment cost can be calculated using a material factor. [41]

The installation cost factor for any material can be determined using Equation (6.1). Where, f_{tc} is the total installed cost factor, $f_{tc,cs}$ is the total cost factor using carbon steel, $f_{eq,cs}$ is the equipment cost factor using carbon steel, $f_{pi,cs}$ is the piping cost factor using carbon steel and f_{mat} is the material cost factor.

$$f_{tc} = f_{tc,cs} - f_{eq,cs} + \left(f_{eq,cs} \cdot f_{mat}\right) - f_{pi,cs} + \left(f_{pi,cs} \cdot f_{mat}\right) \qquad (6.1)$$

Table 6.1: Detailed factor estimation table [40]

| Equipment cost (CS) in kEUR from: | 0 | 10 | 20 | 40 | 80 | 160 | 320 | 640 | 1280 | 2560 | 5120 |
to:	10	20	40	80	160	320	640	1280	2560	5120	10240
Equipment costs	1,00	1,00	1,00	1,00	1,00	1,00	1,00	1,00	1,00	1,00	1,00
Erection cost	0,94	0,64	0,50	0,39	0,31	0,24	0,19	0,15	0,12	0,09	0,07
Piping incl. Erection	0,45	0,31	0,24	0,19	0,15	0,12	0,10	0,08	0,06	0,05	0,04
Electro (equip & erection)	1,20	0,90	0,75	0,63	0,53	0,44	0,37	0,31	0,26	0,22	0,19
Instrument (equip. & erection)	0,60	0,41	0,33	0,26	0,20	0,16	0,13	0,10	0,08	0,06	0,05
Ground work	0,71	0,51	0,42	0,34	0,28	0,23	0,19	0,15	0,13	0,10	0,09
Steel & concrete	1,30	0,96	0,80	0,66	0,55	0,46	0,38	0,32	0,26	0,22	0,18
Insulation	0,28	0,18	0,14	0,11	0,08	0,06	0,05	0,04	0,03	0,02	0,02
Direct costs	6,48	4,92	4,18	3,58	3,10	2,71	2,40	2,15	1,94	1,77	1,63
	-	-	-	-	-	-	-	-	-	-	-
Engineering process	0,44	0,27	0,22	0,18	0,15	0,12	0,10	0,09	0,07	0,06	0,05
Engineering mechanical	0,47	0,27	0,20	0,15	0,11	0,09	0,07	0,05	0,04	0,03	0,03
Engineering piping	0,13	0,09	0,07	0,06	0,05	0,04	0,03	0,02	0,02	0,01	0,01
Engineering el.	0,44	0,27	0,21	0,17	0,14	0,11	0,09	0,08	0,07	0,06	0,05
Engineering instr.	0,32	0,17	0,12	0,09	0,07	0,05	0,04	0,03	0,02	0,02	0,01
Engineering ground	0,16	0,10	0,07	0,06	0,04	0,04	0,03	0,02	0,02	0,02	0,01
Engineering steel & concrete	0,25	0,16	0,13	0,10	0,08	0,07	0,06	0,05	0,04	0,03	0,03
Engineering insulation	0,07	0,04	0,03	0,02	0,01	0,01	0,01	0,01	0,00	0,00	0,00
Engineering	2,30	1,38	1,05	0,82	0,65	0,53	0,43	0,35	0,29	0,24	0,20
	-	-	-	-	-	-	-	-	-	-	-
Procurement	1,15	0,38	0,48	0,48	0,24	0,12	0,06	0,03	0,01	0,01	0,00
Project control	0,11	0,07	0,05	0,04	0,03	0,03	0,02	0,02	0,01	0,01	0,01
Site management	0,32	0,25	0,21	0,18	0,16	0,14	0,12	0,11	0,10	0,09	0,08
Project management	0,39	0,27	0,23	0,19	0,16	0,13	0,12	0,10	0,09	0,08	0,07
Administration	1,98	0,96	0,97	0,89	0,59	0,42	0,32	0,26	0,22	0,19	0,17
	-	-	-	-	-	-	-	-	-	-	-
Commissioning	0,28	0,17	0,13	0,10	0,08	0,06	0,05	0,04	0,03	0,02	0,02
	-	-	-	-	-	-	-	-	-	-	-
Identified costs	11,04	7,44	6,33	5,40	4,42	3,72	3,19	2,79	2,47	2,22	2,01
	-	-	-	-	-	-	-	-	-	-	-
Contingency	2,21	1,49	1,27	1,08	0,88	0,74	0,64	0,56	0,49	0,44	0,40
	-	-	-	-	-	-	-	-	-	-	-
Installation factor 2020	13,24	8,93	7,60	6,48	5,30	4,46	3,83	3,34	2,96	2,66	2,42

Solid handling equipment Installation factors

Adjustment for materials:

SS316 Welded: Equipment and piping factors multiplies with 1,75

SS316 rotating: Equipment and piping factors multiplies with 1,30

Exotic Welded: Equipment and piping factors multiplies with 2,50

Exotic Rotating: Equipment and piping factors multiplies with 1,75

Porsgrunn September 2020 Nils Henrik Eldrup

6.1.2 Capacity factor method

This method utilizes information about a similar existing plant or equipment unit to determine new equipment costs. The accuracy of the method is dependent on the similarities of the equipment compared. The method is an order of magnitude estimate and given by Equation (6.2). [40, 42]

$$C_B = C_A \left(\frac{C_B}{C_A}\right)^e \tag{6.2}$$

Where C_B is the cost of the new equipment, C_A is the cost of old equipment and e is an exponent in the range $0.4 - 0.9$. An average value of $e = 0.65$ is used for many process facilities. [42, 43]
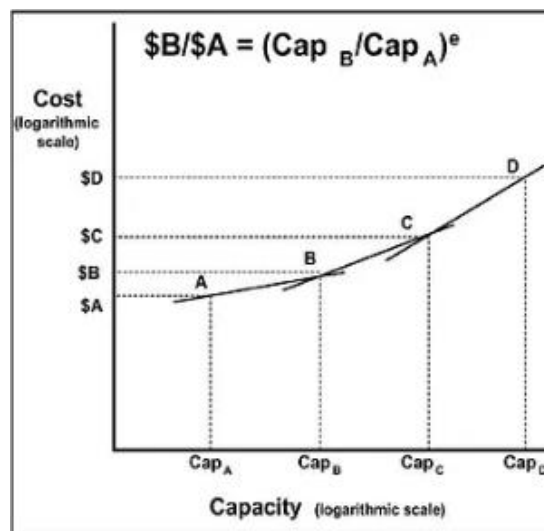
Figure 6.1: Capacity factor illustration [42]

6.1.3 Net present value

The net present value (NPV) is used to analyze the profitability of a project, thus, applied in capital budgeting. By evaluating the difference in present value of cash inflows and outflows over a period of time, the NPV can be determined. [43]

The present value of money is given by Equation (6.3), where PV is the present value (discounted value), F_N is the future value, i is the interest rate (based on the length of one period), and N is the number of interest periods.

$$PV = F_N \frac{1}{(1+i)^{N_i}} \tag{6.3}$$

Table 6.2: Discount factors $\frac{1}{(1+i)^{N_i}}$ vs. number of years. [44]

		2.5	5.0	7.5	10.0	12.5	15.0	17.5	20.0	22.5	25.0	27.5	30.0
		Discount rate (% per year)											
	0	1.00	1.00	1.00	1.00	1.00	1.00	1.00	1.00	1.00	1.00	1.00	1.00
	1	0.98	0.95	0.93	0.91	0.89	0.87	0.85	0.83	0.82	0.80	0.78	0.77
	2	0.95	0.91	0.87	0.83	0.79	0.76	0.72	0.69	0.67	0.64	0.62	0.59
	3	0.93	0.86	0.80	0.75	0.70	0.66	0.62	0.58	0.54	0.51	0.48	0.46
	4	0.91	0.82	0.75	0.68	0.62	0.57	0.52	0.48	0.44	0.41	0.38	0.35
	5	0.88	0.78	0.70	0.62	0.55	0.50	0.45	0.40	0.36	0.33	0.30	0.27
	6	0.86	0.75	0.65	0.56	0.49	0.43	0.38	0.33	0.30	0.26	0.23	0.21
	7	0.84	0.71	0.60	0.51	0.44	0.38	0.32	0.28	0.24	0.21	0.18	0.16
No. of years	8	0.82	0.68	0.56	0.47	0.39	0.33	0.28	0.23	0.20	0.17	0.14	0.12
	9	0.80	0.64	0.52	0.42	0.35	0.28	0.23	0.19	0.16	0.13	0.11	0.09
	10	0.78	0.61	0.49	0.39	0.31	0.25	0.20	0.16	0.13	0.11	0.09	0.07
	11	0.76	0.58	0.45	0.35	0.27	0.21	0.17	0.13	0.11	0.09	0.07	0.06
	12	0.74	0.56	0.42	0.32	0.24	0.19	0.14	0.11	0.09	0.07	0.05	0.04
	13	0.73	0.53	0.39	0.29	0.22	0.16	0.12	0.09	0.07	0.05	0.04	0.03
	14	0.71	0.51	0.36	0.26	0.19	0.14	0.10	0.08	0.06	0.04	0.03	0.03
	15	0.69	0.48	0.34	0.24	0.17	0.12	0.09	0.06	0.05	0.04	0.03	0.02
	16	0.67	0.46	0.31	0.22	0.15	0.11	0.08	0.05	0.04	0.03	0.02	0.02
	17	0.66	0.44	0.29	0.20	0.14	0.09	0.06	0.05	0.03	0.02	0.02	0.01
	18	0.64	0.42	0.27	0.18	0.12	0.08	0.05	0.04	0.03	0.02	0.01	0.01
	19	0.63	0.40	0.25	0.16	0.11	0.07	0.05	0.03	0.02	0.01	0.01	0.01
	20	0.61	0.38	0.24	0.15	0.09	0.06	0.04	0.03	0.02	0.01	0.01	0.01
	21	0.60	0.36	0.22	0.14	0.08	0.05	0.03	0.02	0.01	0.01	0.01	0.00
	22	0.58	0.34	0.20	0.12	0.07	0.05	0.03	0.02	0.01	0.01	0.00	0.00
	23	0.57	0.33	0.19	0.11	0.07	0.04	0.02	0.02	0.01	0.01	0.00	0.00
	24	0.55	0.31	0.18	0.10	0.06	0.03	0.02	0.01	0.01	0.00	0.00	0.00

Equation (6.4) is used to calculate the cumulative discounted cash flow at the end of a project (NPV). [44]

$$NPV = \sum_{N=0}^{N} F_N \frac{1}{(1+i)^N} \tag{6.4}$$

6.1.4 Equivalent annual cost

The equivalent annual cost (EAC) includes all cost aspects of assets over the entire lifespan. This includes owning, operating, and maintaining the asset. To calculate the EAC, an annuity factor needs to be determined. The annuity factor is based on the time value of money and is calculated using Equation (6.5). [26, 45]

$$a_f = \frac{1 - \frac{1}{(1+i)^N}}{i} \tag{6.5}$$

Further, the EAC can be determined by dividing the NPV by the annuity factor, a_f (Equation 6.6).

$$EAC = \frac{NPV}{a_f} \tag{6.6}$$

Since the EAC includes all costs, the capital and operational expenditures can be determined using Equations (6.7, 6.8). Where the net present value of the capital costs (NPV_{CAPEX}) is the total installed cost of all equipment, while the net present value of the operational costs (NPV_{OPEX}), such as electricity for operating the process, salaries, etc.

$$EAC_{CAPEX} = \frac{NPV_{CAPEX}}{a_f} \qquad (6.7)$$

$$EAC_{OPEX} = \frac{NPV_{OPEX}}{a_f} \qquad (6.8)$$

6.2 Material selection

Material selection is a significant cost aspect of the DTR design, and several factors need consideration when selecting the appropriate material:

- Cost
- Manufacturing and fabrication
- Resistance to withstand high temperature
- Good heat transfer properties
- Availability
- Wear of materials
- Sustainability requirements

In this thesis, the two criteria of significance are: 1) Resistance to withstand high temperature, 2) Good heat transfer properties. The challenge is to find a material to satisfy both criteria.

Materials used in high-temperature industrial applications such as calcination reactors, kilns, and heaters must consist of high-quality materials classified as exotic materials. Applying a material that should withstand the high temperature and have good heat transfer properties may ascend the classification of a super-exotic material has to be selected. [46]

Figure 6.2 is an illustration of the categorization of materials when accounting for corrosion and temperature. Material factors are listed and dependent on whether the equipment is machined or welded. [40]
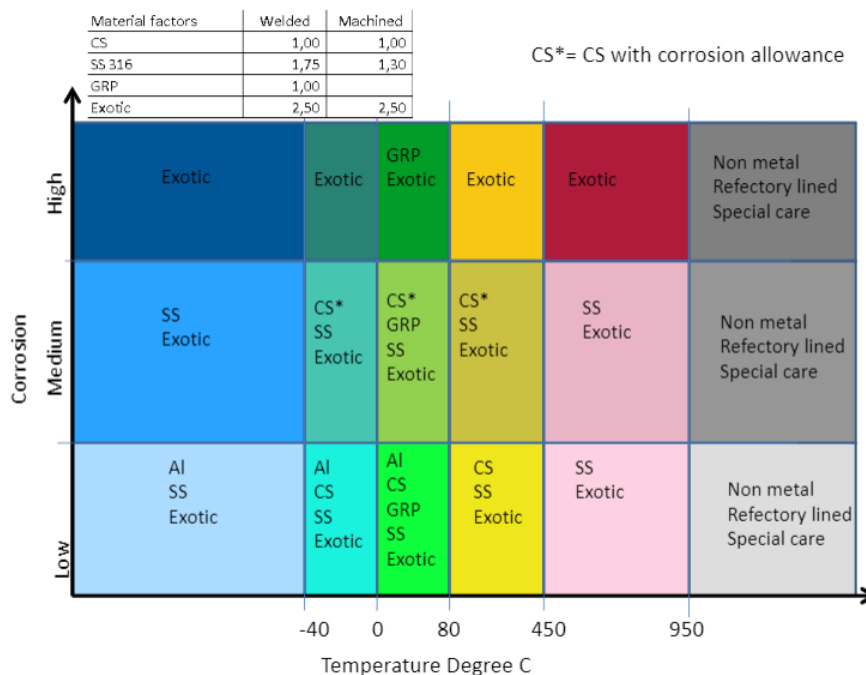
Figure 6.2: Material selection table [40]

6.2.1 DTR material selection

In Chapter 6.2, the important factors of material selection are listed. This thesis is based on the feasibility of an electrically heated DTR concept operating at a high temperature. Thus, a material factor based on an artificial material is discussed.

Given the material requirements of enduring high temperature and have good heat transfer properties, it results in a high material factor. A factor of 3.00 is assumed for the super exotic material when calculating the cost.

Two alternatives of arranging the heating elements in the DTR are evaluated: 1) Heating elements on the outside of the reactor wall, illustrated by Figure 2.1 (Cloak, heating elements, air gap, reactor wall), 2) Heating the DTR construction with a current.

In this thesis, the alternative (1) arrangement is further studied. Alternative (2) may be a valid option. However, there are some problems regarding safety when passing a significant current through the entire construction.

6.2.2 Heating elements

The heating elements must ensure the correct operating temperature of the reactor tube. Kanthal APM delivers heating element solutions, and for this study, Superthal modules are selected. The Superthal concept is based on Kanthal® Super molybdenum disilicide and is sufficient to deliver the required heat flux. O. Stadum at Kanthal APM provided a calculation of a module with the specification of inner diameter 250mm, and height 200 mm, which is included in Appendix M. The cost estimation is based on these dimensions. Figure 6.3 shows the element. [47]

Figure 6.3: Kanthal APM Superthal module, provided by Kanthal APM [47]

6.3 Adjacent units

The adjacent units must be considered when evaluating costs to implement the DTR to an existing cement clinker production system. The units are described in Chapter 2.7 and include a fan, cyclone tower, and a heat exchanger.

6.3.1 Fan

The fan implemented in the system should draw the CO_2 gas through the cyclone and the heat exchanger. The temperature of CO_2 exiting the heat exchanger is calculated in Appendix H to be about 600 K. Thus, the fan needs to fulfill the following requirements:

- Temperature of about 600 K.
- Dilute stream of CO_2 gas (some dust present since the cyclone is not 100% efficient).
- Medium capacity.

A centrifugal radial fan is selected. The details about the fan are neglected as it is not the unit of interest.

6.3.2 Cyclone

The cyclone's purpose is to separate the fine particles in the CO_2 gas exiting the DTR. Different cyclone designs separate dust from gas, such as high throughput (HT), conventional, or a high-efficiency cyclone. However, due to the fine particles, a HE cyclone is applied.

6.3.3 Heat exchanger

Jacob's master thesis, "gas-to-gas heat exchanger for heat utilization in hot CO_2 from an electrically heated calcination process," is used to obtain necessary design values for cost estimation calculations. [26]

Table 6.3: Parameters necessary to calculate the area of heat exchanger

Parameter	Unit	Design basis value
Q	MW	7.6
U	$\dfrac{W}{m^2\,K}$	250
$T_{h,in}$	K	1173.15
$T_{h,out}$	K	616.77
$T_{c,in}$	K	498.15
$T_{c,out}$	K	1073.15

The logarithmic mean temperature becomes $\Delta T_{lm} = 109\ K$, and the area of the heat exchanger $A = 279\ m^2$.

The design of the HX unit is outside the scope of this thesis. Thus, based on Jacob's results, it is assumed that a total of two 1-2 STHE HX's are necessary to cool down the hot CO_2. [26]

6.4 Cost estimation DTR and adjacent units

To estimate the cost of the reactor tubes and the adjacent units, several methods can be applied. However, in this study, the cost is partly based on previously estimated units and adjusted to the appropriate unit price for 2021.

The cost estimation for the reactor tubes is based on the material cost and weight of the tube. To calculate the mass of the hollow cylinder, Equation (6.9) is applied. [48]

$$m_{hollow,cylinder} = \pi \cdot h_t \cdot \left(\left(\frac{D_o}{2} \right)^2 - \left(\frac{D_o}{2} - t \right)^2 \right) \cdot \rho_{mat} \tag{6.9}$$

Where $D_o\ [m]$ is the outer diameter, $h\ [m]$ is the height, $t\ [m]$ is the thickness, and $\rho_{mat}\ \left[\frac{kg}{m^3}\right]$ is the density of the material. Further, the cost can be found by multiplying the mass of the cylinder with the specific cost of material $C_{mat}\ \left[\frac{\$}{kg}\right]$ (Equation (6.10)):

$$C_{tube} = m_{hollow,cylinder} \cdot C_{mat} \qquad (6.10)$$

Cost data for the heat exchanger, centrifugal radial fan, and cyclone is collected from a cost estimation website, which calculates the estimated cost for the year 2002 [49]. To adjust the data to the current year (2021), the time value of money, currency, and installation factor needs to be accounted for.

Adjustment time:

A US inflation calculator has been used to find the inflation of USD from 2002 to 2021, listed in Table 6.4. [50]

Table 6.4: Inflation USD [50]

Year	USD
2002	100
2021	147.24

Equation (6.11) can be used to calculate the present cost of the unit.

$$C_{2021} = C_{2002} \cdot \left(\frac{Value\ of\ present\ money}{Value\ of\ past\ money}\right) \qquad (6.11)$$

Adjustment currency:

To adjust for the currency from dollar to euro, a calculator from Den Norske Bank (DNB) and Equation (6.12) can be used [51]. The currency is changed to euro later to be implemented in the total installation factor.

$$C_{2021,euro} = C_{2021,\$} \cdot \frac{C_{euro}}{C_\$} \qquad (6.12)$$

Where $\frac{C_{euro}}{C_\$}\ \left[\frac{euro}{\$}\right]$ is the exchange ratio.

Installation cost:

The total installation cost in euro is calculated with Equation (6.13) and the total installation factor (Equation (6.1)).

$$C_{unit,newmaterial,2021,euro} = f_{tc} \cdot C_{unit,material,2021,euro} \qquad (6.13)$$

6.5 Electricity cost estimation

The cost of electricity can be calculated as the present cost of electricity per kilowatt-hour, multiplied by the effective operating hours of the system and the total electrical demand

(Equation 6.14). The cost of electricity is excluding taxes and grid rent. Data are listed in Table 6.5 and collected in April 2021 [52].

$$C_{el} = C_{el,NOK/kWh} \cdot t_{op} \cdot E_{el,supply} \qquad (6.14)$$

Table 6.5: Cost of electricity in Norway, April 2021 [52]

Electricity prices in the end-user market, quarterly. Øre/kWh	4th quarter 2020	Change in per cent	
	Øre/KwH	Last 3 mos.	Last 12 mos.
Households. Total price of electricity, grid rent and taxes	82.4	13.0	-26.6
Electricity price	22.2	54.2	-52.6
Grid rent	28.6	0.0	-1.0
Taxes	31.6	5.7	-13.7
Households. Electricity price by type of contract. Exclusive taxes			
New fixed-price contracts-1 year or less [1]	24.3	40.5	-42.6
New fixed-price contracts-1 year or more [1]	32.3	-15.2	-22.7
All other fixed-price contracts	33.7	1.2	-9.4
Contracts tied to spot price	20.2	65.6	-55.4
Variable price (not tied to spot price)	28.5	25.0	-45.8
Business activity. Electricity price. Exclusive taxes			
Services	18.3	77.7	-57.5
Manufacturing excl. energy-intensive manufacturing	17.6	77.8	-59.2
ManufacturiEnergy-intensive manufacturing	28.3	-0.4	-11.0

[1] New fixed-price contracts are entered during the measuring period, and older fixed-price contracts are entered earlier.

6.6 Cost per CO₂ unit captured

Assuming all CO_2 gas exiting the DTR is stored/captured, the amount of produced CO_2 during calcination calculated in Appendix H together with the equivalent CAPEX and OPEX values can estimate the cost per captured unit of CO_2.

Yearly produced CO_2 is the hourly production ($\dot{m}_{CO2,prod}$ $\left[\frac{t}{h}\right]$), multiplied by the operational hours of the system per year (t_{op} $\left[\frac{h}{year}\right]$) given by Equation (6.15).

$$\dot{m}_{CO2,prod,year} = \dot{m}_{CO2,prod} \cdot t_{op} \qquad (6.15)$$

The CAPEX per captured unit of CO_2 can be determined by Equation (6.16):

$$CAPEX_{CO2,captured} = \frac{EAC_{CAPEX}}{\dot{m}_{CO2,prod,year}} \qquad (6.16)$$

The OPEX per captured unit of CO_2 can be calculated with Equation (6.17):

$$OPEX_{CO2,captured} = \frac{EAC_{OPEX}}{\dot{m}_{CO2,prod,year}} \qquad (6.17)$$

The total cost per unit CO₂ captured can be calculated with Equation (6.18):

$$C_{total,CO2,captured} = CAPEX_{CO2,captured} + OPEX_{CO2,captured} \qquad (6.18)$$

7 Results and discussion

This chapter includes both the results and discussion. The first part consists of the general design results obtained from the simulations described in chapter 5. Further, the three design cases are evaluated against the simulations. Finally, the costs are discussed for the most promising cases. The following questions should be answered:

- What are the resulting time, human resources, expenses to alter a system in this manner?
- What is the total footprint area of the new system?
- What is the impact of the new footprint area?
- How many reactors are necessary to meet the required volume of clinker production?

7.1 Simulation results

A modified shrinking core model has been applied to investigate the kinetics of a PSD (0.2-500µm) of calcium carbonate with different requirements in calcination degree, shown in Figure 7.1. A difference is apparent by reducing the calcination degree from 94% to 90%. The calcination degree is a function of particle diameter. Thus, calcining a particle of 180 µm to 94% means that the particles below this size will have a higher calcination degree. Oppositely for the larger particles. The Python 3.8 program used to calculate the conversion time is included in Appendix I.

Several benefits may be achieved by reducing the calcination degree, such as 1) reduced sizing of equipment/units, 2) reduced power demand, 3) reduced CAPEX and OPEX. Negatively, the diffused CO_2 in the reactor reduces. Figure 7.2 shows the conversion of particles as a function of size, where the curves represent the particles when exposed to certain calcination times.
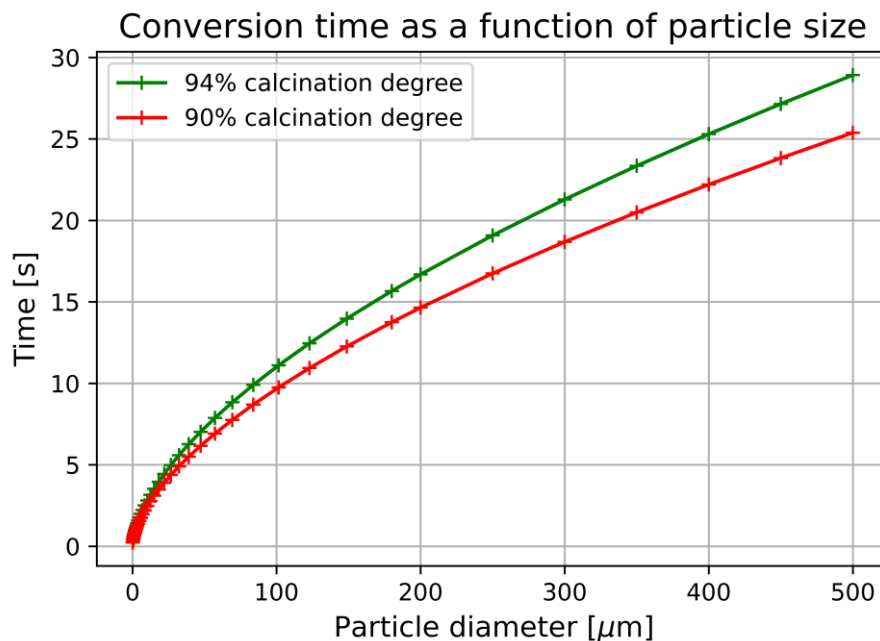
Figure 7.1: Conversion time as a function of particle diameter. Calcination temperature 1173.15 K.
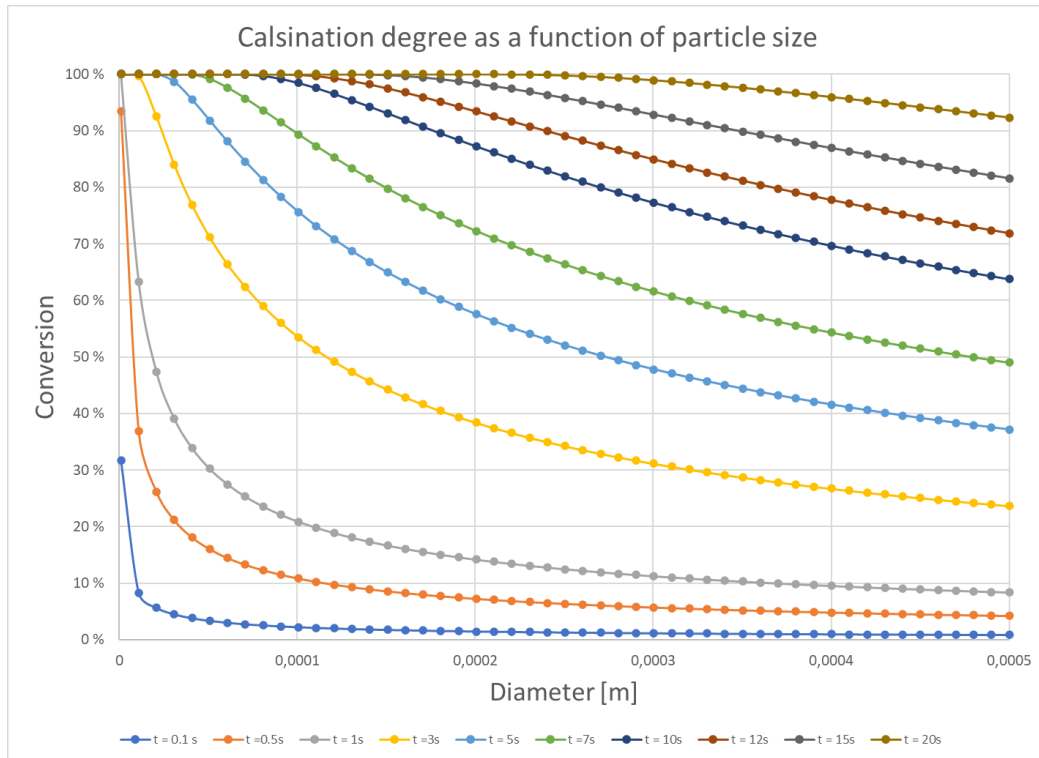
Figure 7.2: Conversion factor of particles. The curves represent the particles calcination degree with a specified calcination time, ranging from 0.1 – 20 seconds. Calcination temperature 1173 K.

Figure 7.3 shows the terminal settling velocity of the PSD. The particles are free falling, and intermolecular interaction is neglected. The terminal settling velocity in the laminar regime increases exponentially. In contrast, the increase is linear after the transition to the turbulent regime due to the particles being slowed down by eddies. The Python 3.8 program used to calculate the terminal settling velocity is included in Appendix J. The smaller particles have a relatively low settling velocity, which is a problem regarding the buoyant CO_2 gas.
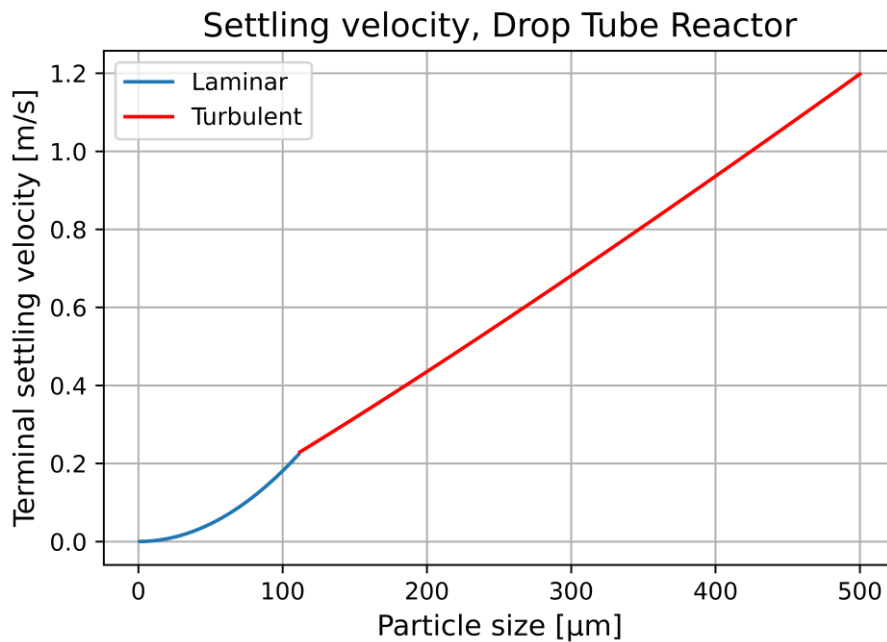
Figure 7.3: Terminal settling velocity, free falling particles in laminar and turbulent regime.

The diameter of the reactor is based on the velocity of the fluid medium. An increase in velocity reduces the diameter, as shown in Figure 7.4. For a fluid velocity of 2 m/s, the diameter must be about 5 meters to process 207 t/h of raw meal in one tube. 0.5 m/s fluid velocity requires a diameter of above 10 meters to process the same amount.

Diameter as a function of raw meal feed rate
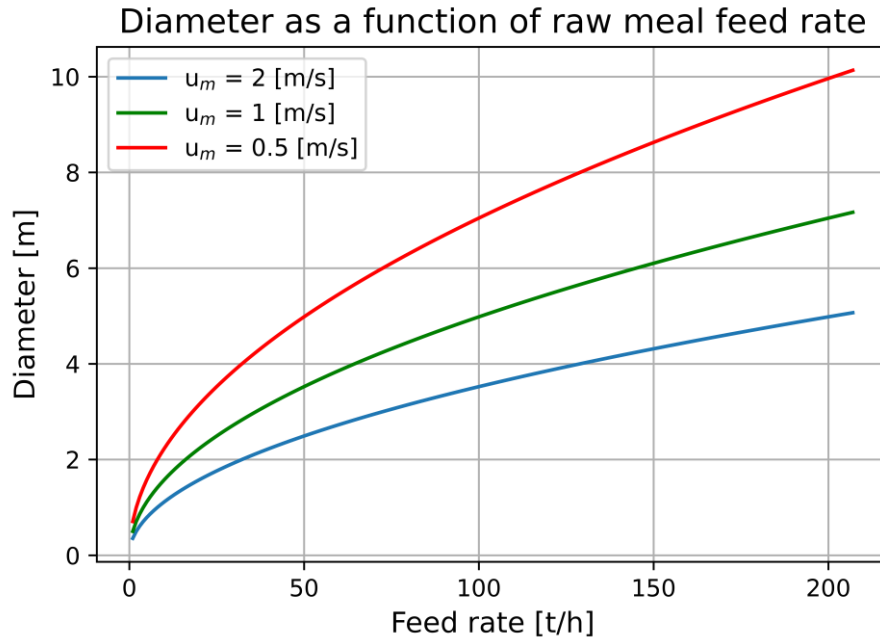
Figure 7.4: Reactor diameter with varying fluid velocity, operating temperature 1323.15 K.

Figure 7.5 shows that increased fluid velocity increases the height of the reactor. Thus, with reduced diameter and increased fluid velocity, the number of tubes to process the meal increases, shown in Figure 7.6.

Height as a function of raw meal feed rate
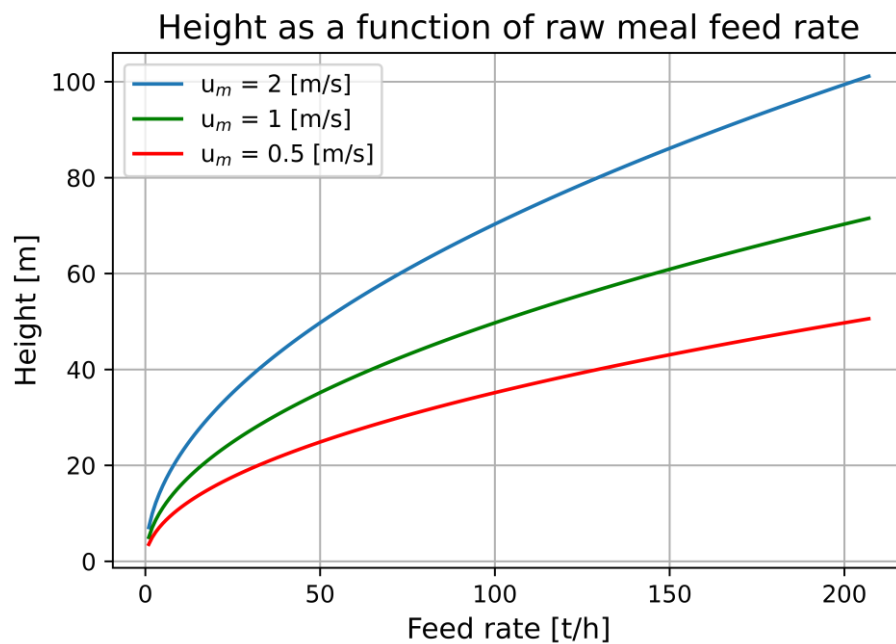
Figure 7.5: Height of the reactor tube, temperature 1323.15 K, 94% calcination degree.

Number of tubes as a function of raw meal feed rate
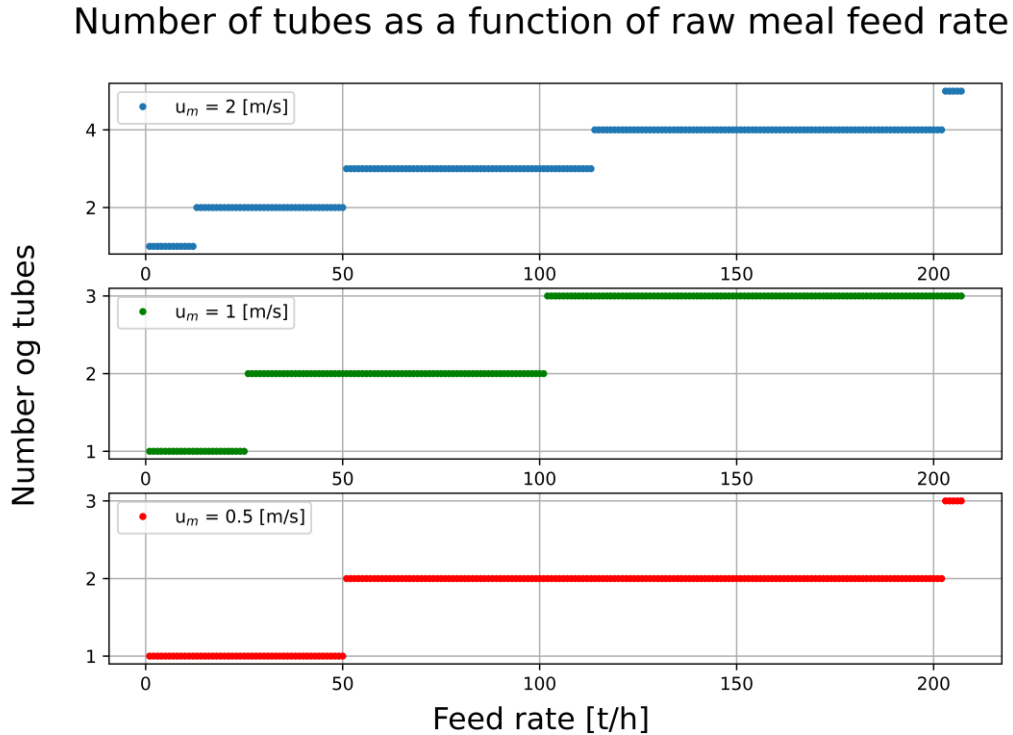
Figure 7.6: Number of reactor tubes. Available height = 25 m, temperature 1323.15 K, calcination degree 94%.

The second key parameter that significantly influences the sizing of the reactor is temperature. Reducing the operating temperature increases the height of the reactor. Between 1200 K to 1323.15 K, there is a substantial difference of several hundred meters. However, when increasing the temperature from 1323.15 K to 1500 K, the reduction in height is minimal, as shown in Figure 7.7. The same phenomenon is shown in Figure 7.8, where the required number of tubes decreases with increased temperature.

Height as a function of raw meal feed rate
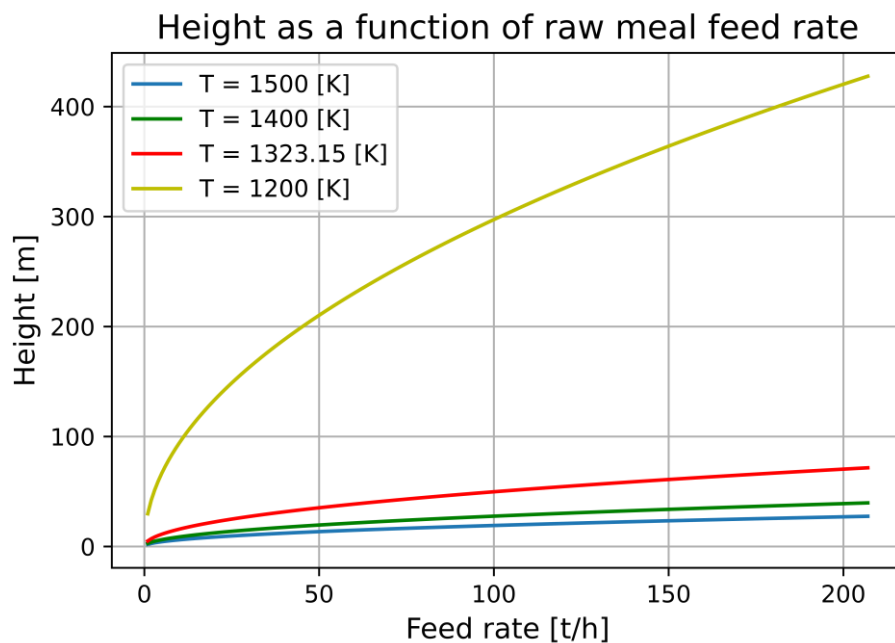
Figure 7.7: Height of tube evaluated at different temperatures, fluid velocity = 1.0 m/s.

Number of tubes as a function of raw meal feed rate
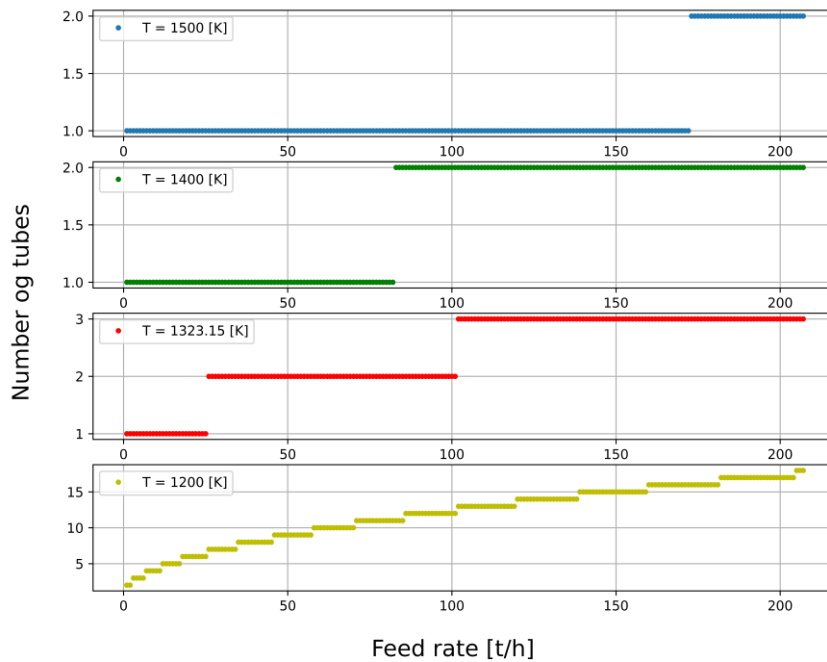
Figure 7.8: Number of reactor tubes with varying temperature. Fluid velocity = 1.0 m/s, calcination degree 94%, available height = 25 m.

The radiation heat flux for the preheating and calcination section was simulated with varying operating temperatures, shown in Figure 7.9 and Figure 7.10.

The energy balances show that the preheating of the raw meal requires less heat than the calcination reaction, which resulted in a big difference in section height. As a result of the preheating section's short height, the required flux becomes much larger than for the calcination section. The preheating flux is about 93 kW/m^2. In comparison, the calcination flux is about 60 kW/m^2, operating with an inner wall temperature of 1323.15 K. The critical flux indicates amount of energy the heating elements must deliver to the system. Thus, heating modules from Kanthal ® APM seem a reasonable choice.
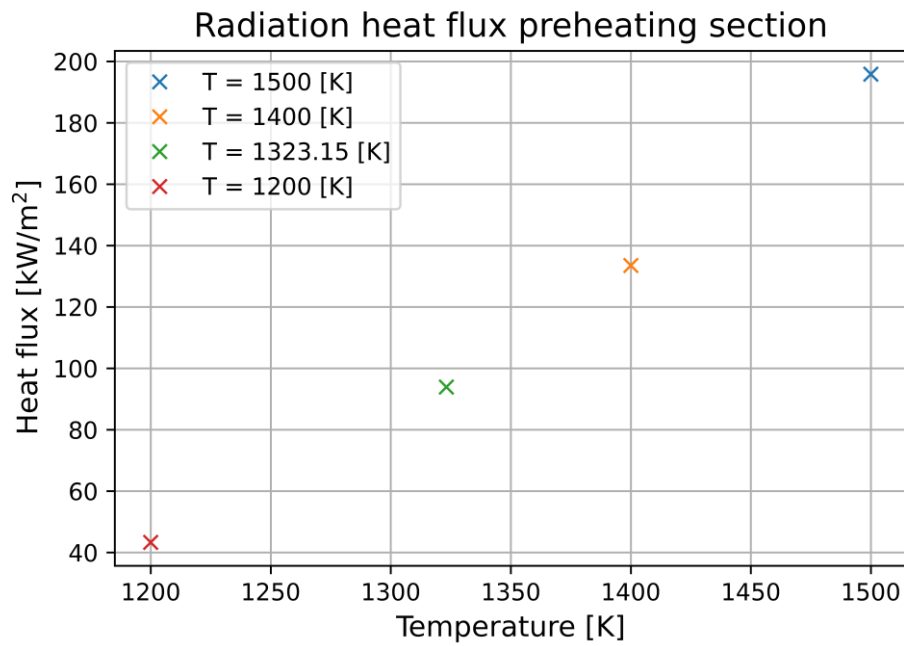
Figure 7.9: Radiation heat flux in preheating zone with varying temperature. The simulation was done with a constant fluid velocity of 1.0 m/s and 94% calcination degree.
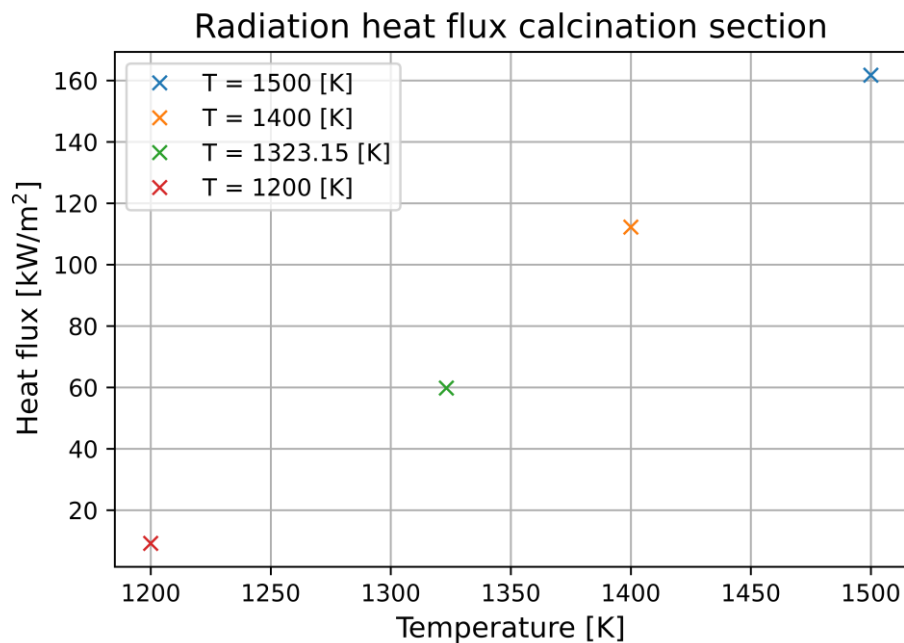
Figure 7.10: Radiation heat flux in calcination zone with varying temperature. The simulation was done with a constant fluid velocity of 1.0 m/s and 94% calcination degree.

7.2 Design cases

Three design cases were evaluated in Chapter 4: 1) counter-current flow of gas and particles, 2) counter-current flow of gas and particles applying a clustering effect, 3) co-current flow of gas and particles. Each case is evaluated in the following sub-chapters against the simulation results. The operating temperature is set optimal to 1323.15 K (1050 °C) based on the simulation results in Figure 7.7.

7.2.1 Counter-current flow – single-particle theory

Chapter 4.1.1 is a calculation example, where 10 t/h of raw meal is processed. At this low feed rate, the diameter of the tube must be above 3.5 meters because of the low terminal settling velocity of the particles and the requirement of low fluid velocity. If 207 t/h of $CaCO_3$ were to be processed, the diameter was calculated to be about 16 meters. This design is proven not feasible and will not be further discussed.

7.2.2 Counter-current flow – applying clustering effect

By applying a clustering effect, the effective particle diameter was evaluated at 500 µm. The fluid flow can be relatively high, resulting in a much smaller diameter (1.76 meters) than obtained with single-particle theory.

The effective particle size results in a terminal settling velocity of about 1.2 m/s. By implementing a fluid velocity of 0.4 m/s, the terminal settling velocity becomes 0.8 m/s. Simulation by a modified SCM (Figure 7.1) shows that a calcination degree of 90% and 94 % is achievable with calcination times of about 25 and 29 seconds, respectively. The minimum required height of the tubes for calcination is calculated: 1) 90 % calcination = 20 meters, 2) 94 % calcination = 23.2 meters. Design results are listed in Table 7.1.

Increasing the fluid velocity reduces essential design factors, such as the diameter, because of the increased residence time of the particles. A fluid velocity of 0.8 m/s, resulting in a terminal settling velocity of 0.4 m/s, was investigated. 90 % and 94 % calcination can be achieved in tube heights of 10 and 11.6 meters. Design results are listed in Table 7.1.

There are no specifications on the available space regarding the height or floor area available for the tubes. Thus, 30 meters, including the framework, and a 30 cm spacing between each tube are assumed. The footprint results in Table 7.1 are only based on floor area.

Table 7.1: Results design counter-current flow

Calc.	$\dot{m}_{in}\left[\frac{t}{h}\right]$	Diameter [m]	Height [m]	T_{op} [K]	N_{tubes}[−]	A_{foot}[m^2]	$u_m\left[\frac{m}{s}\right]$	$v_t\left[\frac{m}{s}\right]$
90 %	207	11.1	20	1323.15	3	293	0.4	0.8
90 %	50	5.5	20	1323.15	8	193	0.4	0.8
90 %	10	2.43	20	1323.15	21	104	0.4	0.8
90 %	1	0.77	20	1323.15	207	159	0.4	0.8
90 %	207	7.84	10	1323.15	7	340	0.8	0.4
90 %	50	3.85	10	1323.15	16	191	0.8	0.4
90 %	10	1.72	10	1323.15	42	111	0.8	0.4
90 %	1	0.55	10	1323.15	207	112	0.8	0.4
94 %	207	11.4	23.2	1323.15	2	205	0.4	0.8
94 %	50	5.3	23.2	1323.15	4	90	0.4	0.8
94 %	10	2.36	23.2	1323.15	21	99	0.4	0.8
94 %	1	0.79	23.2	1323.15	207	164	0.4	0.8
94 %	207	8.01	11.6	1323.15	6	305	0.8	0.4
94 %	50	3.94	11.6	1323.15	12	150	0.8	0.4
94 %	10	1.76	11.6	1323.15	42	115	0.8	0.4
94 %	1	0.56	11.6	1323.15	207	114	0.8	0.4

Based on the above results, the most promising designs are with a feed rate of 50 t/h or 10 t/h. These configurations have a height that utilizes most of the available space. The diameter is not too big, which eases the manufacturing. The optimal designs are highlighted in green, and the worst designs are in orange, in Table 7.1.

The cost of the different "green" designs is calculated by applying the cost estimation theory from Chapter 6.4. As stated for the material selection of the DTR, a super exotic material is used, but this is not specified. Thus, the calculations are based on the material properties of Inconel 718, which may be similar to the desired material. An estimate is shown for the 90%, 10 t/h feed rate design. The rest are listed in Table 7.2.

The mass of the hollow cylinder is calculated by Equation (6.9), where the outer diameter and height are collected from Table 7.1, the thickness from the stress analysis in Chapter 4.6.1, and the density of Inconel 718 is 8193 kg/m^3 [34].

$$m_{90\%,10t/h} = \pi \cdot h_t \cdot \left(\left(\frac{D_o}{2}\right)^2 - \left(\frac{D_o}{2} - t\right)^2\right) \cdot \rho_{mat} = 26043 \; kg$$

The cost per kg Inconel 718 is evaluated from several vendors, and the average cost of 30 \$/kg is used [53]. Thus, the cost of one tube can be calculated with Equation (6.10).

$$C_{90\%,10t/h} = m_{90\%,10t/h} \cdot C_{In718} = 26043 \cdot 30 = 781268 \; \$$$

The cost for all tubes become:

$$C_{90\%,21,10t/h} = C_{90\%,10t/h} \cdot N_{tubes} = 781268 \cdot 21 = 16406633 \ \$$$

Adjustment to NOK:

$$C_{90\%,21,10t/h,nok} = C_{90\%,21,10t/h} \cdot \frac{8.67 NOK}{\$} = 142.25 \ MNOK$$

Table 7.2: Cost estimation of tubes, counter-current flow.

%	$D_o [m]$	$h_t [m]$	$t [m]$	$\rho_m \left[\frac{kg}{m^3}\right]$	$m [kg]$	$C_{IN} \left[\frac{\$}{kg}\right]$	N_{tubes}	$C_{NOK} [MNOK]$
90	2.43	20	0.021	8193	26043	30	21	142.25
90	1.72	10	0.021	8193	9184	30	42	100.32
94	5.3	23.2	0.021	8193	66199	30	4	68.88
94	2.36	23.2	0.021	8193	29331	30	21	160.21
94	1.76	11.6	0.021	8193	10904	30	42	119.11

Based on the cost estimation of the tube, it can be argued that the cheapest set of tubes are the most viable option. However, the impact of the diameter in terms of manufacturing is not included. This could be assessed in future work.

An important observation is that the 94% calcination degree design is the most promising. This results from the increased time required for calcination - the height of the tubes increases – making the total number of tubes less than the design of 90% calcination. However, the diameter is large, and manufacturing may be costly. The tubes are tall, and it may be necessary to implement an elevator for raw meal transport. An elevator will impact the system, where the temperature of the preheated meal reduces due to heat losses, which alters the requirement of the preheated zone and ultimately affects the total cost.

7.2.3 Co-current flow of gas and particles

Forcing the gas down through the effluent of the DTR seems to be a promising concept. Problematics such as the particles being dragged with the gas upwards, as for the counter-current concept, are eliminated. This concept makes it so smaller PSDs can be processed in smaller process facilities. The fan can alter the velocity of the fluid flow and particles.

The fluid velocity is chosen 0.8 m/s, making the terminal settling velocity of the particles to be 1.1 m/s (180 µm). The relatively high velocity has a significant impact on the residence time and required height for calcination. To achieve a calcination degree of 90 % and 94 %, the required height of the tube becomes 15.4 and 17.1 meters, respectively. If the effective particle size is 500 µm, it would require about 50.6 and 77 meters to achieve the necessary residence time. Thus, the feasibility of processing large clusters of particles with this design is not further discussed.

The sizing required to process particles of 180 µm is evaluated at both a fluid velocity of 0.8 and 1.0 m/s. The results are listed in Table 7.3.

Table 7.3: Results co-current flow of 180 µm particles

Calc.	$\dot{m}_{in}\left[\frac{t}{h}\right]$	Diameter [m]	Height [m]	T_{op} [K]	$N_{tubes}[-]$	$A_{foot}[m^2]$	$u_m\left[\frac{m}{s}\right]$	$v_t\left[\frac{m}{s}\right]$
90 %	207	7.84	15.4	1323.15	5	243	0.8	1.1
90 %	50	3.86	15.4	1323.15	12	144	0.8	1.1
90 %	10	1.73	15.4	1323.15	21	56	0.8	1.1
90 %	1	0.54	15.4	1323.15	207	110	0.8	1.1
90 %	207	7.01	18.2	1323.15	4	155	1.0	1.3
90 %	50	3.45	18.2	1323.15	8	78	1.0	1.3
90 %	10	1.54	18.2	1323.15	21	46	1.0	1.3
90 %	1	0.49	18.2	1323.15	207	102	1.0	1.3
94 %	207	8.01	17.1	1323.15	4	203	0.8	1.1
94 %	50	3.94	17.1	1323.15	8	100	0.8	1.1
94 %	10	1.76	17.1	1323.15	21	58	0.8	1.1
94 %	1	0.56	17.1	1323.15	207	114	0.8	1.1
94 %	207	7.17	20.2	1323.15	4	163	1.0	1.3
94 %	50	3.52	20.2	1323.15	8	81	1.0	1.3
94 %	10	1.58	20.2	1323.15	21	48	1.0	1.3
94 %	1	0.50	20.2	1323.15	207	103	1.0	1.3

The green design options listed in Table 7.3 are most promising based on the dimensions. Similarly, with the counter-current flow, the feed rates of 50 t/h and 10 t/h have the most favorable results.

Table 7.4: Cost estimation tubes, co-current flow

%	$D_o[m]$	$h_t[m]$	$t[m]$	$\rho_m\left[kg/m^3\right]$	$m\ [kg]$	$C_{IN}[\$/kg]$	N_{tubes}	$C_{NOK}\ [MNOK]$
90	1.73	15.4	0.021	8193	14226	30	21	77.70
90	3.45	18.2	0.021	8193	33733	30	8	70.19
90	1.54	18.2	0.021	8193	14943	30	21	81.62
94	1.76	17.1	0.021	8193	16074	30	21	87.79
94	3.52	20.2	0.021	8193	38204	30	8	79.49
94	1.58	20.2	0.021	8193	17022	30	21	92.98

The cheapest set of tubes are eight tubes, each processing 50 t/h, at the cost of 70.19 MNOK (90%) and 79.49 MNOK (94%). Reduced height of the pipes is desirable as the necessity of an

elevator may not be needed. Thus, processing 10 t/h to 90 % calcination with 21 tubes 15.5 meters high may be optimal.

7.2.4 Cost of heating elements

As described in Chapter 6.2.2, Kanthal Superthal modules are chosen to heat the reactor tube. It is assumed that the entire height of the tubes is covered with elements. Thus, the total number of elements required for each design is calculated as the tube height, divided by the element's height.

$$N_{elements} = \frac{h_t}{h_{element}}$$

The designs evaluated are the two cost optimum ones, and the cost of elements are listed in Table 7.5. The cost of one element is based on websites, such as Alibaba, to select an assumed cost of 10 kNOK/unit. [53]

Table 7.5: Cost of heating elements based on the required number of elements.

Case	h_t [m]	$h_{element}$ [m]	N_{tube}	$N_{element}$	$C_{el,unit}[\frac{NOK}{unit}]$	$C_{el}[MNOK]$
C.C[5] 94%	23.2	0.200	4	116	10000	1.16
C.O[6] 90%	18.2	0.200	8	91	10000	0.91

7.3 Footprint

Two footprints, both in height and floor space, are compared illustratively from the above-determined values. Figure 7.11 is the isometric view of the arrangements to emphasize the height difference, while Figure 7.12 highlights the circular floor arrangement. The most cost optimum result from Table 7.4 and the second most cost optimum from Table 7.2 is used to illustrate the differences. The required footprint for each tube includes the tube, spacing for refractory, and space needed for maintenance. Thus, fewer tubes may be more viable if it is limiting floor space.
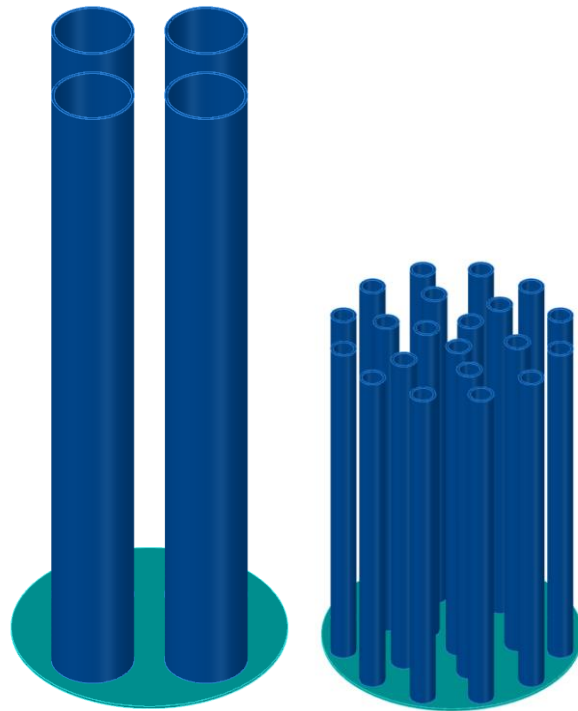
[5] Counter-current.

[6] Co-current.

Figure 7.11: 4 tubes, 23.2 meters vs. 21 tubes, 15.4 meters.
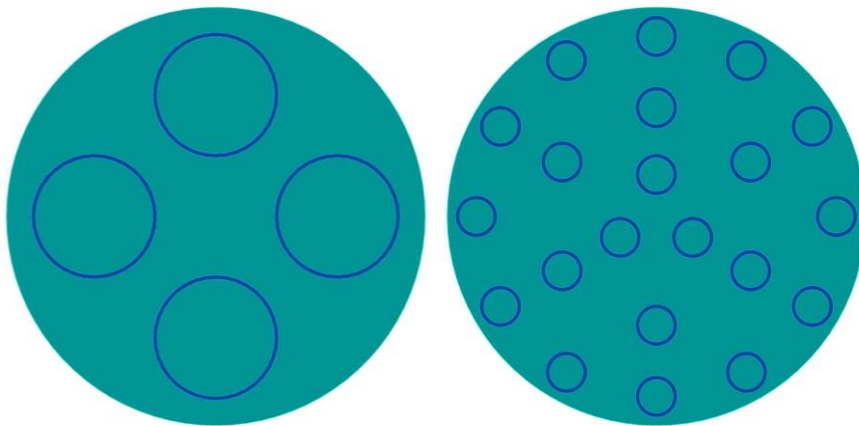
Figure 7.12: Arrangement 4 tubes vs. 21 tubes.

7.4 Pressure drop and fan power

The pressure losses across each unit can be determined as described in Chapter 3.4. Across the DTR, there is a slight pressure drop due to elevation. The height of the two most promising cases previously described is used to calculate the pressure drop (Table 7.6).

Table 7.6: Pressure drop across DTR.

Case	$\rho_{gas}\left[kg/m^3\right]$	$g\left[m/s^2\right]$	$h_t\left[m\right]$	$\Delta P_{DTR}\left[Pa\right]$
Counter-current	0.457	9.807	23.2	104.0
Co-current	0.457	9.807	20.2	90.5

Pressure drop across the heat exchangers are calculated by Jacob [26]:

$$\Delta P_{HX} = 18000 \; Pa$$

The HX's described in Jacobs' thesis are designed for a similar system described in this thesis. Thus, the same HX's are assumed to fit the system. Two 1-2 STHE units are chosen. [26]

Only one cyclone unit is described in this thesis. A high-efficiency cyclone is used for both the counter-current and co-current cases. The meal is sent through the lines into a manifold from the exit tubes, which further collects the flows into one line and sends it to the cyclone. The counter-current cyclone's purpose is to de-dust the gas before it is cooled down by the HX's and sent to storage. Thus, this cyclone needs to separate fine particles from the gas. The co-current cyclone must process the entire flow of gas and calcined meal. As described in Chapter 4.5.2, the maximum allowed pressure drop across the cyclone is 1000 Pa.

The total pressure drop across all units of interest evaluated for the largest pressure drop across the DTR in the system becomes:

$$\Delta P_{tot} = \Delta P_{DTR} + \Delta P_{HX} + \Delta P_{cyclone} = 104 + 18000 + 1000 = 19104 \; Pa$$

To compensate for the pressure drop, a radial centrifugal fan with an efficiency of 75% is implemented, as described in Chapter 3.4.4 and 6.3.1. The power required to run this fan is calculated using Equation (3.52):

$$W_{el} = \frac{C_p \cdot T_{in} \cdot \dot{n}_{CO2}}{\eta} \cdot \left(\left[\frac{p_{out}}{p_{in}} \right]^{\frac{R}{C_p}} - 1 \right)$$

$$W_{el} = \frac{47.32 \cdot 616 \cdot 416.76}{0.75} \cdot \left(\left[\frac{101325}{82221} \right]^{\frac{8.314}{47.32}} - 1 \right) = 0.61 \; MW$$

7.5 Cost of adjacent units

Applying the theory from Chapter 6, the unit cost can be estimated.

7.5.1 Centrifugal radial fan

The fan is assumed to have the capacity to process all CO_2 produced during calcination. Thus, the volumetric flow of CO_2 calculated in Appendix H is the design basis for the calculation. Table 7.7 consists of cost estimation data collected. [49]

Table 7.7: Cost estimation data centrifugal radial fan 2002. [49]

Unit	Material	Size	Year	Currency	Cost
Centrifugal radial fan	Carbon steel	$41 \frac{m^3}{s}$	2002	USD	26259

Equation (6.11) adjustment time:

$$C_{fan,CS,2021,41m^3} = C_{fan,CS,2002,41m^3} \cdot \left(\frac{Value\ of\ present\ money}{Value\ of\ past\ money} \right)$$

$$C_{fan,CS,2021,41m^3} = 26259 \cdot \left(\frac{147.24}{100} \right) = 38664\ USD$$

Equation (6.12) adjustment currency (USD to euro):

$$C_{fan,CS,2021,41m^3,euro} = 38664 \cdot 0.9103 = 35195\ euro$$

Total installation factor:

Carbon steel can withstand the temperature of the CO_2 gas due to effective cooling by the HX's. Thus, the total installed factor (Equation (6.1)) does not need to be altered regarding the material.

$$f_{tc} = f_{tc,CS} = 8.54$$

$$C_{fan,CS,2021,41m^3,euro} = 8.54 \cdot 35195 = 300570\ euro$$

Adjustment currency (euro to NOK):

$$C_{fan,CS,2021,41m^3,NOK} = 300570 \cdot 10.48 = 3149979\ NOK = 3.15\ MNOK$$

Table 7.8: Estimated cost of centrifugal radial fan 2021.

Unit	Material	Size	Year	Currency	Cost
Centrifugal radial fan	Carbon steel	$41\ m^3$	2021	MNOK	3.15

7.5.2 Heat exchangers

The heat exchanger cost estimation is calculated applying the area specified in Chapter 6.3.3 and the total installed cost factor calculated for Inconel 718 by Jacob ($f_{tic} = 19.26$). [26]

The information presented in Table 7.9 has been collected from the cost estimation website for the calculated area. [49]

Table 7.9: Cost estimation heat exchanger 2002. [49]

Unit	Material	Size	Year	Currency	Cost
Heat exchanger	Carbon steel	$279\ m^2$	2002	USD	40689

Adjustment time:

$$C_{HX,CS,2021,279m^2} = C_{HX,CS,2002,279m^2} \cdot \left(\frac{Value\ of\ present\ money}{Value\ of\ past\ money} \right)$$

$$C_{HX,CS,2021,279m^2} = 40689 \cdot \left(\frac{147.24}{100}\right) = 59910 \; USD$$

Adjustment currency (USD to NOK):

$$C_{HX,CS,2021,279m^2,NOK} = 59910 \cdot 8.63 = 517027 \; NOK$$

Equations (6.1) and (6.13) adjusts material and installation:

$$C_{HX,inconel,2021,279m^2} = f_{tic} \cdot C_{HX,CS,2021,279m^2,NOK}$$

$$C_{HX,inconel,2021,279m^2} = 19.26 \cdot 517027 = 9957949 \; NOK = 9.96 \; MNOK$$

To sufficiently cool down the CO_2 gas, two of the chosen HX are necessary for the system. Thus, the total cost of the HX is multiplied by two.

$$C_{HX,2} = 9.96 \cdot 2 = 19.92 \; MNOK$$

Table 7.10: Estimated cost heat exchanger 2021.

Unit	Material	Size	Year	Currency	Cost
Heat exchanger	Inconel 718	$279 \; m^2$	2021	MNOK	9.96
Total	Inconel 718	$279 \; m^2 \; x \; 2$	2021	MNOK	19.92

7.5.3 Cyclone

The cyclone must endure the high temperature CO_2 gas, and stainless steel 316 (SS316) can be applied for this unit.

Table 7.11 shows the cost estimation data collected for a cyclone from the cost estimation website. [49]

Table 7.11: Cost estimation for cyclone 2002. [49]

Unit	Material	Size	Year	Currency	Cost
Cyclone	Carbon steel	$90 \; \dfrac{m^3}{s}$	2002	USD	123601

Adjustment size:

$$C_{cyc,CS,2002,144.5m^3/s} = C_{cyc,CS,2002,90m^3/s} \cdot \left(\frac{New \; size}{Old \; size}\right)^e$$

$$C_{cyc,CS,2002,144.5m^3/s} = 123601 \cdot \left(\frac{41}{90}\right)^{0.65} = 74143 \; USD$$

Adjustment time:

$$C_{cyc,CS,2021,144.5m^3/s} = 74143 \cdot \left(\frac{147.24}{100}\right) = 109168 \; USD$$

Adjustment currency (USD to euro):

$$C_{cyc,CS,2021,144.5m^3/s,euro} = 109168 \cdot 0.9103 = 99376 \; euro$$

Total installed cost factor and material:

$$f_{tc,ss316} = f_{tc,cs,cyclone} - f_{eq,CS,cyclone} + \left(f_{eq,CS,cyclone} \cdot f_{mat,cyclone}\right) - f_{pi,CS,cyclone}$$
$$+ \left(f_{pi,CS,cyclone} \cdot f_{mat,cyclone}\right)$$

$$f_{tc,ss316} = 8.54 - 1 + (1 \cdot 1.75) - 1.22 + (1.22 \cdot 1.75) = 10.21$$

$$C_{cyc,ss316,2021,144.5m^3/s} = 10.21 \cdot 99376 = 1014627 \; euro$$

Adjustment currency (euro to NOK):

$$C_{cyc,ss316,2021,144.5m^3/s,NOK} = 1014627 \cdot 10.48 = 10633287 \; NOK = 10.63 \; MNOK$$

Table 7.12: Estimated cost cyclone 2021.

Unit	Material	Size	Year	Currency	Cost
Cyclone	SS316	$41\dfrac{m^3}{s}$	2021	MNOK	10.63

7.5.4 CAPEX

Table 7.13 includes all previously calculated capital expenditures. Both options of tube costs are implemented in the table. The value to the left is the cost of the counter-current case.

Table 7.13: Total capital cost DTR and adjacent units

Unit	Material	Currency	Cost	
Reactor tubes	Chapter 6.2.1	MNOK	68.88	70.19
Heating elements	Superthal module	MNOK	1.16	0.91
Fan	Carbon steel	MNOK	3.15	
Heat exchanger	Inconel 718	MNOK	19.92	
Cyclone	Stainless steel 316	MNOK	10.63	
Total	-	MNOK	103.74	104.80

7.6 Cost of electricity

The cost of electricity is based on the necessary electrical supply to the reactor and running the fan. By implementing Equation (6.14), the yearly cost of electricity can be calculated. The systems operational hours per year are based on a similar system and are assumed to be 7315 h/y [4].

$$C_{el} = C_{el,NOK/kWh} \cdot t_{op} \cdot E_{el,supply}$$

The process is considered an energy-intensive manufacturing process. Thus, according to Table 6.5, $C_{el,NOK/kWh} = 0.283 \frac{NOK}{kWh}$. The total energy consumption is the necessary energy supply calculated in 4.2 and the fan.

$$C_{el} = 0.283 \cdot 7315 \cdot \left((107.855 + 0.61) \cdot 10^3\right) = 224.54 \; \frac{MNOK}{y}$$

7.6.1 NPV electricity

The NPV of electricity is calculated applying Equation (6.4), assuming an interest rate of 8%, and the number of years to buy electricity is 25, based on Samani's master thesis. [6]

$$NPV_{Cel} = \sum_{N=0}^{N} C_{el} \frac{1}{(1+i)^N}$$

$$NPV_{Cel} = C_{el} + C_{el} \cdot \frac{1}{(1+i)} + C_{el} \cdot \frac{1}{(1+i)^2} + C_{el} \cdot \frac{1}{(1+i)^3} + \cdots + C_{el} \cdot \frac{1}{(1+i)^{N-1}}$$

$$NPV_{Cel} = 224.54 + 224.54 \cdot \frac{1}{(1+0.08)} + \cdots + 224.54 \cdot \frac{1}{(1+0.08)^{25-1}}$$

$$NPV_{Cel} = 2588.67 \; MNOK$$

7.6.2 Equivalent annual cost estimation

The NPV of capital expenditures (CAPEX) is the total installed cost previously calculated.

Counter-current case:

$$NPV_{CAPEX} = 103.74 \; MNOK$$

Co-current case:

$$NPV_{CAPEX} = 104.80 \; MNOK$$

Assuming the only operational cost is electricity:

$$NPV_{OPEX} = NPV_{Cel} = 2588.67 \; MNOK$$

The annuity factor is calculated using Equation (6.5):

$$a_f = \frac{1 - \frac{1}{(1+i)^N}}{i} = \frac{1 - \frac{1}{(1+0.08)^{25}}}{0.08} = 10.67$$

Thus, the equivalent annual cost of CAPEX (Equation (6.7)) is:

Counter-current case:

$$EAC_{CAPEX} = \frac{NPV_{CAPEX}}{a_f} = \frac{103.74}{10.67} = 9.72 \frac{MNOK}{year}$$

Co-current case:

$$EAC_{CAPEX} = \frac{NPV_{CAPEX}}{a_f} = \frac{104.80}{10.67} = 9.82 \frac{MNOK}{year}$$

Furthermore, the equivalent annual cost of OPEX (Equation 6.8) is:

$$EAC_{OPEX} = \frac{NPV_{OPEX}}{a_f} = \frac{2588.67}{10.67} = 242.61 \frac{MNOK}{year}$$

7.6.3 Cost per captured CO_2 unit

Assuming all CO_2 gas exiting the DTR is stored/captured, the amount of produced CO_2 during calcination, together with the equivalent CAPEX and OPEX values, can estimate the cost per

captured unit of CO_2 with Equation (6.15). Yearly produced CO_2 is the hourly production ($\dot{m}_{CO2,prod}$ $\left[\frac{t}{h}\right]$), multiplied by the operational hours of the system per year (t_{op} $\left[\frac{h}{year}\right]$).

$$\dot{m}_{CO2,prod,year} = \dot{m}_{CO2,prod} \cdot t_{op} = 66.03 \cdot 7315 = 483009.5 \frac{t}{y}$$

The CAPEX per captured unit of CO_2 (Equation 6.16)):

Counter-current case:

$$CAPEX_{CO2,captured} = \frac{EAC_{CAPEX}}{\dot{m}_{CO2,prod,year}} = \frac{9.72 \cdot 10^6}{483009.5} = 20.12 \frac{NOK}{t_{CO2,captured}}$$

Co-current case:

$$CAPEX_{CO2,captured} = \frac{EAC_{CAPEX}}{\dot{m}_{CO2,prod,year}} = \frac{9.82 \cdot 10^6}{483009.5} = 20.33 \frac{NOK}{t_{CO2,captured}}$$

The OPEX per captured unit of CO_2 (Equation (6.17)):

$$OPEX_{CO2,captured} = \frac{EAC_{OPEX}}{\dot{m}_{CO2,prod,year}} = \frac{242.61 \cdot 10^6}{483009.5} = 502.29 \frac{NOK}{t_{CO2,captured}}$$

The total cost per unit CO_2 captured for both designs are shown in Table 7.14 and calculated with Equation (6.18):

Table 7.14: Cost per avoided CO_2 unit

Design	EAC_{CAPEX}	EAC_{OPEX}	$C_{NOK/cap}$
Counter-current	20.12 NOK/t	502.29 NOK/t	522.41 NOK/t
Co-current	20.33 NOK/t	502.29 NOK/t	522.62 NOK/t

8 Conclusion

The main objective of this study was to investigate how the calciner in a cement kiln process could be designed as an electrically heated DTR and evaluate the applicability and cost of this concept. The combination of buoyant gaseous CO_2 and the fine particle size proved to be a challenge.

Various system designs were studied:

- Counter-current flow of gas and particles, not considering cluster formations.
- Counter-current flow of gas and particles, applying clustering effect.
- Co-current flow of gas and particles.

A modified SCM was implemented to study the kinetics of $CaCO_3$. The only gas inside the reactor is CO_2. Thus, the partial pressure of CO_2 is approximately 1 atm which favors carbonation and inhibits the calcination reaction. The equilibrium pressure and the partial pressure of CO_2 were implemented to the reaction rate to account for the inhibition. Required time for calcination for a PSD ranging from $0.2 - 500$ µm, with 94% and 90% calcination requirements, were simulated in Python 3.8.

Python 3.8 was used to simulate the design cases. The terminal settling velocity was evaluated based on the PSD, flow regime, and the assumption of free-falling particles. The fluid velocity reduces the velocity of particles in the counter-current design, and some of the smaller particles will exit with the gas at the top of the DTR. Oppositely for the co-current case, where the particle velocity is increased by the fluid velocity, making this design has a degree of freedom to choose a broader range of fluid velocities, which the counter-current is impaired.

The diameter, height, and the number of tubes necessary to process the meal were determined by altering the key parameters fluid velocity and operating temperature. The fluid velocity showed a significant impact on the overall design, as it is the determining factor of the tube diameter and terminal settling velocity. The temperature showed a great impact of the sizing in the temperature range 1200 - 1323.15K, where the total height reduced from several hundred meters at 1200 K to about 80 meters with an operating temperature of 1323.15 K. By increasing the temperature from $1323.15 - 1500$ K, the height-reduction was minimal.

The sizing of the most optimum designs for the counter-current case was:

1) 90% calcination – 1.72 meters diameter, 10 meters height, and 42 tubes,
2) 94% calcination – 5.3 meters diameter, 23.2 meters height, and 4 tubes.

Co-current case yielded:

1) 90% calcination – 3.45 meters diameter, 18.2 meters height, and 8 tubes,
2) 94% calcination – 3.52 meters diameter, 20.2 meters height, and 8 tubes.

Arrangement of tubes and the footprint, both to respect of floor space and height, were studied. More tubes reduces the height but increase the floor space. If the tubes are tall, there is need of an elevator to transport the meal. The elevator is a source of heat loss, and the preheated meal will be fed into the reactor at a lower preheated temperature. Also, by having tall tubes, it may be necessary to skip preheating cyclones, which ultimately increases the reactor's preheating time.

Implementing the DTR to an existing cement kiln system requires few modifications. A de-dusting cyclone to separate the buoyant gas containing fine particles (counter-current) or separate the exiting meal and gas at the effluent of the DTR (co-current). Heat exchangers to

cool down the pure CO_2 gas before further processing and storing. Elevator to transport meal (long tubes). Centrifugal radial fan to compensate for the pressure drop. From the existing system, the quencher, bag filter, and recycle lines can be removed.

Energy and mass balances were implemented to determine the net energy transfer required to preheat and calcine the meal to 94%. The reactor's electrical power supply was found to be about 108 MW. To generate and transfer the heat, Superthal modules from Kanthal® APM are chosen.

Recycle lines are proven not to be necessary for the DTR system. However, sources of waste heat are present. Some heat is lost through the refractory of the reactor, 0.224 MW. The most significant heat loss is apparent in the gas exiting the HX's – the gas holds a temperature of about 600 K – which results in a heat loss of 6.42 MW.

The material of the reactor is not specified in this study. However, to determine several design values and costs, the material properties of Inconel 718 alloy have been used as inspiration. By evaluating buckling and wind force, the thickness of the tube walls is calculated to be a minimum of 21 mm.

Detailed factor estimation and the capacity factor method are applied to calculate the CAPEX for units of interest in the system. The CAPEX of both the counter-current and co-current designs was 103.74 MNOK and 104.80 MNOK, respectively. The highest impact of costs originates from the OPEX – because of electricity – and was calculated to be 224.54 MNOK/year. The cost per captured CO_2 unit (ton) for both designs was calculated 522.41 NOK/t_{CO2} for the counter-current and 522.62 NOK/t_{CO2} for the co-current. The cost of the designs is almost equal, and which concept to implement into an existing cement clinker system should be based on the PSD to be processed and the available space (footprint).

The way forward for this project should include:

- Reactor material study.
    - Material's resistance to high temperature.
    - Material's heat transfer properties.
- Manufacturing costs, i.e., how much does the sizing impact manufacturing.
- CFD analysis to study particle behavior.
- Effectiveness and sizing of co-current design on very fine PSDs (0.1-10µm).
- Need of an elevator.

References

[1] "Cement production and emisisons," Norcem Heidelbergcement Group. [Online]. Available at: url: https://www.norcem.no/en/Cement_and_CCS Accessed: (08.01.2021).

[2] "Climate change: the massive CO_2 emitter you may not know about," BBC News. [Online]. Available at: url: https://www.bbc.com/news/science-environment-46455844 Accessed: (08.01.2021).

[3] "Calcination," Lenntech. [Online]. Available at: url: https://www.lenntech.com/chemistry/calcination.htm Accessed: (09.01.2021).

[4] L. A. Tokheim, A. Mathisen, L.E. Øi, C. Jayarathna, N. H. Eldrup, T. Gautestad, "Combined calcination and CO_2 capture in cement clinker production by use of electrical energy," *TCCS-10. CO_2 Capture, Transport and Storage. Trondheim 17th -19th June 2019. Selected papers from the 10th International Trondheim CCS Conference,* 2019: SINTEF Academic Press.

[5] "Cement," IEA. [Online]. Available at: url: https://www.iea.org/reports/cement Accessed: (12.01.2021).

[6] N. A. Samani, "Calcination in an electrically heated bubbling fluidized bed applied in calcium looping," Master thesis, Faculty of Technology, Natural sciences and Maritime sciences, University of South-eastern Norway, Porsgrunn, 2020.

[7] "Innovating for the Earth," Calix. [Online]. Available at: url: https://www.calix.global/our-technology/ Accessed: (19.01.2021).

[8] P. Hodgson, M. Sceats, A. Vincent, D. Rennie, P. Fennell, T. Hills, "Direct separation calcination technology for carbon capture: demonstrating a low cost solution for the lime and cement industries in the LEILAC project," GHGT-14. Melbourne 21st -25th October 2018.

[9] G. Rovero, M. Curti, G. Cavaglia, "Optimization of spouted bed scale-up by square-based multiple unit design," Politecnico di Torino, torino, Italy, March 2012. Accessed: Feb. 02. 2021. [Online]. doi: 10.5772/33395

[10] D. Geldart, "Characterization of Fluidized Powders," Gas Fluidization Technology, University of Bradford, UK: John Wiley & Sons, 1986, Chapter 3, pp. 33-38.

[11] A. Augustyn, "Terminal velocity," Britannica. [Online]. Available at: url: https://www.britannica.com/science/terminal-velocity Accessed: (12.02.2021).

[12] University of South-eastern Norway, "Gas Purification and Energy Optimization (PEF2006-1)," 2020.

[13] O. levenspiel, *The chemical reactor omnibook,* chemical reactor omnibook. 2nd ed. Corvallis Oregon, USA, 1989.

[14] S. Li, *Reaction Engineering,* Oxford, UK, 2017. [Online]. Available: https://ebookcentral.proquest.com/lib/ucsn-ebooks/reader.action?docID=4914158#

[15] A. Amiri, G. D. Ingram, N. E. Maynard, I. Livk, A. V. Bekker, "An unreacted shrinking core model for calcination and similar solid-to-gas reactions," *Chemical Engineering Communications*, vol. 202, pp. 1161-1175, 2015. [Online]. Available: doi: 10.1080/00986445.2014.910771

[16] A. Amiri, G. D. Ingram, N. E. Maynard, I. Livk, A. V. Bekker, "A multi-stage, multi-reaction shrinking core model for self-inhibiting gas-solid reactions," *Advanced Powder Technology*, vol. 24, pp. 728-736, 2013. [Online]. Available: https://doi.org/10.1016/j.apt.2013.01.016

[17] C.R. Milne, G.D. Silcox, D.W. Pershing, D.A. Kirchgessner, "Calcination and sintering models for application to high-temperature, short-time sulfation of calcium-based sorbents," *American Chemical society,* vol. 29, pp139-149, 1990. [Online]. Available: https://doi.org/10.1021/ie00098a001

[18] Y. Wang, S. Lin, Y. Suzuki, "Study of limestone calcination with CO_2 capture: decomposition behavior in a CO_2 atmosphere," *Energy & Fuels*, vol. 21, pp. 3317-3321, 2017.

[19] M. D. Jeronimo, K. Zhang, D. E. Rival, "Direct lagrian measurements of particle residence time," *Experiments in Fluids*, vol. 60, 2019. [Online]. Available: https://doi.org/10.1007/s00348-019-2718-1

[20] B. Arias, M. Alonso, C. Abanades, "CO_2 capture by calcium looping at relevant conditions for cement plants: experimental testing in a 30 kW pilot plant," *American Chemical Society*, vol. 56, pp. 2634-2640, 2017. [Online]. Available: https://doi.org/10.1021/acs.iecr.6b04617

[21] X Ariyaratne, W. K. H.: Utilization of Waste-derived Biofuels and Partly CO2-neutral Fuels in Cement Kilns, PhD dissertation, Telemark University College, 2014. (Chap. Figure modern cement kiln system)

[22] L. A. Tokheim, "Kiln system modification for increased utilization of alternative fuels at Norcem Brevik," *Cement International*, vol. 4, pp. 52-58, 2006.

[23] F. P. Incropera, "Introduction," in *Incropera's principles of heat and mass transfer*, 8th ed. Singapore: John Wiley & Sons, 2017, pp.3-10.

[24] D. Kunii and O. Levenspiel, *Fluidization engineering*. Elsevier, 2013.

[25] L. A. Tokheim, "ELSE, Combined calcination and CO_2 capture in cement clinker production by use of CO_2-neutral energy – Phase 1: Technical feasibility and early-phase cost-estimate (6CP)," 30.10.2018.

[26] R. M. Jacob, "Gas-to-gas heat exchanger for heat utilization in hot CO_2 from an electrically heated calcination process," Master thesis, Faculty of Technology, Natural sciences and Maritime sciences, University of South-eastern Norway, Porsgrunn, 2019.

[27] R. M. Felder, R. W. Rousseau, *Elementary principles of chemical* processes, 3rd ed. Hoboken, John Wiley & Sons, 2005. p.663.

[28] "Fluid pressure drop along pipe length of uniform diameter," Engineers Edge. [Online]. Available at: url: https://www.engineersedge.com/fluid_flow/pressure_drop/pressure_drop.htm Accessed: (16.04.2021).

[29] C. J. Brown, J. Nielsen, *Silos, Fundamentals of theory, behaviour and design,* CRC Press, 1998, [Online]. Available: doi:10.1201/9781482271744

[30] T. R. Pereira, A. E. Patterson, Y. H. Lee, S. L. Messimer, "Critical buckling load of thin-walled plastic cylinders in axial and radial loading: overview and FEA case study," *EngrXiv,* 2019. [Online]. Available: doi: 10.31224/osf.io/2mtfu

[31] L. Sharp, "NORSOK Standard N-003," Silo.Tips. [Online]. Available at: url: https://silo.tips/download/norsok-standard-n-003 Accessed: (17.04.2021).

[32] "Wind forces," Vishay Precision Group. [Online]. Available at: url: http://www.weightech.com.br/arquivos/vpg-07_forcas-vento.pdf Accessed: (17.04.2021).

[33] "Observasjoner og værstatistikk," Norsk Klimaservicesenter. [Online]. Available at: url: https://seklima.met.no/ Accessed: (17.04.2021).

[34] "Inconel® alloy 718," Special Metals. [Online]. Available at: url: https://www.specialmetals.com/assets/smc/documents/inconel_alloy_718.pdf Accessed: (13.04.2021).

[35] R. Zevenhoven, P. Kilpinen, *Control of pollutants in flue gases and fuel gases,* 3rd ed. Helsinki University of Technology Espoo, Finland, 2004

[36] University of South-eastern Norway, "Gas Purification and Energy Optimization (PEF2006-1)," 2020.

[37] F. P. Incropera, "Internal flow," in *Incropera's principles of heat and mass transfer*, 8th ed. Singapore: John Wiley & Sons, 2017, pp.502-504.

[38] J. C. Geankoplis, *Transport processes and unit operations,* 3rd ed. Prentice-Hall, inc. 1993.

[39] F. P. Incropera, "Radiation: Processes and properties," in *Incropera's principles of heat and mass transfer*, 8th ed. Singapore: John Wiley & Sons, 2017, p.740.

[40] University of South-eastern Norway, "Project Management and Cost Engineering (FM3110-1)," 2020.

[41] W. Saeed, "The factorial method of cost estimation," Chemical Engineering Projects. [Online]. Available at: url: https://chemicalprojects.net/2014/05/09/the-factorial-method-of-cost-estimation/ Accessed: (06.03.2021).

[42] "The cost-to-capacity method and scale factors," evcValuation. [Online]. Available at: url: https://evcvaluation.com/the-cost-to-capacity-method-and-scale-factors/ Accessed: (06.03.2021).

[43] J. Fernando, "Net Present Value," Investopedia. [Online]. Available at: url: https://www.investopedia.com/terms/n/npv.asp Accessed: (07.03.2021).

[44] University of South-eastern Norway, "Project Management and Cost Engineering (FM3110-1)," 2020.

[45] J. Kagan, "Present Value Interest Factor of an Annuity (PVIFA)," Investopedia. [Online]. Available at: url: https://www.investopedia.com/terms/n/npv.asp Accessed: (08.03.2021).

[46] W. D. Callister, D. G. Rethwisch, *Materials Science and Engineering*, 9th ed. John Wiley & Sons, 2014.

[47] "Superthal® SHC," Kanthal®, Part of Sandvik Group. [Online]. Available at: url: https://www.kanthal.com/en/products/furnace-products/heating-modules/superthal-heating-modules/superthal-SHC/ Accessed: (06.05.2021).

[48] "Hollow cylinder - mass," vCalc. [Online]. Available at: url: https://www.vcalc.com/wiki/Carol/Hollow+cylinder+-

+Mass#:~:text=The%20Math,mass%20of%20the%20hollow%20cylinder. Accessed: (02.05.2021).

[49] "Mcgraw-hill," *Chemical data.* [Online]. Available at: url: http://www.mhhe.com/engcs/chemical/peters/data/ce.html Accessed: (23.04.2021).

[50] "Inflation Calculator," US Inflation Calculator. [Online]. Available at: url: https://www.usinflationcalculator.com/ Accessed: (23.04.2021).

[51] "Valutakalkulator," DNB. [Online]. Available at: url: https://m.dnb.no/valutakalkulator Accessed: (23.04.2021).

[52] "Electricity prices," Statistisk sentralbyrå. [Online]. Available at: url: https://www.ssb.no/en/elkraftpris Accessed: (24.04.2021).

[53] "Inconel 718 sheet," Alibaba. [Online]. Available at: url: https://www.alibaba.com/showroom/inconel-718-plate.html Accessed: (03.05.2021).

Appendices

Appendix A: Signed task description

Appendix B: Work break down structure

Appendix C: Scheduling

Appendix D: PSD raw meal data

Appendix E: Chemical composition calculation

Appendix F: Conveection and radiation absorption by CO_2 gas.

Appendix G: Stress calculations

Appendix H: Mass and energy balances

Appendix I: Python 3.8 - calcination time

Appendix J: Python 3.8 - terminal settling velocity

Appendix K: Python 3.8 - diameter, height, and number of tubes with varying fluid flow velocity

Appendix L: Python 3.8 - diameter, height, and number of tubes with varying temperature

Appendix M: Excel calculation heating element. Kanthal® APM [47]

Appendix A: Signed task description

FMH606 Master's Thesis

Title: Calcination in an electrically heated drop tube calciner

USN supervisors: Lars-André Tokheim (main supervisor) and Ron M. Jacob (co-supervisor)

External partners: Norcem AS Brevik

Task background:
USN is one of the partners in the research project *"Combined calcination and CO_2 capture in cement clinker production by use of CO_2-neutral electrical energy"*. The acronym ELSE[1] is used as a short name for the project. Phase 1 of the project was completed in April 2019, and Phase 2 was started in April 2020. The goal of the ELSE project is to utilize electricity (instead of carbon-containing fuels) to decarbonate the raw meal in the cement kiln process while at the same time capturing the CO_2 from decarbonation of the calcium carbonate in the calciner. A regular kiln system is shown in Figure 1.
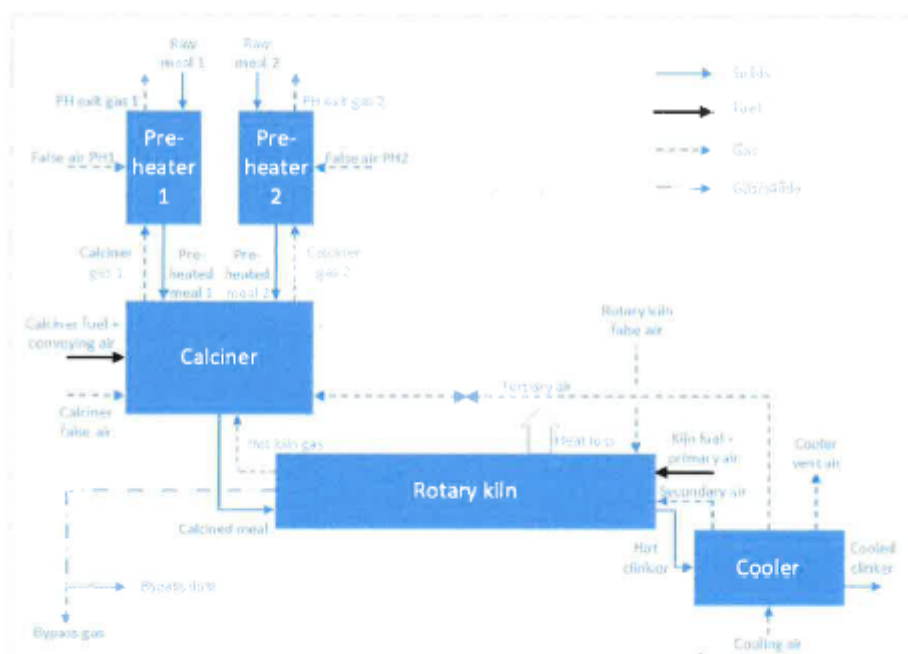
Figure 1: A regular cement kiln process with two preheater strings.

Different concepts to implement electrification of the calciner have been discussed. One alternative is to use electricity (through resistance heating) to generate heat that is indirectly transferred to the calciner, where it is used to calcine the meal ($CaCO_3 \rightarrow CaO + CO_2$). Different reactor types may be used as a calciner, for example a drop tube. The meal is then fed at the top

---

1 ELSE is short for 'ELektrifisert SEmentproduksjon' (Norwegian) meaning 'electrified cement production'.

of the tube and will drop down as it is heated and calcined by the heat being transferred from the electrically heated tube wall.

When the hot kiln gas, the tertiary air and the carbon-containing fuels are no longer supplied to the calciner, then N_2 can be eliminated from the calciner exit gas, which will be more or less pure CO_2, which can be stored (or utilized in some way).

Such a concept may be less expensive than a regular post-combustion system applied to CO_2 capture from the cement plant. Moreover, as the fuel generated CO_2 will be eliminated, less CO_2 is produced in the calcination process.

Task description:
The task may include the following:

- Describe the drop tube concept and explain how a drop tube may be used to calcine the meal

- Describe how heat generated by resistance heating may be transferred to the meal in the drop tube

- Suggest a drop tube design and make a sketch to illustrate it

- Investigate whether any gas recycling is required in the system

- Identify and quantify waste heat streams in the new system

- Make a mass and energy balance of the system and calculate mass flow rates, temperatures, duties, etc.

- Make a process simulation model of (part of) the system and simulate different cases, varying key parameters in the system

- Make a process flow diagram with process values for selected cases

- Describe required constructional changes to the kiln system

- Determine the required size of the drop tube and other relevant equipment units

- Make estimates of investment costs (CAPEX) and operational costs (OPEX) of the suggested process, including calculation of costs per avoided CO_2 unit ($€/t_{CO2}$)

Student category: EET or PT students

Is the task suitable for online students (not present at the campus)? Yes, both online and campus students may select the task.

Practical arrangements:
There may be meetings with Norcem to discuss the task and the progress, most likely via Skype/Teams/Zoom (due to the corona situation).

Supervision:

As a general rule, the student is entitled to 15-20 hours of supervision. This includes necessary time for the supervisor to prepare for supervision meetings (reading material to be discussed, etc).
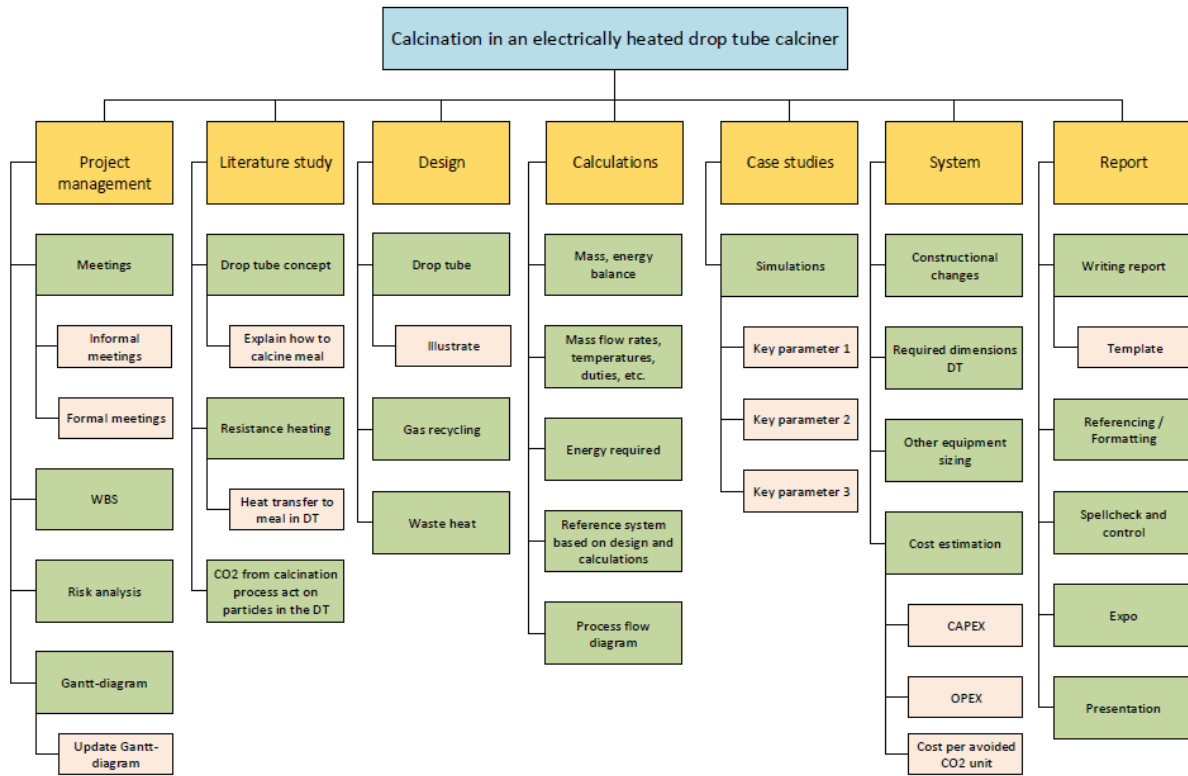
Signatures:

Supervisor (date and signature): 14.01.2021, *[signature]*

Student (write clearly in all capitalized letters): MARTIN HAGENLUND USTERUD

Student (date and signature): 14.01.2021 *[signature]*

Appendix B: Work break down structure

Appendix C: Scheduling
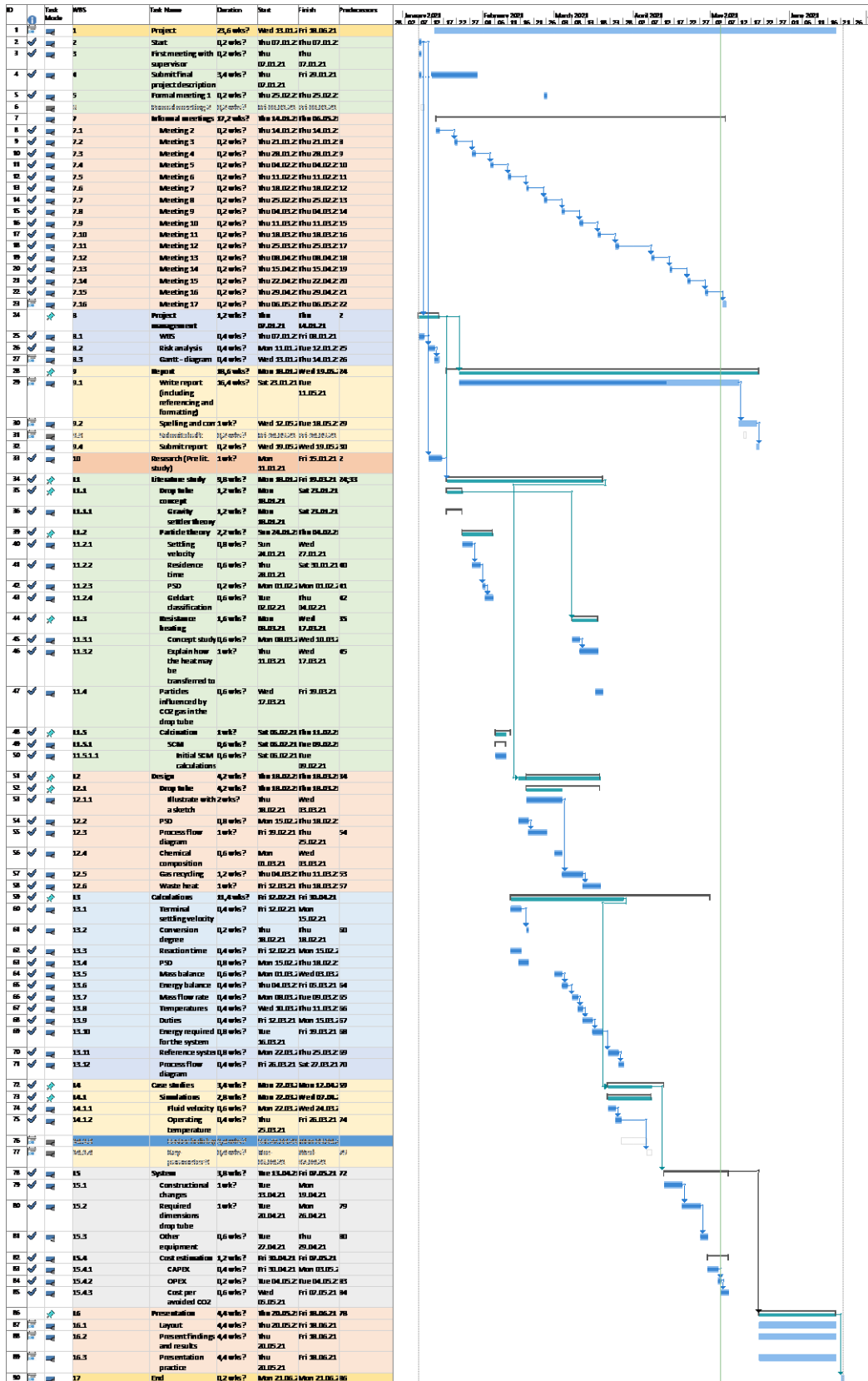
Appendix D: PSD raw meal data

STD-råmel

Version 1.2   28. Nov 1996 13:10

Kalkmel   :Run Number   28

Dato:96.11.28. Kl.
Laborant:il
CaCO3:

Sample File Name: KALKMEL , Record: 1112   Source: Analysed
Measured on: 28. Nov 1996 13:07   Last saved on: 28. Nov 1996 13:07

Presentation: 2$$D
Very Polydisperse model   Volume Result   Focus = 100 mm.
                                           Kill Result Low = 1 High = 0
Residual = 0.128 %   Concentration = 0.012 %   Obscuration = 15.00 %
d (0.5) =   21.25 µm   d (0.1) =   1.91 µm   d (0.9) = 104.93 µm
D [4, 3] =   38.10 µm   Span =   4.85   Slope (D75/D25) = 7.832
Sauter Mean (D[3,2]) =   6.03 µm   Gj.24 µm =   53.27 µm   Mode = 36.38 µm
Blaine = 0.9954 sq. m. / gm   Gj.30 µm =   59.31 µm   Density = 1.00 gm. / c.c.

Size (Lo) µm	Result In %	Size (Hi) µm	Result Below %	Size (Lo) µm	Result In %	Size (Hi) µm	Result Below %
0.20	0.77	0.48	0.77	8.48	3.67	10.27	32.42
0.48	0.77	0.59	1.54	10.27	4.11	12.43	36.53
0.59	0.77	0.71	2.32	12.43	4.52	15.05	41.05
0.71	1.02	0.86	3.34	15.05	4.88	18.21	45.93
0.86	1.27	1.04	4.61	18.21	5.04	22.04	50.97
1.04	1.50	1.26	6.10	22.04	5.16	26.68	56.14
1.26	1.69	1.52	7.80	26.68	5.18	32.29	61.32
1.52	1.83	1.84	9.63	32.29	5.31	39.08	66.63
1.84	1.90	2.23	11.53	39.08	5.21	47.30	71.84
2.23	1.92	2.70	13.46	47.30	4.93	57.25	76.78
2.70	1.99	3.27	15.44	57.25	4.48	69.30	81.25
3.27	2.13	3.95	17.57	69.30	4.15	83.87	85.40
3.95	2.35	4.79	19.91	83.87	3.94	101.52	89.34
4.79	2.61	5.79	22.52	101.52	3.75	122.87	93.09
5.79	2.94	7.01	25.46	122.87	3.58	148.72	96.67
7.01	3.28	8.48	28.74	148.72	3.33	180.00	100.00

Appendix E: Chemical composition

Symbol	Unit	Basis	Raw meal	New raw meal	% of components	Remark
mbasis	kg	LoI-free	1,0000			XRF analysis
wCaO	kg/kg	LoI-free	0,6599			XRF analysis
mCaO	kg	LoI-free	0,6599			Calculated here
m_Other_old	kg	-	0,3401			Calculated here
wSiO2	kg/kg	LoI-free	0,4824			XRF analysis
wAl2O3	kg/kg	LoI-free	0,1257			XRF analysis
wFe2O3	kg/kg	LoI-free	0,0432			XRF analysis
wMgO	kg/kg	LoI-free	0,0141			XRF analysis
wSO3	kg/kg	LoI-free	0,0091			XRF analysis
wK2O	kg/kg	LoI-free	0,0266			XRF analysis
wNa2O	kg/kg	LoI-free	0,0061			XRF analysis
MCaO	kg/mol	-	0,0560			Constant
nCaO	mol	-	11,7839			Calculated here
nCO2	mol	-	11,7839			Calculated here
MCO2	kg/mol	-	0,0440			Constant
mCO2	kg	-	0,5185			Calculated here
mCaCO3	kg	Raw	1,1784			Calculated here
mnew	kg	Raw	1,5185			Calculated here
wCaCO3	kg/kg	Raw	0,7760	0,7760		Calculated here
m_other_new	kg	Raw	0,2240			
wSiO2_new	kg/kg	Raw	0,3177	0,1528	0,6821	Calculated here
wAl2O3_new	kg/kg	Raw	0,0828	0,0398	0,1777	Calculated here
wFe2O3_new	kg/kg	Raw	0,0284	0,0137	0,0611	Calculated here
wMgO_new	kg/kg	Raw	0,0093	0,0045	0,0199	Calculated here
wSO3_new	kg/kg	Raw	0,0060	0,0029	0,0129	Calculated here
wK2O_new	kg/kg	Raw	0,0175	0,0084	0,0376	Calculated here
wNa2O_new	kg/kg	Raw	0,0040	0,0019	0,0086	Calculated here
Sum weight				1,0000	1,0000	
Sum other			0,4657			

Appendix F: Convection and radiation absorption by CO₂ gas.

Calculation heat absorbed by the CO₂ gas:

The heat flux between the CO₂ gas and the reactor walls is described:

$$q''_{CO2,rad} = \sigma \cdot (\varepsilon_G \cdot T_G^4 - \alpha_G \cdot T_{sur}^4)$$

Here:

σ: Stefan-Boltzmann constant $= 5.67 \cdot 10^{-8} \left[\frac{W}{m^2 \, K^4}\right]$

ε_G: Emissivity = to be calculated

α_G: Absorptivity = to be calculated

T_G: Temperature of gas $= 1173.15 \, [K] = 900 \, [°C]$

T_{sur}: Wall temperature $= 1323.15 \, [K] = 1050 \, [°C]$

The characteristic mean beam length can be determined with a chosen diameter of $0.3m$:

$$L = 0.60 \cdot D = 0.60 \cdot 0.3m = 0.18m$$

The partial pressure of CO₂ in the reactor is assumed to be equal to $1 \, atm$, thus:

$$P_G \cdot L = 1atm \cdot 0.18m = 0.18 \, atm \cdot m$$

Read of the emissivity using emissivity figure:

$$\varepsilon_G = 0.13$$

Calculate the absorptivity of the gas using $P_G \cdot L \cdot \frac{T_{sur}}{T_G}$:

$$\alpha_G = 0.162$$

The heat flux to the gas is then:

$$q''_{CO2,rad} = 5.67 \cdot 10^{-8} \cdot (0.13 \cdot (1323.15)^4 - 0.162 \cdot (1173.15)^4) = 5193.15 \frac{W}{m^2}$$

Convection heat transfer, diameter 0.3m and height of reactor 3m:

The heat flux of convection can be calculated:

$$q''_{conv} = h \cdot (T_s - T_m)$$

Where:

T_s: Wall temperature $= 1323.15 \, [K] = 1050 \, [°C]$

T_m: Guessed value fluid $= 1173.15 \, [K] = 900 \, [°C]$

The convective heat transfer coefficient is described by:

$$h = \frac{k \cdot Nu}{D}$$

k: thermal conductivity coefficient $= 0.0651 \, \left[\frac{W}{m \, K}\right]$

μ: dynamic viscosity $= 4.65 \cdot 10^{-5} \, \left[N \cdot \frac{s}{m^2}\right]$

The Nusselt number is determined using the empirical correlation:

$$Nu = 0.027 \cdot Re_D^{\frac{4}{5}} \cdot Pr^{\frac{1}{3}} \left(\frac{\mu}{\mu_s}\right)^{0.14}$$

$0.7 \leq Pr \leq 16700$
$Re_D \geq 10000$
$\dfrac{L}{D} \geq 10$

Determine the flow regime by calculating the Reynolds number:

$$Re_D = \frac{\rho_{CO2} \cdot u_m \cdot D}{\mu}$$

The mean velocity u_m of the fluid needs to be determined based on the terminal settling velocity of the particles. The velocity of the gas must not drag the majority of particles upwards in the reactor. Hence, a guessed value of the mean velocity of the gas:

$$u_m = 0.4 \frac{m}{s}$$

The density of CO₂ is found by using the ideal gas law at the calcination temperature (1173 [K], $P_{CO2} \, [Pa]$ is the partial pressure of CO₂, $M_{CO2} \, \left[\frac{kg}{mol}\right]$ is the molecular mass of CO₂, $R \, \left[\frac{m^3 \cdot Pa}{K \cdot mol}\right]$ is the universal gas constant:

$$\rho_{CO2} = \frac{P_{CO2} \cdot M_{CO2}}{R \cdot T} = \frac{101325 \cdot 44.01 \cdot 10^{-3}}{8.314 \cdot 1173.15} = 0.457 \frac{kg}{m^3}$$

$Re_D = 20763 \, (Ok! \, according \, to \, Nu \, correlation)$

$Pr = 0.706 \, (Ok! \, according \, to \, Nu \, correlation)$

Ratio of the length (height) to diameter:

$$\frac{L}{D} = \frac{3}{0.3} = 10 \, (Ok! \, according \, to \, Nu \, correlation)$$

The dynamic viscosity evaluated at the wall temperature:

$$\mu_s = 5.08 \cdot 10^{-5} \, N \cdot \frac{s}{m}$$

The Nusselt number is then:

$$Nu = 67.52$$

The convective heat transfer coefficient is then:

$$h = 14.65 \frac{W}{m^2 K}$$

Finally:

$$q''_{conv} = 14.65 \cdot (1323.15 - 1173.15) = 2197.5 \frac{W}{m^2}$$

Maximum temperature of CO₂ gas heated by radiation and convection. What is the average temperature of the gas?

The total heat flux that is heating the gas:

$$q''_{tot} = q''_{rad} + q''_{conv} = 5193.15 + 2197.5 = 7390.65 \frac{W}{m^2 K}$$

The maximum temperature of the gas can be found:

$$T_{CO2,max}(x) = T_m + \frac{q''_{tot} \cdot P}{\dot{n}_{CO2} \cdot C_{p,CO2}} x$$

Where:

P: Perimeter of the cylinder (not top and bottom)

$$P = 2 \cdot \pi \cdot r = 2 \cdot 3.14 \cdot \left(\frac{0.3}{2}\right) = 0.942 \, m$$

Choosing x = 0.15 (center of reactor).

The maximum temperature is then:

$$T_{CO2,max} = 1173.15 + \frac{7390.65 \cdot 2.826}{417.76 \cdot 0.0589} \cdot 0.15 = 1300.5 \, K$$

The average temperature:

$$T_{CO2,ave} = \frac{T_{CO2,max} + T_m}{2} = 1236.8 \, K = 963.7 \, °C$$

Convective heat transfer by gas absorption:

Preheat section:

Wall to fluid. The operating temperature $T_{wall} = 1323.15 \, K$, and the fluid is assumed to have a temperature equal to the calcination temperature $T_{cal} = 1173.15 \, K$ at which the gas is produced.

$$q''_{ph,wall,gas,conv} = h_{wall,gas} \cdot (T_{wall} - T_{cal})$$

The convective heat transfer coefficient evaluated at the fluid calcination temperature:

$$h_{wall,gas} = \frac{k_{T,cal} \cdot Nu_{wall,gas}}{D}$$

Where $k_{T,cal} = 0.0651 \frac{W}{m\,K}$

The Nusselt number can be calculated using the empirical correlation, if the criteria for Reynolds number, Prandtl number and the ratio of length to diameter are within the limits.

$$Nu_D = 0.027 \cdot Re_D^{\frac{4}{5}} \cdot Pr^{\frac{1}{3}} \cdot \left(\frac{\mu}{\mu_s}\right)^{0.14}$$

Where $Pr(T = 1173.15) = 0.7024$, $\mu = 4.65 \cdot 10^{-5}\,[Pa\,s]$, $\mu_s = 5.08 \cdot 10^{-5}\,[Pa\,s]$

Reynolds number is:

$$Re_D = \frac{\rho_g \cdot u_m \cdot D}{\mu}$$

$$Re_D = \frac{0.457 \cdot 1.0 \cdot 1.57}{4.65 \cdot 10^{-5}} = 15489$$

Both the Prandtl number and Reynolds number are valid. Thus, the calculation with the Nusselt number correlation continues.

$$Nu_D = 0.027 \cdot 15489^{\frac{4}{5}} \cdot 0.7024^{\frac{1}{3}} \cdot \left(\frac{4.65 \cdot 10^{-5}}{5.08 \cdot 10^{-5}}\right)^{0.14}$$

$$Nu_D = 53.15$$

The convective heat transfer coefficient becomes:

$$h_{wall,gas} = \frac{0.0651 \cdot 53.15}{1.57} = 2.2 \frac{W}{m^2\,K}$$

Finally, the heat flux:

$$q''_{ph,wall,gas,conv} = 2.2 \cdot (1323.15 - 1173.15) = 330 \frac{W}{m^2}$$

Fluid to the particles. The convective heat transfer is evaluated at T_{cal} for the fluid and an average temperature $T_{m,phm}$ for the particles.

$$q''_{ph,gas,part,conv} = h_{gas,part} \cdot (T_{cal} - T_{m,phm})$$

The average temperature:

$$T_{m,phm} = \frac{T_{cal} + T_{phm}}{2} = 1052.15\,K$$

Convective heat transfer coefficient is evaluated at the average temperature:

$$h_{gas,part} = \frac{k_{Tm,phm} \cdot Nu_{gas,part}}{D}$$

Where: $k_{Tm,phm} = 0.0771 \frac{W}{m^2\,K}$

$$Nu_D = 0.027 \cdot Re_D^{\frac{4}{5}} \cdot Pr^{\frac{1}{3}} \left(\frac{\mu_{Tm,phm}}{\mu}\right)^{0.14}$$

Where:

$Pr(T = 1052.15) = 0.77095 : ok!$

$\mu_{Tm,phm} = 4.30 \cdot 10^{-5} \; Pa\,s, \mu = 4.65 \cdot 10^{-5} \; Pa\,s$

The Reynolds number becomes:

$$Re_D = \frac{0.510 \cdot 1.0 \cdot 1.57}{4.30 \cdot 10^{-5}} = 18620 : ok!$$

Nusselt number:

$$Nu_D = 0.027 \cdot 18620^{4/5} \cdot 0.77095^{1/3} \cdot \left(\frac{4.30 \cdot 10^{-5}}{4.65 \cdot 10^{-5}} \right)^{0.14}$$

$Nu_D = 63.82$

The convective heat transfer coefficient:

$$h_{gas,part} = \frac{0.0771 \cdot 63.82}{1.57} = 3.13 \; \frac{W}{m^2 \, K}$$

And the heat flux:

$$q''_{ph,gas,part,conv} = 3.13 \cdot (1173.15 - 1052.15) = 379 \; \frac{W}{m^2}$$

The radiation heat absorption:

$$q''_{ph,abs,rad} = \sigma \cdot (\varepsilon_G \cdot T_G^4 - \alpha_G \cdot T_{wall}^4)$$

Where $\sigma = 5.67 \cdot 10^{-8} \; \frac{W}{m^2 \, K^4}, T_G = 1173.15 \; K, T_{wall} = 1323.15 \; K$

To find the emissivity ε_G and absorptivity α_G of the gas, the mean beam length must be calculated, using the geometry of enclosure "infinite cylinder":

$L = 0.95 \cdot D = 0.95 \cdot 1.57 = 1.49 \; m$ Further, the parameter $P_G L$ can be calculated assuming a partial pressure of CO_2 ($P_G = 1 \; atm$):

$P_G L = 1 \cdot 1.49 = 1.49 \; atm \cdot m$

Using the appropriate temperature and the $P_G \cdot L$ value, the emissivity is found.

$\varepsilon_G = 0.2$

The absorptivity is determined with $P_G \cdot L \cdot \left(\frac{T_{wall}}{T_G} \right)$.

$$P_G \cdot L \cdot \left(\frac{T_{wall}}{T_G} \right) = 1.68 \; atm \cdot m$$

$\alpha_G = 0.25$

The heat absorbed by the gas:

$$q''_{ph,abs,rad} = 5.67 \cdot 10^{-8} \cdot (0.2 \cdot (1173.15)^4 - 0.25 \cdot (1323.15)^4) = -19819 \; \frac{W}{m^2}$$

Further, the actual heat flux from the heated gas ($T_{m,gas}$) to the particles is calculated using the convective heat transfer correlations:

$$q''_{abs,conv,ph} = h_{abs,conv} \cdot \left(\overline{T_m} - T_{m,phm} \right)$$

The temperature of the heated gas:

$$T_m = T_{cal} + \frac{q''_{ph,abs,rad} \cdot P}{\dot{m} \cdot C_p} = 1173.15 + \frac{19819 \cdot \pi \cdot 1.57}{2.78 \cdot 120.4} = 1465.2 \ K$$

Where: $P = perimeter \ [m]$

The average temperature of the heated gas:

$$\overline{T_m} = \frac{1465.2 + 1173.15}{2} = 1319.2 \ K$$

Reynolds number:

$$Re_D = 12578.5$$

Prandtl number:

$$Pr = 0.706$$

Nusselt number:

$$Nu = 46.86$$

Convective heat transfer coefficient:

$$h_{abs,conv} = 2.9 \ \frac{W}{m^2 \ K}$$

And the heat flux:

$$q''_{abs,conv,ph} = 2.9 \cdot (1319.2 - 1052.15) = 774.5 \ \frac{W}{m^2}$$

Calcination section:

The convective heat flux from the wall to fluid is the same as the preheat section.

$$q''_{cal,wall,gas,conv} = q''_{ph,wall,gas,conv} = 330 \ \frac{W}{m^2}$$

The particles and the fluid in the calcination section have the same temperature. i.e., no heat exchange.

Radiation from the wall to the gas calculations is the same as in the preheated meal section. However, it is the mean heated gas temperature $\overline{T_m}$ and the calcination temperature T_{cal} that apply.

$$q''_{abs,conv,cal} = h_{abs,rad}\left(\overline{T_m} - T_{cal}\right)$$

The temperature difference is minor. The parameters describing the Nusselt number, Reynolds number, and convective heat transfer coefficient are approximately the same as the calculated parameters in the preheat section of the example.

$$q''_{abs,conv,cal} = 2.9(1319.2 - 1173.15) = 423.5 \ \frac{W}{m^2}$$

Appendix G: Stress calculations

Wall thickness calculation:		
Wall thickness	0,021	m
Buckling stress		
Outer diameter	1,11	m
Inner diameter	1,089	m
Cross-sectional area	0,0362689	m2
Density Inconel 718	8193	kg/m3
Height	30	m
Volume	1,08806705	m3
Mass cylinder	8914,53337	kg
Gravitational acceleration	9,807	m/s2
Force, dead load	87424,8288	N
Calculated buckling stress	2,41046253	MPa
Maximum allowed stress	36	MPa

Wall thickness calculation:		
Wall thickness	0,021	m
Bending - Shear stress		
Outer diameter	1,11	m
Inner diameter	1,089	m
Cross-sectional area (not shell)	52,3075177	m2
Height	30	m
Drag coefficient	0,8	-
Ambient pressure	101325	Pa
Universal gas constant	8,314	m3 Pa/K mol
Ambient temperature	293,15	K
Molar mass	0,02897	kg/mol
Density air	1,20438459	kg/m3
Velocity air	40	m/s
Wind force	40318,9556	N
Even distributed load	1343,96519	N/m2
Bending moment	151196,083	MPa
Moment of inertia	0,00548119	m4
Bending stress	27,5845593	MPa
Safety factor	1,3	-
Bending stress w/ safety factor	35,8599271	
Maximum allowed stress	36	MPa

Appendix H: Mass and energy balances

Calculation example: Determine the calcined meal flow rate $\dot{m}_{meal,cal}$ $\left[\frac{t}{h}\right]$ out of the DTR.

Mass balance:

$$\dot{m}_{phm,in} = \dot{m}_{CO2,prod} + \dot{m}_{meal,cal}$$

Find the weight of CO_2 produced during calcination:

$$w_{CO2,prod} = w_{CaCO3} \frac{M_{CO2}}{M_{CaCO3}}$$

The molecular mass of CO_2 and $CaCO_3$ are $44.01 \frac{kg}{kmol}$ and $100.087 \frac{kg}{kmol}$, respectively.

$$w_{CO2,prod} = 0.77 \cdot \frac{44.1}{100.087} = 0.3393$$

The mass flow rate of produced CO_2 when the meal is 100% converted is:

$$\dot{m}_{CO2,phm,100\%} = w_{CO2,prod}\dot{m}_{phm,in}$$

$$\dot{m}_{CO2,phm,100\%} = (0.3393 \cdot 207)\frac{t}{h} = 70.24\frac{t}{h}$$

To find the correct flow rate of CO_2 produced, the calcination degree X needs to be accounted for:

$$\dot{m}_{CO2,prod} = \dot{m}_{CO2,phm,100\%}X$$

$$\dot{m}_{CO2,prod} = (70.24 \cdot 0.94)\frac{t}{h} = 66.03\frac{t}{h}$$

The outflow of calcined meal:

$$\dot{m}_{meal,cal} = \dot{m}_{phm,in} - \dot{m}_{CO2,prod}$$

$$\dot{m}_{meal,cal} = (207 - 66.03)\frac{t}{h} = 140.97\frac{t}{h}$$

Calculation example: how much energy [MW] must be supplied the calciner in the preheat zone and the reaction zone? What is the total necessary supply assuming the electricity to heat efficiency is 98%?

The energy balance for the preheat zone of the reactor assuming a steady state system:

$$E_{phm,in} + E_{gen,ph} = E_{meal,900°C}$$

To find the energy provided by the preheated meal:

$$E_{phm,in} = \dot{m}_{phm,in} C_{p,phm} (T_{phm} - T_{ref})$$

The specific heat of the preheated meal:

$$C_{p,phm} = 0.13352 \cdot 10^3 \frac{J}{mol\ K}$$

The specific heat capacity has the unit mole, thus, either the mass flow rate needs to be converted to mole flow rate or the specific heat needs to be converted to mass basis. In this calculation example mole basis is used.

Molar flow rate of the preheated meal into the system can be calculated by dividing the mass flow rate $\dot{m}_{phm,in}$ with the molecular weight of the raw meal (in this example assumed $CaCO_3$):

$$\dot{n}_{phm,in} = \frac{\dot{m}_{phm,in}}{M_{w,CaCO_3}} = \frac{207}{100.0869 \cdot 10^{-3}} \cdot \frac{10^3}{3600} = 574.5 \frac{mol}{s}$$

$$E_{phm,in} = 574.5 \cdot 0.13352 \cdot 10^3 \cdot (658 - 25) = 48.56\ MW$$

The generated energy for the preheat zone is the electrical energy for preheating the meal, and the electric energy:

$$E_{el,ph} = E_{meal,900°C} - E_{phm,in}$$

The energy necessary to preheat the meal to 900 °C:

$$E_{meal,900°C} = \dot{m}_{phm,in} C_{p,phm} (T_{cal} - T_{ref})$$

$$E_{meal,900°C} = 574.5 \cdot 0.13352 \cdot 10^3 \cdot (900 - 25) = 67.12\ MW$$

The energy of the preheated meal is then:

$$E_{el,ph} = (67.12 - 48.56)MW = 18.56\ MW$$

The required supply of electrical energy is then:

$$E_{el,supply,ph} = \frac{18.56}{0.98} MW = 18.94\ MW$$

A second energy balance is used to describe the reaction zone of the DTR:

$$E_{meal,900°C} + E_{gen,cal} = E_{out,cal}$$

Further the energy out of the calciner can be found:

$$E_{out,cal} = E_{CO2,cal} + E_{meal,900°C}$$

$$E_{CO2,cal} = \dot{m}_{CO2,cal} \cdot C_{p,CO2,cal} \cdot (T_{cal} - T_{ref})$$

The mass flow rate of CO_2 produced needs to be changed to molar basis – same procedure as for the inlet mass flow rate – to determine $E_{CO2,cal}$.

$$\dot{n}_{CO2,cal} = 416.76 \frac{mol}{s}$$

$$C_{p,CO2,cal} = 0.0589 \frac{kJ}{mol\,K}$$

$$E_{CO2,cal} = 416.76 \cdot 0.0589 \cdot 10^3 \cdot (900 - 25) = 21.479\ MW$$

Thus, the outlet energy:

$$E_{out,cal} = (21.479 + 67.12)\ MW = 88.60\ MW$$

The energy generated in the reaction zone:

$$E_{gen,cal} = E_{el,cal} + E_{cal} + E_{other,cal}$$

Where:

$$E_{cal} = \dot{m}_{CO2,cal} \cdot H_{cal},\ E_{other,cal} = \dot{m}_{CO2,cal} \cdot H_{other}$$

The enthalpies are converted to molar basis:

$$H_{cal} = -3.6 \frac{MJ}{kg_{CO2}} \cdot 44.01 \cdot 10^{-3} \frac{kg_{CO2}}{mol} = -0.158436 \frac{MJ}{mol}$$

$$H_{other,cal} = 0.3 \frac{MJ}{kg_{CO2}} \cdot 44.01 \cdot 10^{-3} \frac{kg_{CO2}}{mol} = 0.013203 \frac{MJ}{mol}$$

The reaction energies become:

$$E_{cal} = \dot{n}_{CO2,cal} \cdot H_{cal} = 416.76 \cdot (-0.158436) = -66.03\ MW$$

$$E_{other,cal} = 416.76 \cdot 0.013203 = 5.50\ MW$$

The electric energy can be found:

$$E_{el,cal} = E_{out,cal} - E_{meal,900°C} - E_{cal} - E_{other}$$

$$E_{cal} = (88.60 - 67.12 - (-66.03) - 5.50)\ MW = 82.01\ MW$$

The supply of electrical energy can be calculated:

$$E_{el,supply,cal} = \frac{E_{el,cal}}{\eta_{el,heat}} = \frac{82.009}{0.98} = 83.683\ MW$$

Finally, the total energy supply can be calculated as the sum of the electrical energy supply:

$$E_{el,supply} = E_{el,supply,ph} + E_{el,supply,cal} = (18.94 + 83.683)MW = 107.855\ MW$$

Heat exchanger: determine the temperature of the cooled CO₂ gas.

This calculation example is molar based.

First, determine the specific heat capacity of the air and the CO₂ gas, then select the proper temperature equation.

$$C \overset{def}{=} \dot{m}_{gas} C_{p,gas}$$

To determine the heat capacity, an average temperature of 900 K is guessed for the CO₂ side.

$$C_{p,CO2,HX} = 1.204 \frac{kJ}{kg\,K} \cdot 44.01 \cdot 10^{-3} \frac{kg}{mol} = 0.0530 \frac{kJ}{mol\,K}$$

The average temperature of the air side is guessed to be 600 K and the air is regarded as dry, thus, the molecular weight is 28.97 kg/mol:

$$C_{p,air,HX} = 1.05 \frac{kJ}{kg\ K} \cdot 28.97 \cdot 10^{-3} \frac{kg}{mol} = 0.0304 \frac{kJ}{mol\ K}$$

The specific heat capacities for CO_2 and air are then:

$$C_{CO2} = 416.76 \cdot 0.0530 = 22.088$$

$$C_{air} = 680.78 \cdot 0.0304 = 20.696$$

$$C_{CO2} > C_{air}$$

$$\Delta T_{HX,min} = 100\ K$$

$$T_{CO2,in} = 900\ °C = 1173.15\ K$$

$$T_{air,in} = 225\ °C = 498.15\ K$$

$$T_{air,exc,hot} = T_{CO2,cal} - \Delta T_{HX,min} = 1173.15 - 100 = 1073.15 K$$

The average temperature of airstream can then be calculated:

$$T_{average,air} = \frac{T_{air,in} + T_{air,exc,hot}}{2} = \frac{498.15 + 1073.15}{2} = 785.65\ K$$

Then the specific heat capacity of air at the average temperature is found:

$$C_{p,air,HX} = 1.0897 \cdot 28.97 \cdot 10^{-3} = 0.03157 \frac{kJ}{mol\ K}$$

The temperature of the cooled CO_2 can then be found:

$$T_{CO2,cooled} = T_{CO2,in} - \frac{\dot{n}_{air} C_{p,air,HX}\left(T_{air,exc,HX} - T_{air,in}\right)}{\dot{n}_{CO2} C_{p,CO2,HX}}$$

$$T_{CO2,cooled} = 1173.15 - \frac{680.76 \cdot 0.03157 \cdot (1073.15 - 498.15)}{416.76 \cdot 0.0530} = 613.67\ K$$

To get a more correct answer, more iterations are required determine the proper outlet temperature of the cooled CO_2 gas.

The average temperature of CO_2 gas:

$$T_{average,CO2} = \frac{T_{CO2,in} + T_{CO2,cooled}}{2} = \frac{1173.15 + 613.67}{2} = 893.41\ K$$

The new specific heat capacity of CO_2 is then:

$$C_{p,CO2,HX,new} = 1.211 \cdot 44.01 \cdot 10^{-3} = 0.053296 \frac{kJ}{mol\ K}$$

The new temperature:

$$T_{CO2,cooled,new} = T_{CO2,in} - \frac{\dot{n}_{air} C_{p,air,HX}\left(T_{air,exc,HX} - T_{air,in}\right)}{\dot{n}_{CO2} C_{p,CO2,HX,new}}$$

$$T_{CO2,cooled,new} = 616.77\ K$$

The temperature of the cooled CO_2 is relatively close to the first iterated temperature, thus the second iteration might not be necessary.

Appendix I: Python 3.8 - calcination time

```python
@author: Martin Hagenlund Usterud
"""
#%% Shrinking core model reaction time calculations
#%% Libraries

import numpy as np
import matplotlib.pyplot as plt
from xlwt import Workbook, easyxf

#%%Input parameters
# PSD [micron]
D_p = [0.2, 0.48, 0.59, 0.71, 0.86, 1.04, 1.26, 1.52, 1.84, 2.23,
       2.7, 3.27, 3.95, 4.79, 5.79, 7.01, 8.48, 10.27, 12.43, 15.05,
       18.21, 22.04, 26.68, 32.29, 39.08, 47.3, 57.25, 69.3, 83.87,
       101.52, 122.87, 148.72, 180, 200, 250, 300, 350, 400, 450, 500]

T = 1173.15         # [K] Calcination temperature
X = 0.94            # Conversion factor (1 = 100% conversion)
X1 = 0.90           # Reduced conversion factor
A = 0.012           # [mol/m2 s kPa] Frequency factor
E = 33.47           # [kJ/mol] Activation energy
R = 8.314           # [m3 Pa/K mol] Universal gas constant
P_eq = 1.087276653  # [atm] Equilibrium pressure
P_CO2 = 1           # [atm] Partial pressure of CO2
#%% Empty store arrays for plotting
t = np.zeros(len(D_p))
t_X1 = np.zeros(len(D_p))

#%% Equation(s)
k = 0.003440816*(P_eq-P_CO2)    # Reaction rate

#%% Simulation loop
for i in range(0, len(D_p)):
    t[i] = ((1-(1-X))**3)*(D_p[i]*10**-6)**0.6/k
    t_X1[i] = ((1-(1-X1))**3)*(D_p[i]*10**-6)**0.6/k

#%% Plotting
plt.figure(1)
plt.title('Conversion time as a function of particle size', size = 14)
plt.plot(D_p, t, 'g-+', label = '94% calcination degree')
plt.plot(D_p, t_X1, 'r-+', label = '90% calcination degree')
plt.grid()
plt.legend()
plt.ylabel('Time [s]', size = 12)
plt.xlabel('Particle diameter ' r'[$\mu$m]', size = 12)

plt.savefig('Conversion time as a function of particle size',
            transparent = True, dpi = 1000)
#%% Export to Excel

wb = Workbook()
ns = wb.add_sheet('Reaction time')          #new sheet
style = easyxf('font: name Calibri')        #change font
```

```python
ns.write(0,0, 'Particle diameter' r'$\[mu$m]', style)
ns.write(0,1,'Time [s]', style)

#Store data in excel cells
for i in range(0, len(D_p)):
    ns.write(i+1,0, D_p[i], style)
    ns.write(i+1,1, t[i], style)

wb.save('Reaction time.xls')
```

Appendix J: Python 3.8 - terminal settling velocity

```python
@author: Martin Hagenlund Usterud
"""

import numpy as np
import matplotlib.pyplot as plt

#%% Parameters
g = 9.807                             # [m/s2] Gravitational acceleration
D_p = np.linspace(1, 500, 500)*10**-6 # [m] Particle diameter
rho_p = 1590                          # [kg/m3] Density product particle
rho_1 = 1.9022                        # [kg/m3] Density CO2 at T 1
rho_2 = 1.7730                        # [kg/m3] Density CO2 at T 2
T = 928 + 273.15                      # [K] Inlet temperature
T_1 = 1200                            # [K] Min temperature
T_2 = 1250                            # [K] Max temperature
my_1 = 478*10**-7                     # [Pa s] Dynamic viscosity at 1200 K
my_2 = 493*10**-7                     # [Pa s] Dynamic viscosity at 1250 K

#%% Interpolated values
rho_g = rho_1+((rho_2-rho_1)/(T_2-T_1))*(T-T_1)   # Density CO2 at T
my = my_1 +((my_2-my_1)/(T_2-T_1))*(T-T_1)        # Dynamic viscosity at T

#%% Arrays for storing
Ar = np.zeros(len(D_p))
v_t_turb = np.zeros(len(D_p))
Re_D_t = np.zeros(len(D_p))
Re_D = np.zeros(len(D_p))
v_t_lam = np.zeros(len(D_p))
v_t = np.zeros(len(D_p))
v_t2 = np.zeros(len(D_p))
D_p_lam = np.zeros(len(D_p))
D_p_turb = np.zeros(len(D_p))
```

```python
#%% Simulation loop
for i in range(0, len(D_p)):
    v_t_lam[i] = (g*(D_p[i]**2)*(rho_p-rho_g))/(18*my)    # Laminar velocity
    Re_D[i] = (rho_g*v_t_lam[i]*D_p[i])/my    # Reynoldsnumber Stokes regime
    if Re_D[i] <= 1:                # If Re is less than 1 = Stokes Regime
        v_t[i] = v_t_lam[i]         # Velocity is laminar
        D_p_lam[i] = D_p[i]        # Particle size laminar in laminar regime
    else:
        Ar[i] = (rho_g*(rho_p-rho_g))*g*(D_p[i]**3)/(my**2)# Archimedes nr.
        Re_D_t[i] = 0.1334*Ar[i]**0.7016  # Turbulent Reynolds number
        v_t_turb[i] = (Re_D_t[i]*my)/(rho_g*D_p[i]) # Turbulent velocity
        D_p_turb[i] = D_p[i]            # Particle size turbulent regime
        v_t2[i] = v_t_turb[i]           # Velocity storing array


#%% Sorting values of interest
v_t_lam = np.array(v_t)              # Laminar array for plotting
v_t_lam = v_t_lam[v_t_lam != 0]
D_p_lam = D_p_lam[D_p_lam !=0]       # Exclude all particle sizes that are
not laminar




v_t_turb = np.array(v_t2)            # Turbulent array for plotting
v_t_turb = v_t_turb[v_t_turb != 0]
D_p_turb = D_p_turb[D_p_turb != 0]   # Exclude all particle sizes that are
not turbulent


#%% Plotting
plt.figure(1)
plt.title('Settling velocity, Drop Tube Reactor', size = 14)
plt.plot(D_p_lam*10**6, v_t_lam , '-', label = 'Laminar')
plt.plot(D_p_turb*10**6, v_t_turb, 'r-', label = 'Turbulent')
plt.grid()
plt.legend()
plt.xlabel('Particle size [µm]', size = 12)
plt.ylabel('Terminal settling velocity [m/s]', size = 12)
plt.savefig('Terminal settling velocity', transparent = True, dpi = 1000)
```

Appendix K: Python 3.8 - diameter, height and number of tubes with varying fluid flow velocity

```python
@author: Martin Hagenlund Usterud
"""

# Simulations varying fluid flow velocity


#%% Libraries
import numpy as np
import math
from matplotlib import pyplot as plt
#%% Design values
m_total = 207        # [t/h] Max feedrate of raw meal
T_phm = 931.15       # [K] Temperature preheated meal inlet of DTR
T_cal = 1173.15      # [K] Calcination temperature
T_ref = 298.15       # [K] Reference temperature (ambient)
T_wall = 1323.15     # [K] Operating temperature (Reactor wall temperature)
eta = 0.98           # [-] Efficienct conversion from electricity to heat
U = 250              # [W/m2 K] Overall heat transfer coefficient,
                     # contribution from convection and radiation.
P_CO2 = 101325       # [Pa] Partial pressure of CO2 = 1 atm
R = 8.314            # [m3 Pa/K mol] Universal gas constant
k = 0.0651           # [W/m K] thermal conductivity coefficient (calculated
from excel)
k_T_m = 0.0771       # [W/m K] 1052.15K thermal conductivity coefficient
(calculated from excel)
k_2 = 0.0971         # Thermal conductivity at average Tm gas
my = 4.65*10**-5     # [Pa s] Dynamic viscocity evaluated at 1173.15 K
my_s = 5.08*10**-5   # [Pa s] Dynamic viscocity evaluated at 1323.15 K
my_g_p = 4.30*10**-5 #[Pa S] Dynamic viscosity evaluated at 1052.15 K
eps = 0.22           # Emissivity gas absorption graph.
eps1 = 0.9           # Emissivity grey body (Textbook page 740 and 939)
alpha = 0.25         # Absorptivity -"-
sigma = 5.67*10**-8  # Stefan Boltzmann constant
X = 0.94             # calcination degree
u_m = 2.0            # [m/s] mean velocity fluid
```

```python
u_m2 = 1.0          # [m/s] mean velocity fluid
u_m3 = 0.8          # [m/s] mean velocity fluid
C_p_CO2 = 120.4     # [J/kg K]  Specific heat capacity CO2 gas at
L_max = 24.8        # [m] Available height tubes


#%% Feedrate
m_phm = np.linspace(1, 207, 207)    # feedrate t/h
m_phm_in = m_phm*10**3/3600 # feedrate kg/s


#%%How much CO2 is produced during calcination with specified feedrate
w_CaCO3 = 0.7760 # Design basis value
Mw_CO2 = 44.01*10**-3   # Molecular weight CO2
Mw_CaCO3 = 100.087*10**-3 # Molecular weight Calcium carbonate
w_CO2_prod = w_CaCO3*(Mw_CO2/Mw_CaCO3) # Weight fraction of CO2


# Array for storing mass flow rate calculations
m_CO2_prod = np.zeros(len(m_phm))
m_CO2_prod_94 = np.zeros(len(m_phm))
n_CO2_prod_94 = np.zeros(len(m_phm))
# Find mass flow rate of CO2 w/ 100 % calcination
for i in range(len(m_phm)):
    m_CO2_prod[i] = w_CO2_prod*m_phm_in[i]  # produced CO2
    m_CO2_prod_94[i] = m_CO2_prod[i]*X  # produced CO2
    n_CO2_prod_94[i] = m_CO2_prod_94[i]/Mw_CO2 # produced CO2


#%% Volumetric flow of CO2
rho_CO2 = (P_CO2*Mw_CO2)/(R*T_cal)  # Density of CO2 at 900 °C


# Arrays for storing dimensional data
V_flow_CO2 = np.zeros(len(m_phm))
A_cross = np.zeros(len(m_phm))
D = np.zeros(len(m_phm))
A_cross2 = np.zeros(len(m_phm))
D2 = np.zeros(len(m_phm))
A_cross3 = np.zeros(len(m_phm))
D3 = np.zeros(len(m_phm))


for i in range(len(m_phm)):
```

138

```python
    V_flow_CO2[i] = m_CO2_prod_94[i]/rho_CO2   # [m3/s]
    A_cross[i] = V_flow_CO2[i]/u_m      # The cross sectional area of the DTR
    A_cross2[i] = V_flow_CO2[i]/u_m2
    A_cross3[i] = V_flow_CO2[i]/u_m3
    D[i] = np.sqrt(4*A_cross[i]/np.pi)    # The required diameter of the DTR
    D2[i] = np.sqrt(4*A_cross2[i]/np.pi)
    D3[i] = np.sqrt(4*A_cross3[i]/np.pi)


#%% Preheat section
# Wall to particle radiation - Preheating
T_m_ph = (T_cal+T_phm)/2
h_rad_ph = sigma*eps1*(T_m_ph+T_wall)*((T_m_ph)**2+(T_wall)**2)
q_rad_ph_wall_part_flux = h_rad_ph*(T_m_ph-T_wall)
# Total heat flux - preheating
q_tot_ph = abs(q_rad_ph_wall_part_flux)


#%% Calcination section
# Wall to particle radiation - Calcination
h_rad_cal = sigma*eps1*(T_cal+T_wall)*((T_cal)**2+(T_wall)**2)
q_rad_cal_wall_part_flux = h_rad_cal*(T_cal-T_wall)


# Total heat flux - Calcination
q_tot_cal = abs(q_rad_cal_wall_part_flux)


#%% Energy supply required to heat meal (Heat rate)
# From energy balances / Preheat zone
n_phm_in = m_phm_in/Mw_CaCO3 # Molar flow rate of preheated meal
Cp_phm = 0.13352*10**3 # Specific heat capacity of raw meal at 1052.15 K


E_meal_900 = n_phm_in*Cp_phm*(T_cal-T_ref)*10**-6 # Energy of the meal at
T_cal
E_phm_in = n_phm_in*Cp_phm*(T_phm-T_ref)*10**-6 # Energy of the preheated
meal


E_el_ph = E_meal_900-E_phm_in
E_supply_ph = (E_el_ph/eta) # Necessary electricity supply of ph in MW
Q_ph = E_supply_ph


# From energy balances / Calcination zone
```

```python
Cp_CO2_cal = 0.0589*10**3 # Specific heat capacity of CO2 at T_cal
E_CO2_cal = n_CO2_prod_94*Cp_CO2_cal*(T_cal-T_ref)*10**-6 # Energy of CO2
E_out_cal = (E_CO2_cal + E_meal_900) # Energy out of the reactor


H_cal = -3.6*Mw_CO2      #Enthalpy of calcination
H_other = 0.3*Mw_CO2     #Enthalpy of other reactions
E_cal = n_CO2_prod_94*H_cal # Calcination reaction energy
E_other = n_CO2_prod_94*H_other # Other reactions energy


E_supply_cal = ((E_out_cal-E_meal_900-E_cal-E_other)/eta)
Q_cal = E_supply_cal


# Total heat required
Q = Q_ph+Q_cal


#%% Heat transfer area
# Preheating section
A_heat_ph = (Q_ph*10**6/q_tot_ph)


# Calcination section
A_heat_cal = ((Q_cal*10**6)/q_tot_cal)


#%% Length of sections
# Preheating section
L_ph = A_heat_ph/(D*np.pi)


# u_m2
L_ph2 = A_heat_ph/(D2*np.pi)


# u_m3
L_ph3 = A_heat_ph/(D3*np.pi)


# Calcination section
L_cal = A_heat_cal/(D*np.pi)


#u_m2
L_cal2 = A_heat_cal/(D2*np.pi)
```

```python
#u_m3
L_cal3 = A_heat_cal/(D3*np.pi)


# Total length of DTR at given feedrate
L = L_ph + L_cal


#u_m2
L2 = L_ph2 + L_cal2


#u_m3
L3 = L_ph3 + L_cal3


#%% Number of tubes necessary


n_tubes = (L/L_max)
n_tubes_rounded = [math.ceil(number) for number in n_tubes]


# u_m2
n_tubes2 = (L2/L_max)
n_tubes_rounded2 = [math.ceil(number) for number in n_tubes2]


# u_m3
n_tubes3 = (L3/L_max)
n_tubes_rounded3 = [math.ceil(number) for number in n_tubes3]


#%%Plotting
plt.figure(1)
plt.title('Diameter as a function of raw meal feed rate', size = 14)
plt.plot(m_phm, D, label = 'u$_m$ = 2 [m/s]')
plt.plot(m_phm, D2, 'g', label = 'u$_m$ = 1 [m/s]')
plt.plot(m_phm, D3, 'r', label = 'u$_m$ = 0.5 [m/s]')
plt.grid()
plt.legend()
plt.xlabel('Feedrate [t/h]', size = 12)
plt.ylabel('Diameter [m]', size = 12)


plt.figure(2)
plt.title('Length as a function of raw meal feed rate', size = 14)
```

```python
plt.plot(m_phm, L, label = 'u$_m$ = 2 [m/s]')
plt.plot(m_phm, L2, 'g', label = 'u$_m$ = 1 [m/s]')
plt.plot(m_phm, L3, 'r', label = 'u$_m$ = 0.5 [m/s]')
plt.grid()
plt.legend()
plt.xlabel('Feedrate [t/h]', size = 12)
plt.ylabel('Length [m]', size = 12)


fig, (ax1, ax2, ax3) = plt.subplots(nrows=3, ncols=1, sharex = False)
fig.set_size_inches(9, 6)
plt.suptitle('Number of tubes as a function of raw meal feed rate', size = 20)


ax1.plot(m_phm, n_tubes_rounded, '.', label = 'u$_m$ = 2 [m/s]')
ax1.grid()
ax1.legend(loc = 'upper left')


ax2.plot(m_phm, n_tubes_rounded2,  'g.', label = 'u$_m$ = 1 [m/s]')
ax2.grid()
ax2.legend(loc = 'upper left')


ax3.plot(m_phm, n_tubes_rounded3,  'r.', label = 'u$_m$ = 0.5 [m/s]')
ax3.grid()
ax3.legend(loc = 'upper left')


fig.text(0.5, 0.04, 'Feedrate [t/h]', ha='center', size = 17)
fig.text(0.04, 0.5, 'Number og tubes', va='center', rotation='vertical', size = 17)


#plt.savefig('Diameter of tube with changing gas velocity', transparent = True, dpi = 1000)
```

Appendix L: – Python 3.8 - diameter, height and number of tubes with varying temperature

```python
@author: Martin Hagenlund Usterud
"""

# Simulations impact of temperature

#%% Libraries
import numpy as np
import math
from matplotlib import pyplot as plt

#%% Design values
m_total = 207        # [t/h] Max feedrate of raw meal
T_phm = 931.15       # [K] Temperature preheated meal inlet of DTR
T_cal = 1173.15      # [K] Calcination temperature
T_ref = 298.15       # [K] Reference temperature (ambient)
T_wall = 1500        # [K] Operating temperature (Reactor wall temperature)
T_wall2 = 1400       # [K] Operating temperature (Reactor wall temperature)
T_wall3 = 1323.15    # [K] Operating temperature (Reactor wall temperature)
T_wall4 = 1200       # [K] Operating temperature (Reactor wall temperature)
eta = 0.98           # [-] Efficienct conversion from electricity to heat
U = 250              # [W/m2 K] Overall heat transfer coefficient,
                     # contribution from convection and radiation.
P_CO2 = 101325       # [Pa] Partial pressure of CO2 = 1 atm
R = 8.314            # [m3 Pa/K mol] Universal gas constant
k = 0.0651           # [W/m K] thermal conductivity coefficient
k_T_m = 0.0771       # [W/m K] 1052.15K thermal conductivity coefficient
k_2 = 0.0971         # Thermal conductivity at average Tm gas
my = 4.65*10**-5     # [Pa s] Dynamic viscocity evaluated at 1173.15 K
my_s = 5.08*10**-5   # [Pa s] Dynamic viscocity evaluated at 1323.15 K
my_g_p = 4.30*10**-5 #[Pa S] Dynamic viscosity evaluated at 1052.15 K
eps = 0.22           # Emissivity gas absorption graph.
eps1 = 0.9           # Emissivity grey body (Textbook page 740 and 939)
alpha = 0.25         # Absorptivity -"-
sigma = 5.67*10**-8  # Stefan Boltzmann constant
X = 0.94             # calcination degree
u_m = 1.0            # [m/s] mean velocity fluid
C_p_CO2 = 120.4      # [J/kg K]  Specific heat capacity CO2 gas at
L_max = 25           # [m] Available height tubes
#%% Feedrate
m_phm = np.linspace(1, 207, 207)   # feedrate t/h
m_phm_in = m_phm*10**3/3600 # feedrate kg/s

#%%How much CO2 is produced during calcination with specified feedrate
w_CaCO3 = 0.7760 # Design basis value
Mw_CO2 = 44.01*10**-3   # Molecular weight CO2
Mw_CaCO3 = 100.087*10**-3 # Molecular weight Calcium carbonate
w_CO2_prod = w_CaCO3*(Mw_CO2/Mw_CaCO3) # Weight fraction of CO2

# Array for storing mass flow rate calculations
```

```python
m_CO2_prod = np.zeros(len(m_phm))
m_CO2_prod_94 = np.zeros(len(m_phm))
n_CO2_prod_94 = np.zeros(len(m_phm))
# Find mass flow rate of CO2 w/ 100 % calcination
for i in range(len(m_phm)):
    m_CO2_prod[i] = w_CO2_prod*m_phm_in[i]  # produced CO2
    m_CO2_prod_94[i] = m_CO2_prod[i]*X  # produced CO2 with calcination
degree
    n_CO2_prod_94[i] = m_CO2_prod_94[i]/Mw_CO2 # produced CO2 at molar
basis

#%% Volumetric flow of CO2
rho_CO2 = (P_CO2*Mw_CO2)/(R*T_cal)  # Density of CO2 at T_cal

# Arrays for storing dimensional data
V_flow_CO2 = np.zeros(len(m_phm))
A_cross = np.zeros(len(m_phm))
D = np.zeros(len(m_phm))

for i in range(len(m_phm)):
    V_flow_CO2[i] = m_CO2_prod_94[i]/rho_CO2  # [m3/s]
    A_cross[i] = V_flow_CO2[i]/u_m
    D[i] = np.sqrt(4*A_cross[i]/np.pi)    # The required diameter of the
DTR

#%% Preheat section
# Wall to particle radiation - Preheating
T_m_ph = (T_cal+T_phm)/2
h_rad_ph = sigma*eps1*(T_m_ph+T_wall)*((T_m_ph)**2+(T_wall)**2)
q_rad_ph_wall_part_flux = h_rad_ph*(T_m_ph-T_wall)

h_rad_ph2 = sigma*eps1*(T_m_ph+T_wall2)*((T_m_ph)**2+(T_wall2)**2)
q_rad_ph_wall_part_flux2 = h_rad_ph2*(T_m_ph-T_wall2)

h_rad_ph3 = sigma*eps1*(T_m_ph+T_wall3)*((T_m_ph)**2+(T_wall3)**2)
q_rad_ph_wall_part_flux3 = h_rad_ph3*(T_m_ph-T_wall3)

h_rad_ph4 = sigma*eps1*(T_m_ph+T_wall4)*((T_m_ph)**2+(T_wall4)**2)
q_rad_ph_wall_part_flux4 = h_rad_ph4*(T_m_ph-T_wall4)

# Total heat flux - preheating
q_tot_ph = abs(q_rad_ph_wall_part_flux)
q_tot_ph2 = abs(q_rad_ph_wall_part_flux2)
q_tot_ph3 = abs(q_rad_ph_wall_part_flux3)
q_tot_ph4 = abs(q_rad_ph_wall_part_flux4)

#%% Calcination section
# Wall to particle radiation - Calcination
h_rad_cal = sigma*eps1*(T_cal+T_wall)*((T_cal)**2+(T_wall)**2)
q_rad_cal_wall_part_flux = h_rad_cal*(T_cal-T_wall)

h_rad_cal2 = sigma*eps1*(T_cal+T_wall2)*((T_cal)**2+(T_wall2)**2)
q_rad_cal_wall_part_flux2 = h_rad_cal*(T_cal-T_wall2)

h_rad_cal3 = sigma*eps1*(T_cal+T_wall3)*((T_cal)**2+(T_wall3)**2)
q_rad_cal_wall_part_flux3 = h_rad_cal3*(T_cal-T_wall3)
```

```
h_rad_cal4 = sigma*eps1*(T_cal+T_wall4)*((T_cal)**2+(T_wall4)**2)
q_rad_cal_wall_part_flux4 = h_rad_cal4*(T_cal-T_wall4)
# Total heat flux - Calcination
q_tot_cal = abs(q_rad_cal_wall_part_flux)
q_tot_cal2 = abs(q_rad_cal_wall_part_flux2)
q_tot_cal3 = abs(q_rad_cal_wall_part_flux3)
q_tot_cal4 = abs(q_rad_cal_wall_part_flux4)


#%% Energy supply required to heat meal (Heat rate)
# From energy balances / Preheat zone
n_phm_in = m_phm_in/Mw_CaCO3 # Molar flow rate of preheated meal
Cp_phm = 0.13352*10**3 # Specific heat capacity of raw meal at 1052.15 K

E_meal_900 = n_phm_in*Cp_phm*(T_cal-T_ref)*10**-6 # Energy of the meal at
calcination temp
E_phm_in = n_phm_in*Cp_phm*(T_phm-T_ref)*10**-6 # Energy of the preheated
meal


E_el_ph = E_meal_900-E_phm_in
E_supply_ph = (E_el_ph/eta) # Necessary electricity supply of ph in MW
Q_ph = E_supply_ph

# From energy balances / Calcination zone
Cp_CO2_cal = 0.0589*10**3 # Specific heat capacity of CO2 at calcination
temp
E_CO2_cal = n_CO2_prod_94*Cp_CO2_cal*(T_cal-T_ref)*10**-6 # Energy of CO2
at calcination
E_out_cal = (E_CO2_cal + E_meal_900) # Energy out of the reactor

H_cal = -3.6*Mw_CO2      #Enthalpy of calcination
H_other = 0.3*Mw_CO2     #Enthalpy of other reactions
E_cal = n_CO2_prod_94*H_cal # Calcination reaction energy
E_other = n_CO2_prod_94*H_other # Other reactions energy

E_supply_cal = ((E_out_cal-E_meal_900-E_cal-E_other)/eta)
Q_cal = E_supply_cal

# Total heat required
Q = Q_ph+Q_cal

#%% Heat transfer area
# Preheating section
A_heat_ph = (Q_ph*10**6/q_tot_ph)
A_heat_ph2 = (Q_ph*10**6/q_tot_ph2)
A_heat_ph3 = (Q_ph*10**6/q_tot_ph3)
A_heat_ph4 = (Q_ph*10**6/q_tot_ph4)

# Calcination section
A_heat_cal = ((Q_cal*10**6)/q_tot_cal)
A_heat_cal2 = ((Q_cal*10**6)/q_tot_cal2)
A_heat_cal3 = ((Q_cal*10**6)/q_tot_cal3)
A_heat_cal4 = ((Q_cal*10**6)/q_tot_cal4)

#%% Length of sections
# Preheating section
L_ph = A_heat_ph/(D*np.pi)
L_ph2 = A_heat_ph2/(D*np.pi)
```

```python
L_ph3 = A_heat_ph3/(D*np.pi)
L_ph4 = A_heat_ph4/(D*np.pi)

# Calcination section
L_cal = A_heat_cal/(D*np.pi)
L_cal2 = A_heat_cal2/(D*np.pi)
L_cal3 = A_heat_cal3/(D*np.pi)
L_cal4 = A_heat_cal4/(D*np.pi)

# Total length of DTR at given feedrate
L = L_ph + L_cal
L2 = L_ph2 + L_cal2
L3= L_ph3 + L_cal3
L4 = L_ph4 + L_cal4

#%% Number of tubes necessary
n_tubes = (L/L_max)
n_tubes2 = (L2/L_max)
n_tubes3 = (L3/L_max)
n_tubes4 = (L4/L_max)
n_tubes_rounded = [math.ceil(number) for number in n_tubes]
n_tubes_rounded2 = [math.ceil(number) for number in n_tubes2]
n_tubes_rounded3 = [math.ceil(number) for number in n_tubes3]
n_tubes_rounded4 = [math.ceil(number) for number in n_tubes4]


#%%Plotting
plt.figure(2)
plt.title('Height as a function of raw meal feed rate', size = 14)
plt.plot(m_phm, L, label = 'T = 1500 [K]')
plt.plot(m_phm, L2, 'g', label = 'T = 1400 [K]')
plt.plot(m_phm, L3, 'r', label = 'T = 1323.15 [K]')
plt.plot(m_phm, L4, 'y', label = 'T = 1200 [K]')
plt.grid()
plt.legend()
plt.xlabel('Feed rate [t/h]', size = 12)
plt.ylabel('Height [m]', size = 12)


plt.figure(3)
plt.title('Radiation heat flux preheating section', size = 14)
plt.plot(T_wall, q_tot_ph*10**-3, 'x' , label = 'T = 1500 [K]')
plt.plot(T_wall2, q_tot_ph2*10**-3, 'x' , label = 'T = 1400 [K]')
plt.plot(T_wall3, q_tot_ph3*10**-3, 'x' , label = 'T = 1323.15 [K]')
plt.plot(T_wall4, q_tot_ph4*10**-3, 'x' , label = 'T = 1200 [K]')
plt.grid()
plt.legend()
plt.xlabel('Temperature [K]', size = 12)
plt.ylabel('Heat flux [kW/m$^2$]', size = 12)


plt.figure(4)
plt.title('Radiation heat flux calcination section', size = 14)
plt.plot(T_wall, q_tot_cal*10**-3, 'x' , label = 'T = 1500 [K]')
plt.plot(T_wall2, q_tot_cal2*10**-3, 'x' , label = 'T = 1400 [K]')
plt.plot(T_wall3, q_tot_cal3*10**-3, 'x' , label = 'T = 1323.15 [K]')
plt.plot(T_wall4, q_tot_cal4*10**-3, 'x' , label = 'T = 1200 [K]')
plt.grid()
plt.legend()
plt.xlabel('Temperature [K]', size = 12)
```

146

```python
plt.ylabel('Heat flux [kW/m$^2$]', size = 12)

fig, (ax1, ax2, ax3, ax4) = plt.subplots(nrows=4, ncols=1, sharex = False)
fig.set_size_inches(10, 8)
plt.suptitle('Number of tubes as a function of raw meal feed rate', size =
20)

ax1.plot(m_phm, n_tubes_rounded, '.', label = 'T = 1500 [K]')
ax1.grid()
ax1.legend(loc = 'upper left')

ax2.plot(m_phm, n_tubes_rounded2,  'g.', label = 'T = 1400 [K]')
ax2.grid()
ax2.legend(loc = 'upper left')

ax3.plot(m_phm, n_tubes_rounded3,  'r.', label = 'T = 1323.15 [K]')
ax3.grid()
ax3.legend(loc = 'upper left')

ax4.plot(m_phm, n_tubes_rounded4,  'y.', label = 'T = 1200 [K]')
ax4.grid()
ax4.legend(loc = 'upper left')

fig.text(0.5, 0.04, 'Feed rate [t/h]', ha='center', size = 17)
fig.text(0.04, 0.5, 'Number og tubes', va='center', rotation='vertical',
size = 17)

plt.savefig('Number of tubes with varying temperature', transparent = True,
dpi = 1000)
```

Appendix M: Excel calculation heating element. Kanthal® APM [47]

APM U Tube Element Calculation.

Customer	ELSE II			Date	05.05.2021		
Project	Drop tube calciner			Sign	O Stadum		
Drawing no	xx			Rev no	0		

	Tube element data:				Electrical data:		
Heating zone	Outer dia.	260,00	mm	Rating	No of elements	16	In parallel
	Inner dia.	238,00	mm		Total rating	10,52	MW
	Le	15 000	mm		Element voltage	42,00	Volts DC
	No shanks	1	pcs		Current	251	kA
	c-c A	0	mm				
	Cross section	8605	mm^2	Element data	Tube temp	1175	ºC
	Tube length	15 000	mm		Ct factor	1,042	Ct
	Surface area	122 522	cm^2		Resistance	0,002682	Ohm
	Resistance Le	0,002528	Ohms @20ºC		Res. ratio	98,3	% Le/Lu
					Element rating	657 702	Watts
	No terminals	2	pcs		Element current	15 660	Amperes
Terminals	Terminal W	250,0	mm		Weight Le	1120,35	kg
	Terminal T	250,0			Weight Lu	518,75	kg
	Terminal Lu	500	mm		Weight Bridge	15,12	kg
	Cross section	62 500	mm^2		Element weight	1639,10	kg
	Surface area	5 000	cm^2				
	Resistance Lu	0,000023	Ohms @20ºC				
	Total surface	10000	cm^2				
	Tot resistance	0,000046	Ohms @20ºC				
	No bridges	0	pcs		Process temp:	1050	ºC
Serial bridge	Bridge W	100,0	mm		Element temp calc:	1175	ºC
	Bridge T	36,0	mm				
	Bridge Lu	246	mm				
	Cross section	3 600	mm^2				
	Surface area	669	cm^2				
	Resistance Lu	0,000000	Ohms @20ºC				
	Tot resistance	0,000000	Ohms @20ºC				

Data per element

Voltage	Current	Power Le	Surface Lo. Le	Power per Lu	Surface Load Lu	Elem. power	Tot Power
42,00	15660	645 846	5,27	5 689	1,1	657 225	10515,60
Volts	Amperes	Watts	W/cm^2	Watts	W/cm^2	Watts	kW